VEHICLE CRASH TEST AND EVALUATION OF MEDIAN BARRIERS FOR TEXAS HIGHWAYS

by

T. J. Hirsch
Research Engineer and Principal Investigator

Edward R. Post
Assistant Research Engineer

and

Gordon G. Hayes
Physics Research Associate

Research Report Number 146-4
Studies of Field Adaptation of Impact Attenuation Systems

Research Study Number 2-8-68-146

Sponsored by
The Texas Highway Department
in cooperation with
The United States Department of Transportation
Federal Highway Administration

September 1972
Texas Transportation Institute
Texas A&M University
College Station, Texas

ABSTRACT

Key Words: Median Barriers, Roadway Safety, Vehicle Damage, Vehicle Decelerations, Accidents, Injury Severity, Injury Probability, Maintenance, Luminaire Poles

Full-scale tests were conducted to evaluate and compare the performance of three median barriers of different configuration and lateral stiffness. The three barriers selected by the Texas Highway Department were: (a) the Metal Beam Guard Fence (MBGF) which consists of two back-to-back steel W-beam guardrails on weak breakaway steel posts, (b) the E-3 which consists of two different size strong elliptical steel rail members mounted on strong fabricated steel posts, and (c) the concrete median barrier (CMB) with sloping faces.

All three barriers remained *intact* in restraining and redirecting a standard size 4,000 lb. passenger vehicle under the severe impact conditions of about 60 mph and 25 degrees. However, some snagging occurred on a post of the E-3 barrier as a result of the vehicle mounting the lower rail member.

A 60 mph and 25 degree test demonstrated that luminaire poles and fencing can be safely mounted on the top of the CMB barrier in narrow medians. Flexible guardrail may be unsafe in narrow medians because the lateral displacements of the guardrail may allow the vehicle to contact and knock the luminaire pole onto the roadway.

A comparative study of the three barriers demonstrated that barrier displacements were effective in reducing vehicle decelerations, vehicle

damage, and the probability and severity of injuries to unrestrained occupants. An injury probability of 46 percent represents the apparent division between minor and major injuries. The MBGF barrier, undergoing the largest dynamic displacement of 1.5 ft., was on the *threshold* of major injuries under the impact conditions of 60 mph and 25 degrees.

A graph is presented from which an engineer can examine the probability and severity of injury associated with *rigid* traffic barriers under various combinations of imapct speed, impact angle, and passenger vehicle weight. The results of this and other studies show that the performance of the CMB barrier with sloping faces would be similar to that of a rigid concrete barrier with a vertical wall under those combinations of impact speed and angle exceeding an average lateral vehicle deceleration of 2 G's and a probability injury level of 20 percent.

This study adds support to the vast knowledge obtained from previous testing programs and field experience in demonstrating that maintenance repair increases as barrier flexibility increases. Maintenance of the rigid CMB barrier would require at most an occasional light sandblasting job to remove unsightly tire scrub markings.

The findings of this study indicate that the CMB barrier would best serve the public in narrow medians of roadways located in urban developments and carrying high speed and high traffic volume. Information is presented on the safety, economic, and aesthetic considerations for each of the three barriers investigated.

SUMMARY

Full-scale tests were conducted to evaluate the performance of three median barriers of different configuration and lateral stiffness. The barriers selected by the Texas Highway Department were: (a) the Metal Beam Guard Fence (MBGF) which consists of two standard W-beam guardrails mounted back-to-back on breakaway steel posts, (b) the E-3 which consists of two elliptical steel rails mounted on strong steel posts, and (c) the concrete median barrier (CMB) with sloping faces.

All three barriers remained intact in restraining and redirecting a 4,000 lb. passenger vehicle under the severe impact conditions of about 60 mph and 25 degrees. However, some snagging occurred on a post of the E-3 barrier as a result of the vehicle mounting the lower rail member. Increasing the height of the lower rail member may be one solution for reducing the snagging.

The 150 ft. test section of the CMB barrier, which was not anchored to the roadway and contained continuous #5 longitudinal reinforcing steel, showed no tendency to overturn or slide during the 60 mph and 25 degree collision. The measured rotational displacement at the top of the barrier was 0.09 inches. A 1-in. layer of hot mix asphalt was placed 1-in. above the median and adjacent to the base of the barrier to help prevent sliding.

The breakaway fillet-weld post connections of the MBGF barrier were effective from a standpoint of providing greater flexibility and permitting the posts to displace laterally without significantly reducing the height

of the rail member, and thereby, preventing vehicle ramping.

A 60 mph and 25 degree test showed that luminaire poles and fencing can be safely mounted on the top of the CMB barrier in narrow medians. On the other hand, a luminaire pole protected by flexible guardrail may be unsafe in narrow medians because the lateral displacements of the guardrail may allow the vehicle to contact and knock the luminaire pole onto the roadway.

The departure angles of the vehicles after redirection varied from a low of 6 degrees to a high of 20 degrees. The 20 degree departure angle occurred with the semi-rigid MBGF barrier due to the side ramping effect created by the barrier displacements. On wide shoulders and under high speed and large angle collisions, the large departure angles would most likely not create a hazardous condition for other nearby vehicles because most full-scale tests demonstrate that the colliding vehicle after redirection is pulled back toward the barrier due to the high friction drag forces of the severely damaged front wheel.

A comparative study of the three barriers demonstrated that barrier displacements were very effective in reducing the lateral vehicle decelerations, vehicle damage, and hence, injury severity. During a 60 mph and 25 degree barrier collision, it was predicted from *measured* lateral decelerations that the probability and severity of injury to unrestrained occupants in a standard size 4,000 lb. passenger vehicle would be: 72 percent and major for the rigid CMB barrier; 62 percent and major for the E-3 barrier undergoing a displacement of 0.7 feet; and, 46 percent and on the threshold of major for the MBGF barrier undergoing the largest

displacement of 1.5 feet. An injury probability of 46 percent represents the apparent division between minor and major injuries. An average of nine individual assessments of vehicle damage rating using the National Safety Council (NSC) 7-point rating severity scale were: 5.75 for the CMB barrier; 6.1 for the E-3 barrier; and, 5.2 for the MBGF barrier.

Two additional tests were conducted on the CMB barrier at lower angles of impact of 7 and 15 degrees to evaluate its performance under representative inservice narrow median type collisions. It was predicted that the probability and severity of injuries to unrestrained occupants in a standard size 4,000 lb. passenger vehicle would be: between 19 to 22 percent and minor for a 60 mph and 7 degree collision; and, between 43 to 47 percent and on the threshold of major for a 60 mph and 15 degree collision. The averages of nine individual NSC vehicle damage scale ratings were 2.1 and 5.5 for the 7 and 15 degree collisions, respectively.

The 60 mph and 7 degree CMB barrier test and the tests of other investigators on concrete medians with sloping faces definitely show that minor sheet metal vehicle damage occurs under low impact speeds and/or angles.

As well known from field experience, this study showed that maintenance increases as barrier flexibility increases. Maintenance of the CMB barrier would be nil and would require at most an occasional light sandblasting job. Maintenance of the relatively rigid E-3 barrier would require the replacement of one upper 10 ft. rail, straightening of one post, and a paint touchup for an estimated cost of $290. Maintenance of the semi-rigid MBGF barrier would require the replacement of 25 ft. of the barrier including three breakaway posts for an estimated cost of $440.

Based upon information provided by the Texas Highway Department, the initial construction costs of the three barriers on a linear foot basis are: $13.40 for the CMB barrier; $19.20 for the E-3 barrier; and, $11.75 for the MBGF barrier.

One could conclude from the results presented (see also Table 6) that the MBGF barrier is the most economical concerning initial construction costs, and that the barrier is the safest concerning probability and injury severity to unrestrained occupants during a 4,000 lb. automobile 60 mph/25 deg. impact. However, the MBGF barrier would cost the most to maintain and its use in *narrow* medians is *not* desirable due to the possibility of the vehicle displacing the barrier a sufficient distance and knocking the luminaire pole onto the roadway. It appears that the MBGF barrier would probably be satisfactory for use on rural type roadways with wide shoulders, wide medians and relatively high speed but low traffic volume.

One could further conclude from the results presented that the CMB barrier is the most economical when both initial construction costs and estimated maintenence costs are considered. The CMB barrier with luminaire poles would be very desirable for use on urban type roadways with narrow medians and carrying high speed and high traffic volume. In addition, low maintenance reduces the amount of exposure time, and hence, increases safety to maintenance personnel.

It is important that one keep in mind that all three median barriers investigated in this study have performed adequately while in service on our highways. Also, other factors in addition to those

presented here should be considered when selecting a barrier. For example, information is available which indicates that approximately 75% of the vehicle collisions will occur at angles of 15 deg. or less. At lower impact angles, the safety and maintenance aspects of all three median barriers would improve. A graph (Figure 35) is presented from which a highway engineer can examine the probability and severity of injury associated with *rigid* type traffic barriers under various combinations of impact speed, impact angle, and passenger vehicle weight.

It is the contention of the writers that the safety aspects of the E-3 could be improved by increasing the height of the lower rail member to prevent vehicle snagging on the support posts.

IMPLEMENTATION STATEMENT

In this study, three median barriers were evaluated and compared under full-scale test conditions. The semi-rigid MBGF barrier, the relatively rigid E-3 barrier, and the rigid CMB barrier all remained *intact* in restraining and redirecting a standard size 4,000 lb. passenger vehicle under the severe impact conditions of 60 mph and 25 degrees.

A noticeable amount of snagging occurred on a post of the E-3 barrier as the result of the vehicle front wheel mounting the lower rail member. It appears that snagging could be greatly reduced by increasing the height of the lower rail member. Also, the splice sleeve in each rail member of the E-3 barrier, adjacent to a post support, functions largely as a shear connection distributing the lateral load on a rail member to one or at most two posts. Failure of a splice would allow the colliding vehicle to penetrate the barrier or abruptly snag on the exposed rail member end and the post. It is therefore important that the 1/2-in. diameter bolt connecting the rail member and splice sleeve shown on the shop drawings be *securely tightened.*

The initial construction costs for the three barriers on a linear foot basis are: $19.20 for the E-3 barrier; $13.40 for the CMB barrier; and, $11.75 for the MBGF barrier. The figures on construction were obtained from a Texas Highway Department D-8 Interoffice Memorandum (20) dated April 10, 1972.

The estimated maintenance costs following a 4,000 lb. automobile impact at 60 mph/25 deg. are: $290 for the E-3 barrier; nil for the

CMB barrier; and, $440 for the MBGF barrier.

The initial construction cost of the CMB barrier is about 12 percent higher than the cost of the MBGF barrier. However, the findings in this study indicate that the CMB barrier would *better serve* the public in narrow medians of roadways located in urban developments and carrying high speed and high traffic volume. Maintenance of the CMB barrier would require at the most an occasional light sandblasting job to remove unsightly tire scrub marks. And, low maintenance insures increased safety by reducing the exposure time of repair crews and equipment to high speed and high traffic volumes. A 60 mph and 25 degree test also demonstrated that luminaire poles and fencing can be safely mounted on the top of the CMB barrier. Guardrail, such as the MBGF barrier, may be unsafe in narrow medians because the lateral displacements of the guardrail may allow the colliding vehicle to contact and knock the luminaire pole onto the roadway. Lastly, the majority of the rigid traffic barrier collisions in urban areas would occur under impact conditions in which the probability of vehicle occupant (unrestrained) injury would be low. A graph is presented in this study (see Figure 35) from which a highway engineer can examine the probability and severity of injury associated with *rigid* traffic barriers under various combinations of impact speed, impact angle, and passenger vehicle weight.

TABLE OF CONTENTS

LIST OF FIGURES

LIST OF FIGURES (CONTINUED)

LIST OF FIGURES (CONTINUED)

LIST OF TABLES

DISCLAIMER

The contents of this report reflect the views of the authors who are responsible for the facts and the accuracy of the data presented herein. The contents do not necessarily reflect the official views or policies of the Federal Highway Administration. This report does not constitute a standard, specification, or regulation.

I. INTRODUCTION

Highway engineers in Texas became concerned about the performance of certain median barriers being used or being considered for use on Texas highways. Consequently, three different types of median barriers were selected by the Texas Highway Department for full scale vehicle crash testing in order to determine their behavior under controlled impact conditions.

The three median barriers selected were: (a) the Metal Beam Guard Fence (MBGF) which consists of two standard W-sections mounted on each side of 6 WF 8.5 support posts; (b) the E-3 Railing or Median Barrier (E-3) which consists of two elliptical shaped steel rails mounted on steel posts; and, (c) the concrete median barrier (CMB) with sloping faces.

Median barriers are very effective in preventing serious head-on multiple vehicle accidents. In order to be assured that a barrier has adequate strength to prevent vehicle penetration, the three selected median barriers were subjected to the severe impact conditions recommended by HRB Circular 482 (1). That is, a test shall be conducted at a speed of 60 mph and 25 degrees using a standard size passenger vehicle weighing about 4,000 lbs., with load. Conducting the tests under similar impact conditions also provides a means of comparing the performance of the three barriers from primarily a viewpoint of injury severity and maintenance.

Most CMB type barriers are located in narrow medians of large urban developments. Because of the restricted widths of roadway, most barrier

accidents will occur at relatively shallow angles. Therefore, two additional tests were conducted on the CMB barrier at lower impact angles of 7 and 15 degrees in order to evaluate its performance under representative inservice collisions.

One other objective of this study was to determine if a passenger vehicle would snag or dislodge a luminaire pole mounted on the top of the CMB barrier. One test was conducted under the impact conditions of 60 mph and 25 degrees to investigate this problem.

II. DESCRIPTIONS AND PROCEDURES FOR TESTS

Description of Median Barriers

Descriptions of the three median barriers selected by the Texas Highway Department for evaluation under full scale test conditions are presented in the work to follow:

1. E-3 RAILING OR MEDIAN BARRIER

The E-3 median barrier consists of two elliptical shaped steel rail members mounted on fabricated steel posts as shown in Figure 1. The height from the roadway to the top of the lower rail member is 14 in., and the height to the top of the upper rail member is 30 in. The posts are spaced on 10 ft. centers.

The rail members are rolled from a round to an elliptical shape to increase the moment carrying capacity under lateral loading. Also, the lower rail member is larger than the upper rail member because the larger portion of the lateral load is developed in the area of the wheel hub and structural frame of a passenger vehicle; whereas, the upper rail member is subjected to primarily sheet metal crushing of the passenger vehicle.

A detailed drawing of a post and its connections and of the splices in the rail members is shown in Figure 2. Each post consists of two high strength steel (A441) rectangular shapes. Fillet welds are used to connect the post to the two rail members and the 1-in. high strength steel (A441) base plate. The two rectangular shapes

of the post extend through the lower rail member. The base plate is anchored by two 3/4-in. A325 U-shaped bolts embedded in an 18-in. diameter concrete shaft.

The E-3 median barrier is considered to be a rigid barrier capable of undergoing only small displacements in the redirection of a standard size passenger vehicle because of the relatively *strong* posts and rail members.

2. METAL BEAM GUARD FENCE

The metal beam guard fence or barrier, designated as MBGF(B)-69A, consists of two standard 12-gage steel W-shaped rail members mounted back-to-back on each side of a 6 WF 8.5 support post as shown in Figure 3. The posts are spaced on 6 ft.-3 in. centers, and the height above the roadway to the top of the rail member is 27 in.

The 3/8-in. fillet welds connecting the outer faces of the two post flanges and the 5/8-in. base plate are designed to fracture during the redirection of a standard size passenger vehicle under high impact speeds and moderate to large angles. Failure of the welded connections allows the two back-to-back rail members to displace several feet laterally, thereby, reducing the vehicle decelerations and incidence of injury. Also, failure of the welds allows the posts to displace laterally with the rail member without pulling the rail member down, thereby, preventing vehicle ramping.

3. CONCRETE MEDIAN BARRIER

The concrete median barrier, designated as CMB-70, is a massive solid concrete barrier with inclined plane surfaces as shown in the

cross sectional view of Figure 4. The CMB barrier tested had: a weight of about 507 lb./ft.; a height of 32 in. above the roadway; a lower 10-in. high inclined surface of about 55 degrees; an upper 19-in. high inclined surface of about 84 degrees; a base width of 27 in.; and a top width of 8 in.

The Texas CMB barrier is similar to the New Jersey Median Barrier (2) except that #5 longitudinal reinforcing steel is used in the Texas barrier whereas none is used in the New Jersey barrier. As shown in Figure 5, the CMB barrier was constructed in two longitudinally reinforced continuous length sections of 150 ft. and 50 ft. The construction joint between the two sections offers no lateral restraint.

The luminaire pole was mounted on top of the shorter 50 ft. section. Three 18-in. diameter drilled concrete shafts were used to support the shorter CMB section against possible overturning due to wind and vibratory forces on the luminaire pole. The longer 150 ft. section, on which three tests were conducted, contains no mechanical anchors to the roadway. The 1-in. layer of hot mix asphalt at the base of the CMB barrier provided some restraint to sliding during a vehicle collision.

Details of the chain link fabric fence and of the luminaire pole connection is shown in Figure 6.

The CMB barrier when located in narrow medians provides, as demonstrated in test CMB-1, additional *safety* to motorists because highway luminaire poles can be placed on top of the barrier and thus removed from possible traffic conflict. For example, a luminaire pole

protected by guardrail may be unsafe in narrow medians because the guardrail could be displaced laterally a sufficient distance so that the colliding vehicle could snag on the pole and even conceivably fracture and knock the pole into the stream of traffic.

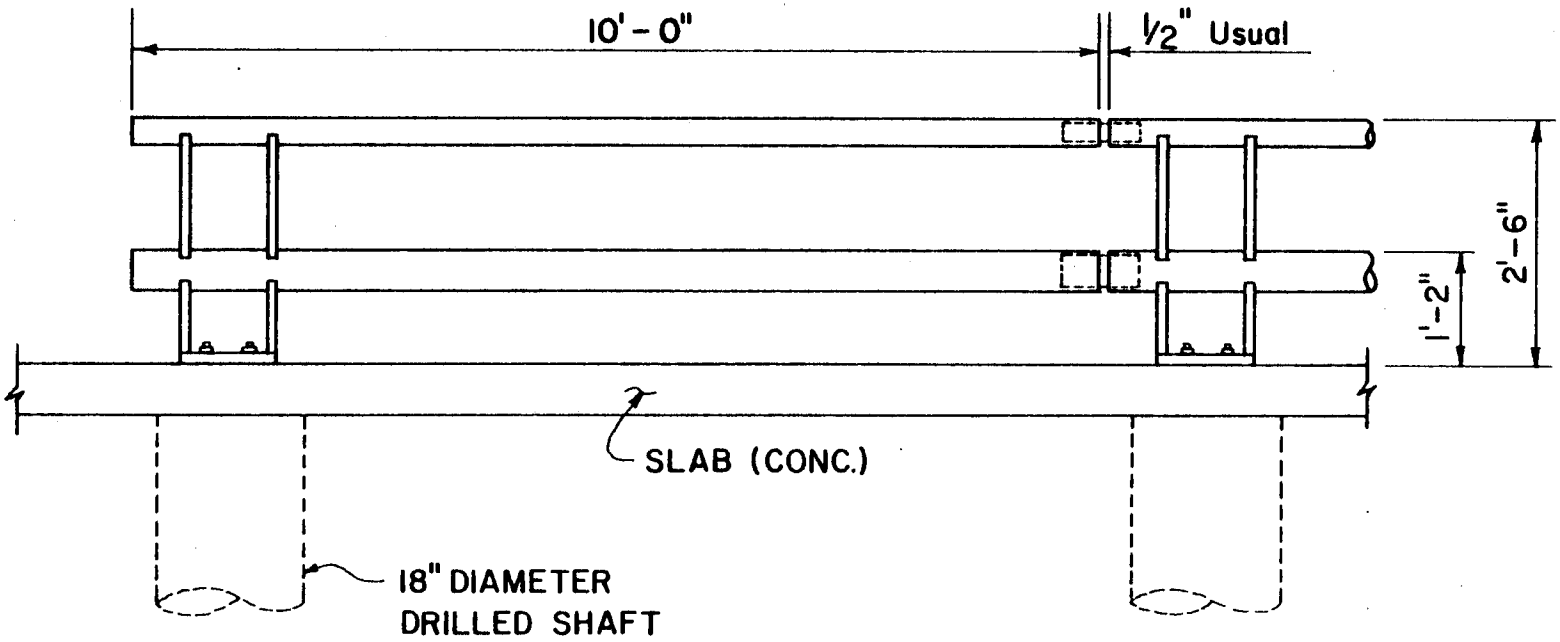

FIGURE 1. TEXAS HIGHWAY DEPT. RAILING TYPE E-3

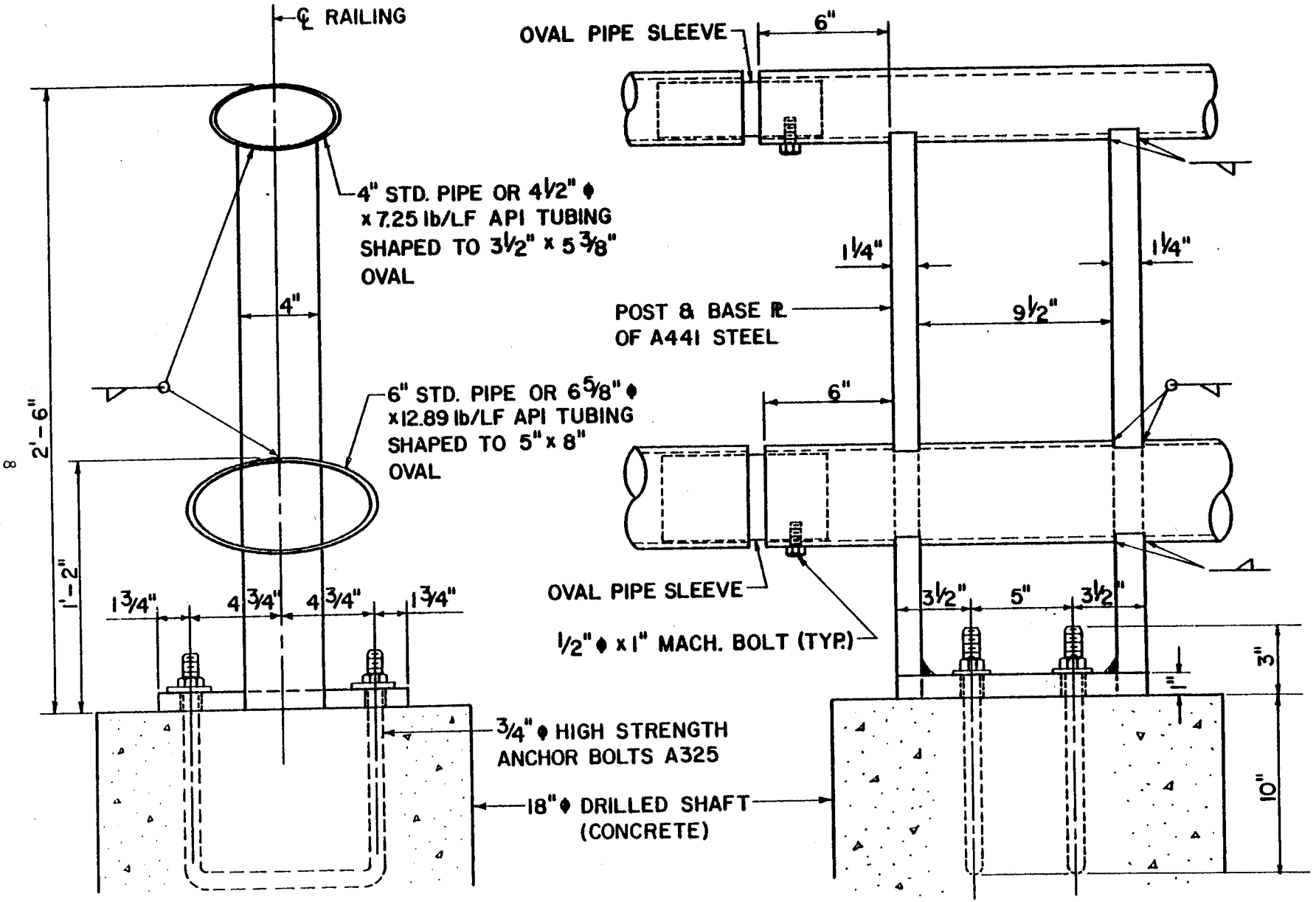

FIGURE 2. TEXAS HIGHWAY DEPT. RAILING TYPE E-3

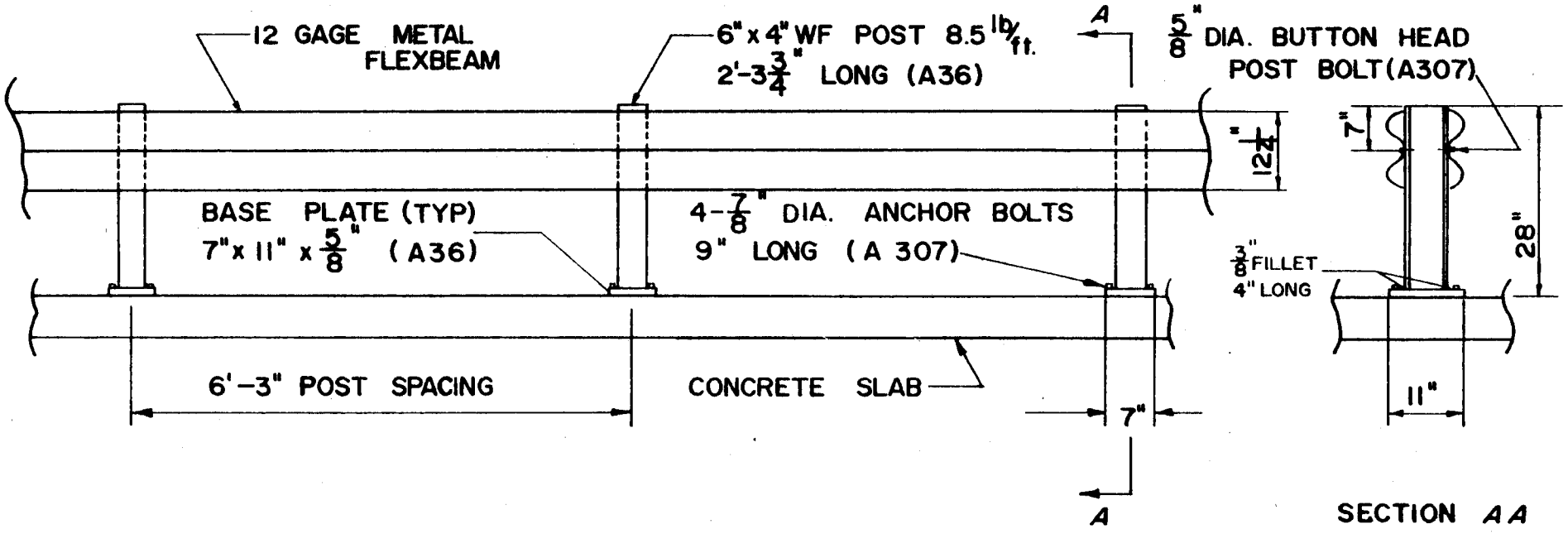

FIGURE 3. TEXAS HIGHWAY DEPT. METAL BEAM GUARD FENCE (BARRIER)
MBGF (B) – 69A

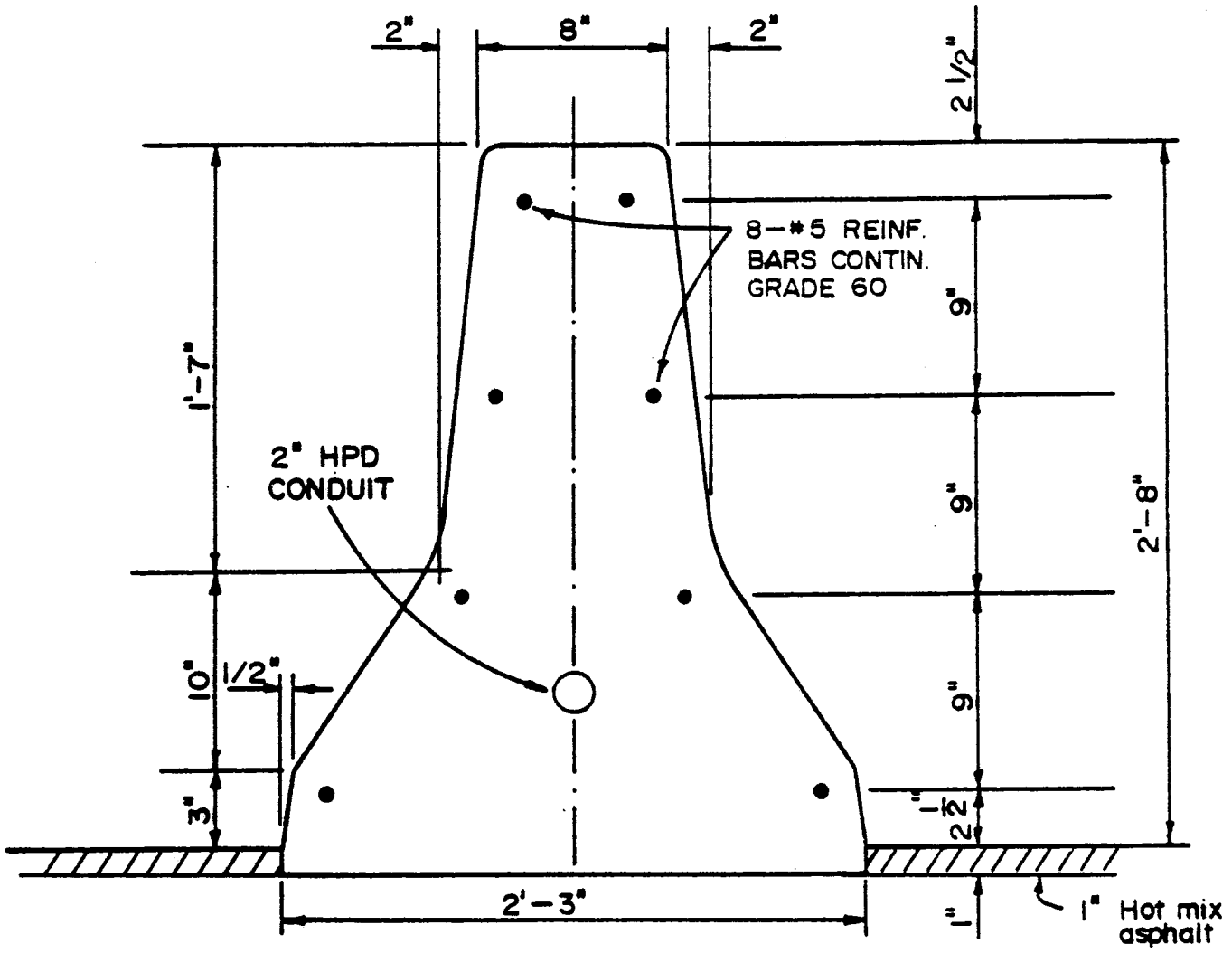

FIGURE 4. TEXAS HIGHWAY DEPT. CONCRETE MEDIAN BARRIER (CMB 70)

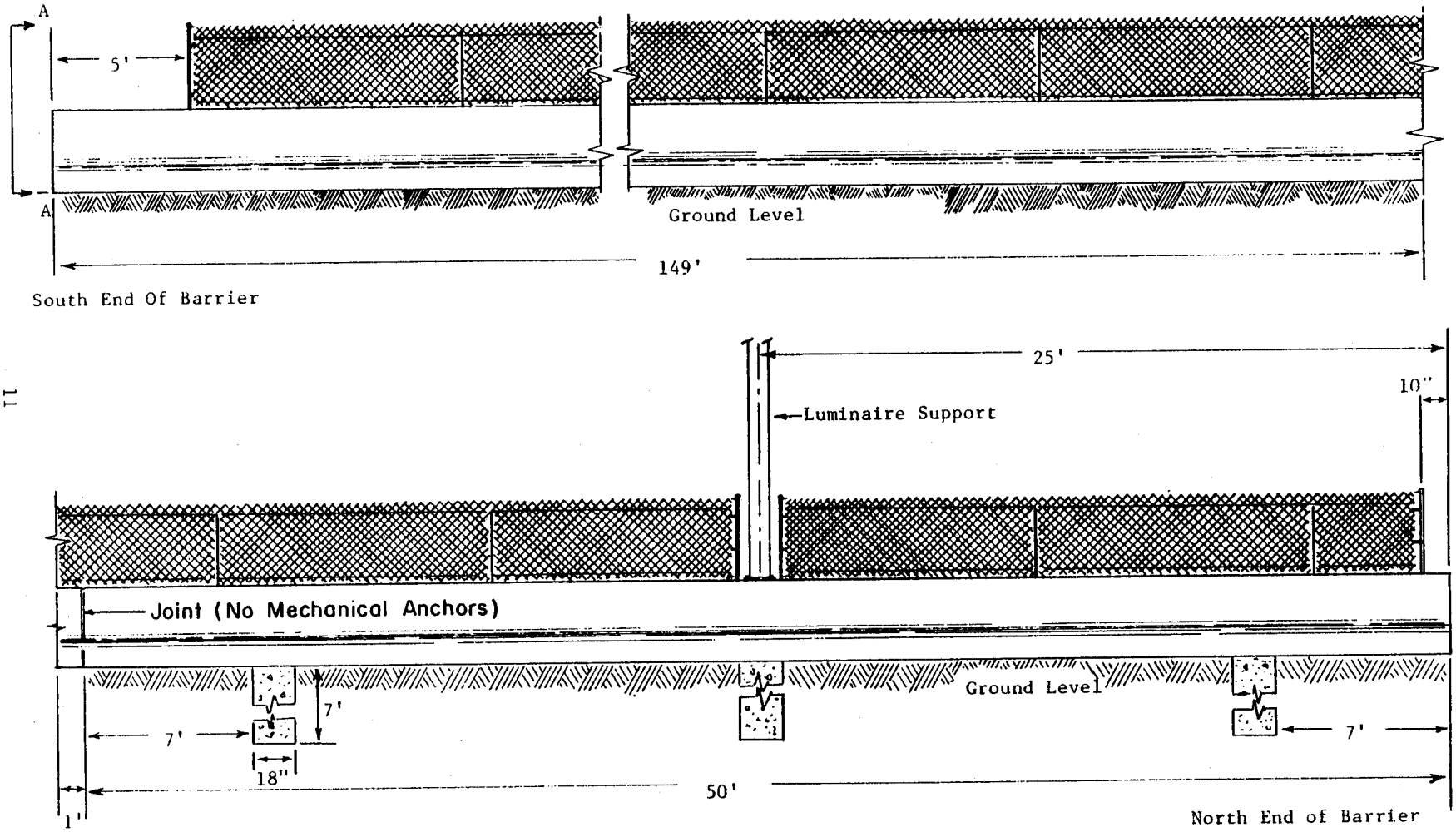

FIGURE 5. CONCRETE MEDIAN BARRIER (CMB 70)

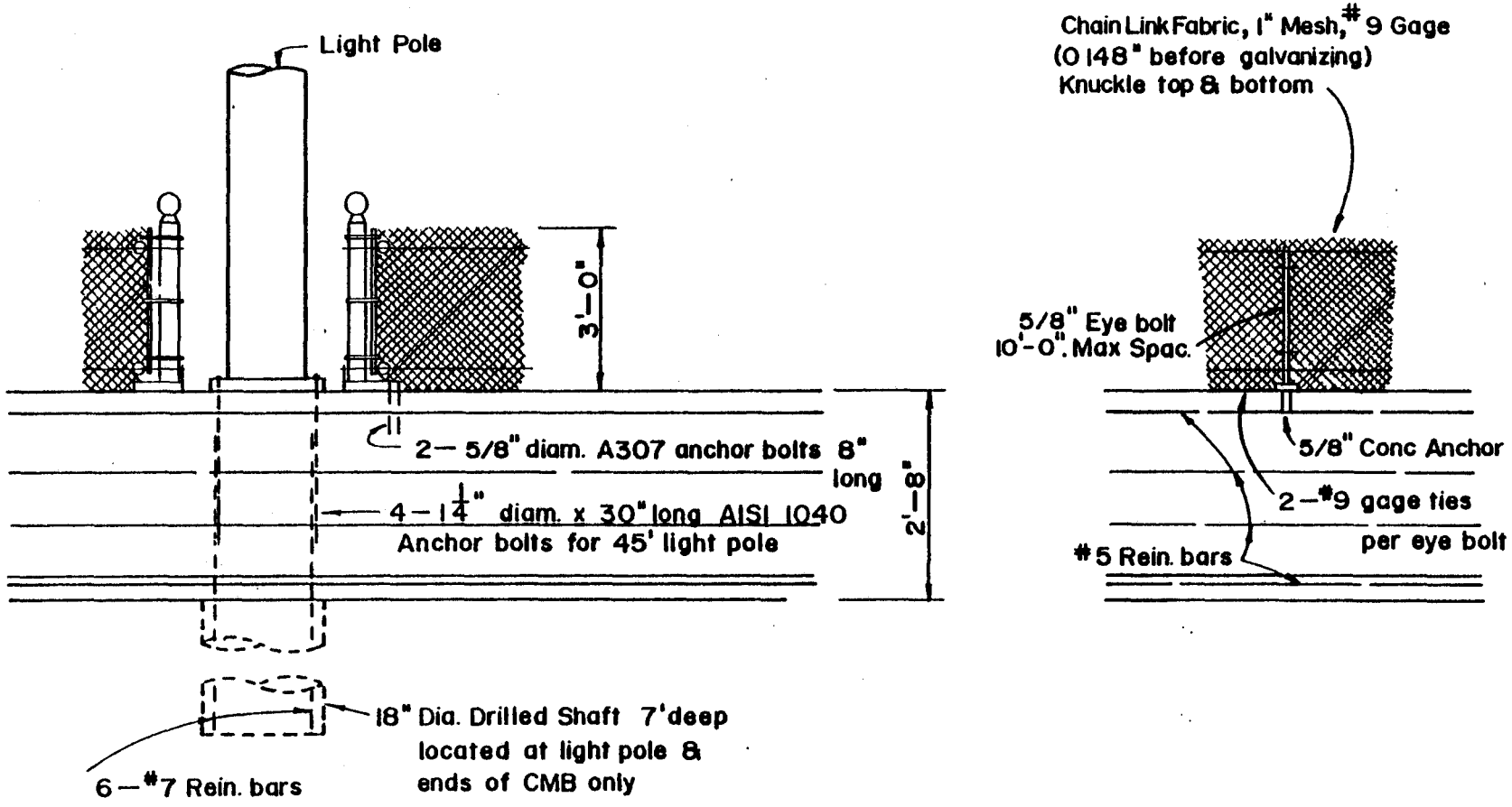

FIGURE 6. TEXAS HIGHWAY DEPT. CONCRETE MEDIAN BARRIER (CMB 70)

Vehicle Control Apparatus

The passenger test vehicles were guided along the desired approach paths by a cable guidance system. In this system, a breakaway flange attached to the left front wheel hub follows a cable stretched along the desired path. Before impact, this device shears off and leaves the vehicle unguided.

The vehicles were brought to the desired test speed by a cable attached through a pulley system to a reverse tow vehicle. The cable has an eye in the end which is looped around a pin welded to the front bumper of the test vehicle. As the test vehicle approaches the impact area, the pulley system exerts a downward force on the cable and causes it to disengage from the towing pin on the bumper. From this point, the test vehicle was unpowered.

Test Instrumentation

All tests were recorded photographically using high-speed and documentary motion picture cameras. The high-speed films (usually 500 frames per second) have accurate timing marks placed on the edge from which elapsed times can be computed. Vehicle displacement can be measured from the films using the stadia boards on the vehicles and other targets and range poles. The position of the vehicle in the horizontal plane can be determined using two cameras and a triangulation technique. However, the roof target over the vehicle's c.g. is used as a tracking point, and if excessive roll or pitch motions are encountered, this method is not effective because at this time it is limited to two dimensions, and a plot of the positions of the roof target would not be representative of the positions of the vehicle's c.g. Tables in the Appendix give either time-position data for the roof target or time-displacement data for the vehicle along its path.

All test vehicles had four accelerometers mounted on the longitudinal frame members behind the front seat. One accelerometer was mounted transversely and one longitudinally on each frame member. The tests of the E-3 and MBGF median barriers were conducted in July of 1970. At that time the signals from the accelerometers were transmitted by shielded cable to a nearby instrumentation van where they were recorded on magnetic tape. In these two tests, piezoelectric accelerometers were mounted transversely and strain-gage-type accelerometers were mounted longitudinally. Although the strain-gage-type accelerometers are considered more suitable for

vehicle crash testing, they require four electrical conductors. The limited number of conductors in the "hard-wired" system required that the two-conductor piezoelectric devices be used.

The tests on the concrete median barrier were conducted in the summer of 1971. At this time, a telemetry data acquisition system had been acquired. This system transmitted the accelerometer data by radio signals to a ground station where they were recorded on magnetic tape. This system eliminated the need for a physical connection to the test vehicle and allowed the use of all strain-gage-type instruments.

In all tests, a 160 lb anthropometric dummy simulated a driver. The dummy was secured by a lap belt attached to a load cell for sensing lap belt force.

Reproductions of the accelerometer and lap belt force traces are shown in the Appendix.

Auxiliary devices were used for quick-look determinations of initial vehicle speed and subsequent accelerations on test day. But these are not considered as accurate as the processed data from the films and accelerometer traces, and they are therefore not presented here. All accelerometer and lap belt data were passed through an 80 Hz low-pass active filter.

Data Reduction Techniques

The initial, or impact, vehicle speeds are determined from films obtained with a camera located for that purpose perpendicular to the vehicle's initial path. These speeds are actually average speeds over an approximately six-foot interval prior to impact. The position or displacement of the vehicle is usually determined at the end of successive small time intervals throughout the interaction, and the speed at any point can be computed over a suitable interval.

The average lateral and longitudinal decelerations from the film data are calculated from impact to the time when the vehicles are parallel to the barriers. These decelerations are the perpendicular and parallel components with respect to the barriers, whereas the decelerations from the accelerometers are perpendicular and parallel to the vehicles' longitudinal axes. The longitudinal deceleration from the film is calculated from the impact angle, impact speed, speed at parallelism, and the distance traveled parallel to the barrier as shown in footnote "a" of Tables 1 and 2. The lateral deceleration is calculated from initial speed and angle, vehicle dimensions, and barrier deflection as shown in footnote "b" of Tables 1 and 2. This method has proven to give values that are comparable to those obtained by triangulation methods.

The peak decelerations are read from the accelerometer traces. The average decelerations from these traces are taken over the interval from impact to the point where significant accelerations have ceased. This point usually occurs before the vehicle has completely lost contact with the barrier. As the vehicle is redirected, the departing angle is such

that ordinarily very little force is exerted on the vehicle even though it is still in contact with the barrier.

The average decelerations from accelerometer traces are determined by measuring the area under the curve with a planimeter, dividing this area by the length to get average height, and converting this height to deceleration. The values reported in Tables 1 and 2 are averages of the decelerations measured on the left and right vehicle frame members.

The accelerometer traces are reproduced in the Appendix.

III. DISCUSSION AND EVALUATION OF TESTS

A discussion and evaluation of the six full scale tests conducted on three median barriers of different configuration and lateral stiffness are presented in the work to follow. Assessments of the damage to the test vehicles and predictions on the probability and severity of injury that would occur under impact conditions similar to the tests are presented later in Section IV. Descriptions and detailed drawings of the median barriers were presented earlier in Section II.

E-3 Median Barrier Test

The E-3 Median Barrier test was conducted at an impact speed of 59.3 mph and an impact angle of 25 degrees using a standard size 1963 Plymouth weighing 3,610 lbs., with instrumentation and dummy. The point of impact was slightly upstream from the splice connections in the rail members and a support post as shown by the location of the vehicle control cable and damaged barrier in the photographs of Figure 7.

Sequential photographs of the vehicle collision and its redirection are shown in Figures 8, 9, and 10 from three camera positions. And, a summary of the test results from an analysis of the film data and accelerometer traces are presented in Table 1.

The longitudinal accelerometer traces on the right and left frame members of the vehicle in Figures 36 and 37 (see appendix) indicate that snagging occurred on a support post during the time interval of 100 to 160 milliseconds after impact. The peak acceleration was 21.3 G's. The tire marks in Figure 7 and the motion of the vehicle in Figure 10 show that the vehicle had climbed on the lower rail member. It is the

opinion of the writers that the snagging on the post could be reduced by placing the lower rail member at a higher height.

It can be seen in Figure 10 that the right front wheel of the vehicle was pulled left toward the barrier. This pulling effect in combination with the severely damaged left wheel caused the vehicle after redirection to travel in a circular arc back toward the barrier as shown in Figure 11. This phenomenon, which is typical of high speed and large angle barrier collisions, is certainly desirable because it minimizes the danger to other vehicles in the vicinity of the collision.

As indicated in Table 1, the change in heading speed of the vehicle during redirection was 30 mph; the departure angle from the barrier was 9 degrees; and, the maximum dynamic lateral displacement of the top rail member was 0.7 ft.

It can be seen in Figure 7 that the barrier remained intact and was not extensively damaged under the severe imposed test conditions. Maintenance would require the replacement of one 10 ft. length of upper rail member, straightening of one support post, and a paint touchup. It appears that the damaged barrier would, prior to repair, be functional under a possible second collision.

The damaged test vehicle is shown in Figure 11. It can be seen that the left front quarter and wheel are severely damaged, the windshield is knocked out, and the passenger compartment area is slightly warped.

TABLE 1

SUMMARY OF TEST DATA FOR E3 AND MBGF TESTS

DATA	BARRIER TEST	
	E3	MBGF
VEHICLE		
Year	1963	1963
Make	Plymouth	Plymouth
W, Weight (lbs)	3610	3640
θ, Impact Angle (deg)	25	25
FILM DATA		
V_I, Initial Impact Speed (mph)	59.3	57.3
V_P, Speed at Parallel (mph)	28.9	32.7
S_{long}, Longitudinal Distance to Parallel (ft)	20.7	17.5
D, Dynamic Barrier Displacement (ft)	0.7	1.5
S_{lat}, Lateral Distance to Parallel (ft)	3.4	4.28
Δt, Time to Parallel (sec)	0.394	0.270
a. G_{long}, Average Longitudinal Deceleration (G's) (Parallel to Barrier)	3.3	3.0
b. G_{lat}, Average Lateral Deceleration (G's) (Normal to Barrier)	6.2	4.6
Departure Angle (deg)	8.7	19.7
ACCELEROMETER DATA		
Longitudinal Deceleration (G's) (parallel to long. axis of vehicle)		
Maximum	21.3	12.8
Average	4.1	3.0
Time (sec)	0.533	0.560
Transverse Deceleration (G's) (normal to long. axis of vehicle)		
Maximum	6.1	--
Average	0.4	--
Time (sec)	0.537	--

a. $$G_{long} = \frac{(V_I \cos\theta)^2 - V_P^2}{2g\ S_{long}}$$

b. $$G_{lat} = \frac{V_I^2 \sin^2\theta}{2g\ S_{lat}}$$ where: $S_{lat} = AL\sin\theta - B(1-\cos\theta) + D$

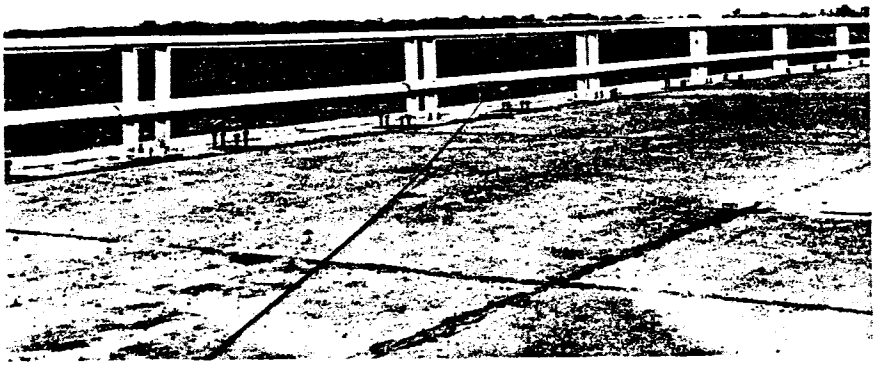

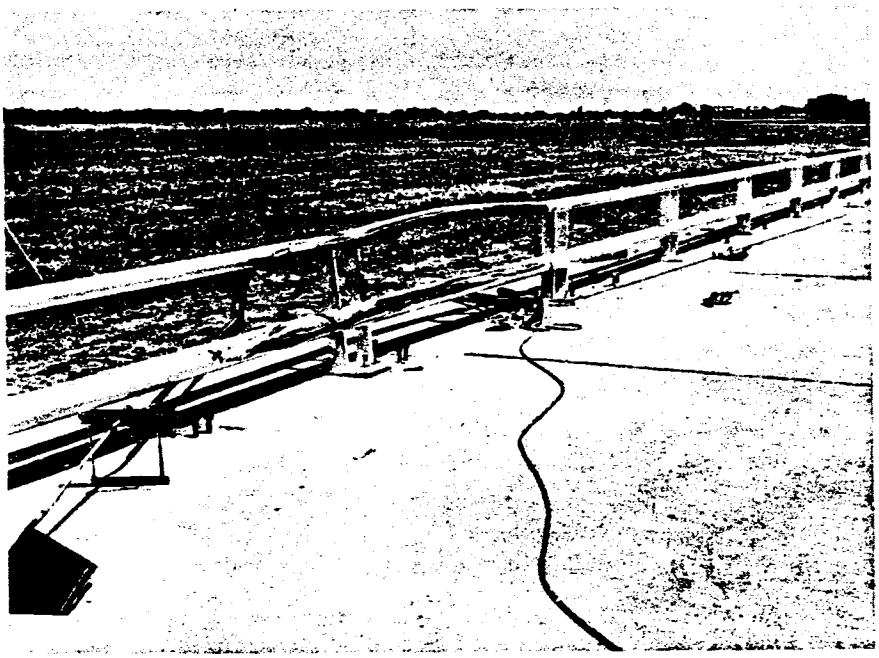

FIGURE 7, E3 BARRIER BEFORE AND AFTER TEST.

t = 0.000 sec

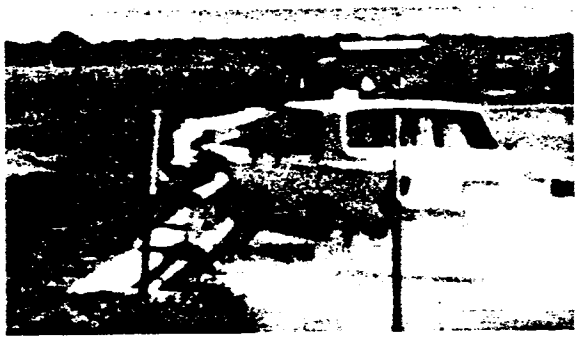

t = 0.063 sec

t = 0.116 sec

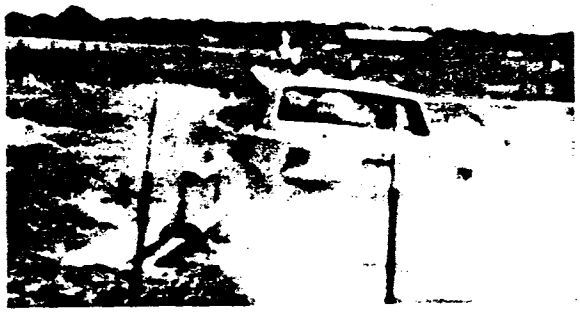

t = 0.213 sec

t = 0.309 sec

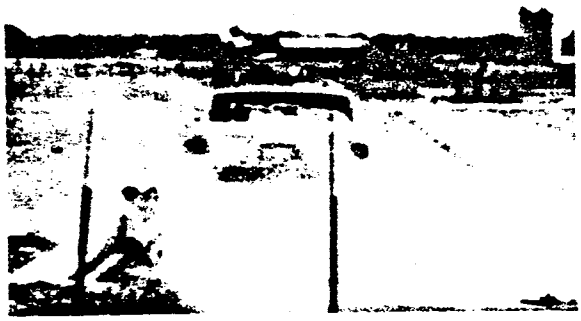

t = 0.382 sec

t = 0.441 sec

t = 0.567 sec

FIGURE 8, SEQUENCE PHOTOGRAPHS OF E-3 BARRIER TEST
(View Parallel To Rail Members)

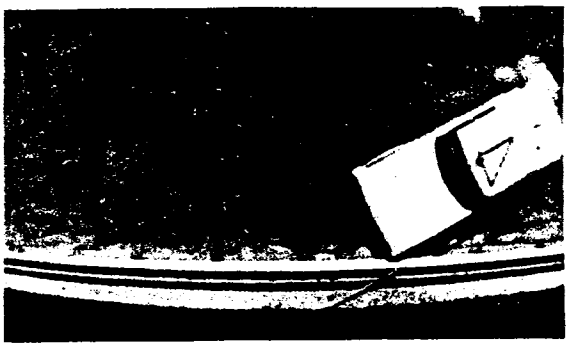

t = -0.010 sec

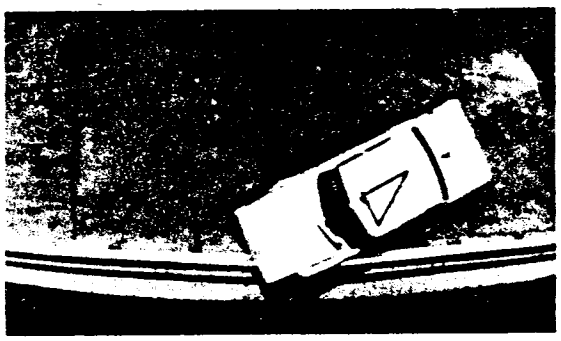

t = 0.066 sec

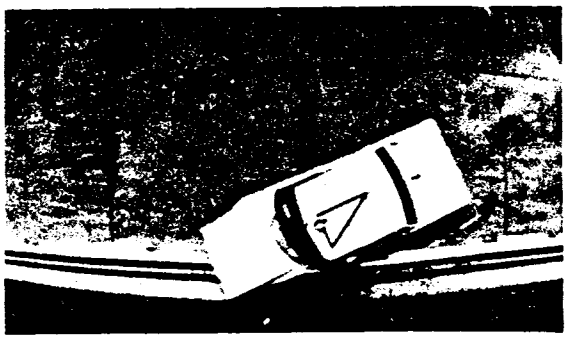

t = 0.139 sec

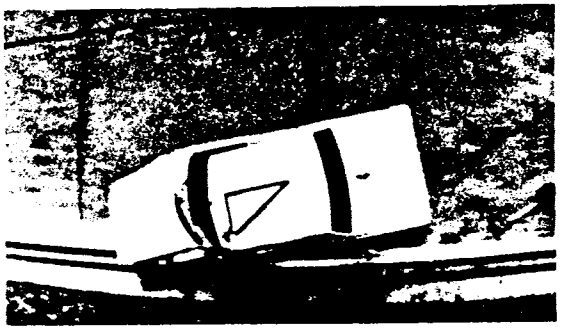

t = 0.230 sec

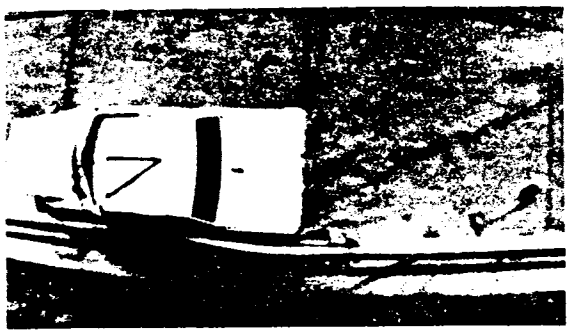

t = 0.345 sec

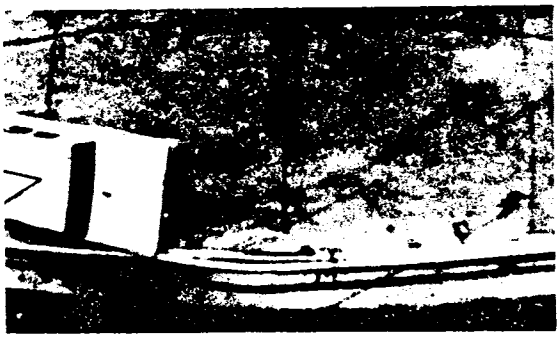

t = 0.485 sec

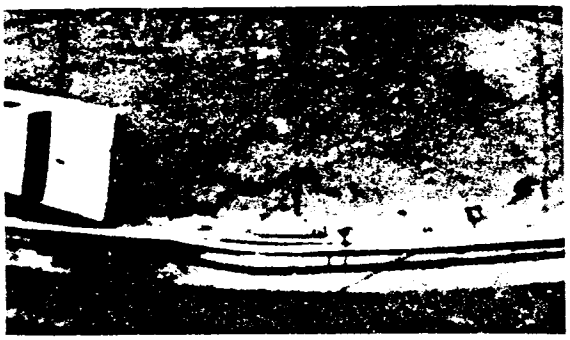

t = 0.578 sec

FIGURE 9, SEQUENCE PHOTOGRAPHS OF E-3 BARRIER TEST
(Overhead View)

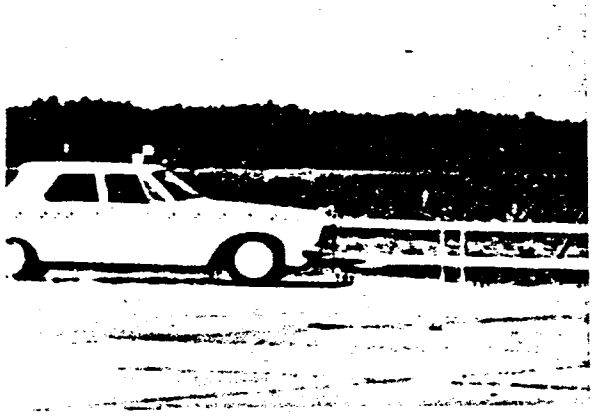

t= -0.022 sec

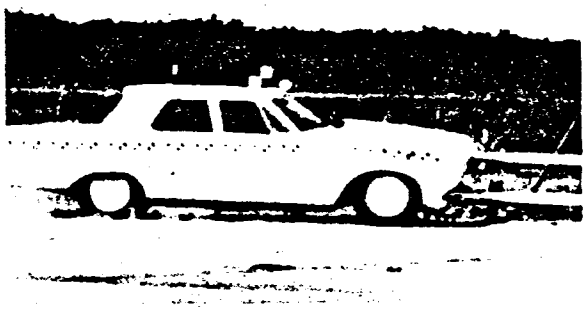

t = 0.057 sec

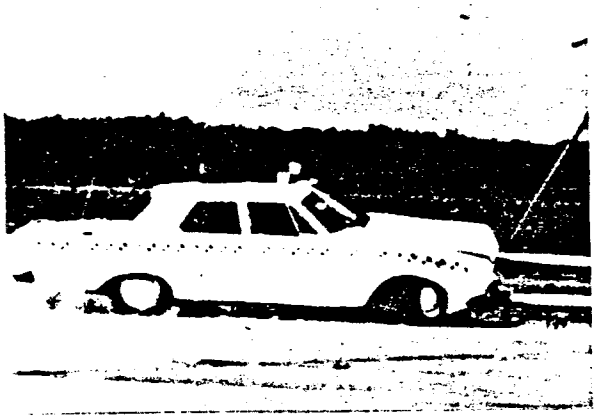

t = 0.095 sec

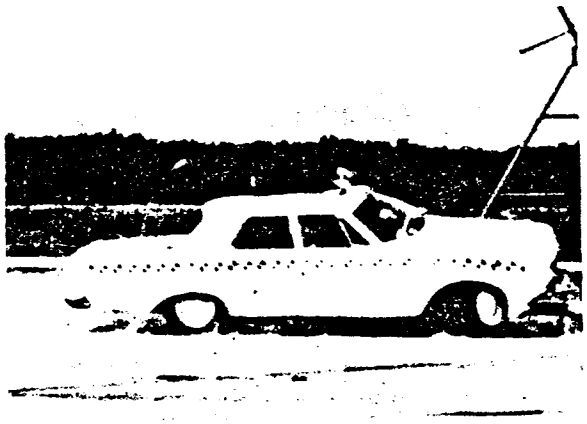

t = 0.160 sec

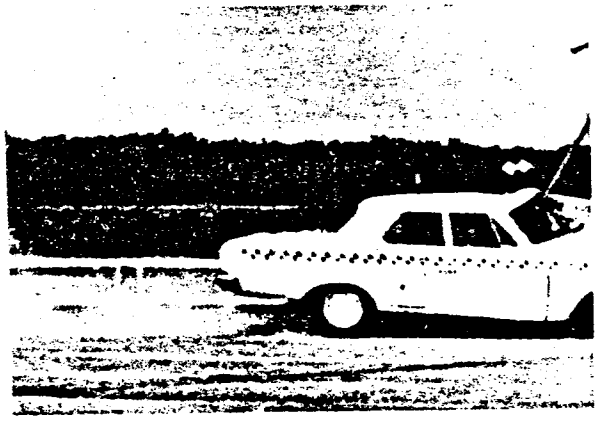

t = 0.244 sec

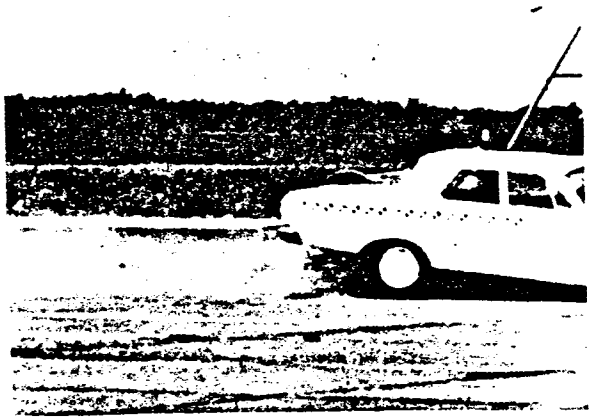

t = 0.339 sec

FIGURE 10, SEQUENCE PHOTOGRAPHS OF E-3 BARRIER TEST
(View Perpendicular To Initial Path of
Vehicle Prior to Impact)

FIGURE 11, VEHICLE AFTER E-3 BARRIER TEST.

MBGF Median Barrier Test

The MBGF Median Barrier test was conducted at an impact speed of 57.3 mph and an impact angle of 25 degrees using a standard size 1963 Plymouth weighing 3,640 lbs., with instrumentation and dummy. The point of impact was near a support post as shown by the location of the vehicle control cable in the photographic views of the barrier before testing in Figure 12.

Sequential photographs of the vehicle collision and its redirection are shown in Figures 13 and 14 from two camera positions. And, a summary of the test results from an analysis of the film data and accelerometer traces are presented in Table 1.

The longitudinal accelerometer traces on the right and left frame of the vehicle in Figures 40 and 41 (see appendix) indicate that the snagging on the weak breakaway posts was not of any great concern. The peak longitudinal acceleration was 12.8 G's.

As indicated in Table 1, the change in heading speed of the vehicle during redirection was 25 mph; the departure angle from the barrier was 20 degrees; and, the maximum dynamic lateral displacement of the barrier was 1.5 ft.

The departure angle was large due to the side ramping effect resulting from the displacements of the single back-to-back rail member. In any event, the large departure angle would probably not create a hazardous condition to other nearby traffic, because it can be seen in Figure 15 that the severely damaged wheel pulled the vehicle after redirection back toward the barrier.

The effectiveness of the breakaway fillet welded post connection in allowing the posts to displace laterally without pulling the rail member down, and thereby, preventing any tendency of the vehicle to ramp is evident in the photographs of the damaged barrier in Figure 15.

It can be seen in Figure 15 that the MBGF barrier remained intact under the severe imposed test conditions. Maintenance would essentially require the replacement of three posts and one 25 ft. length section of the two back-to-back W-beam guardrails. It appears that the damaged barrier would, prior to repair, be functional under a possible low-angle second collision.

The damaged test vehicle is shown in Figure 16. It can be seen that the damage is less severe than the E-3 barrier test vehicle. The left front quarter is severely damaged, but the windshield remained intact and the passenger compartment area is not warped.

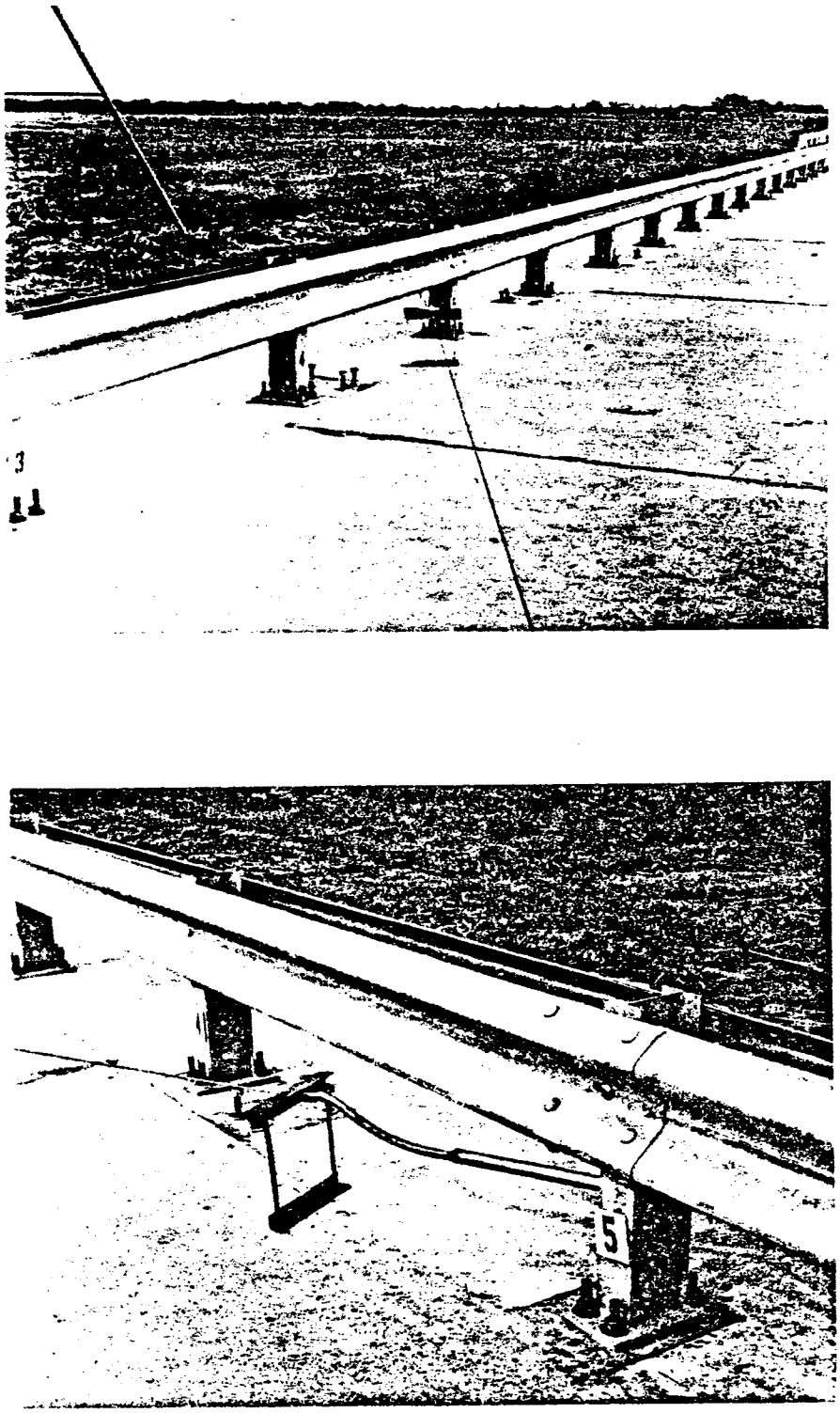

FIGURE 12, VIEWS OF MBGF BARRIER BEFORE TEST.

t = 0.000 sec

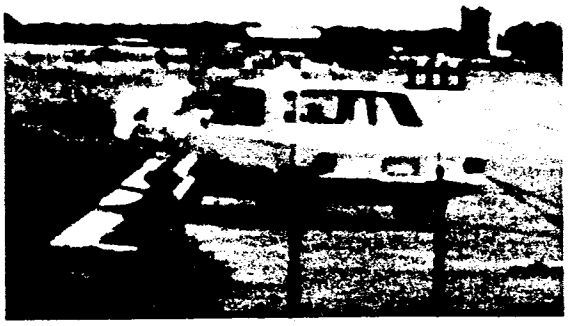

t = 0.079 sec

t = 0.123 sec

t = 0.198 sec

t = 0.277 sec

t = 0.358 sec

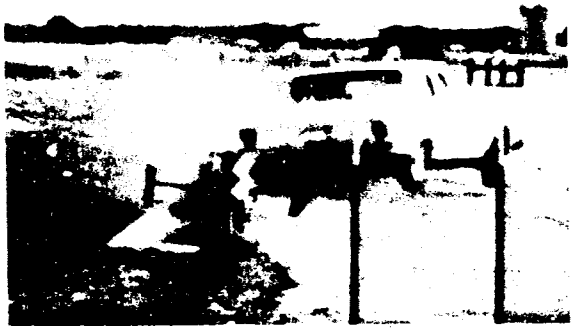

t = 0.512 sec

t = 0.664 sec

FIGURE 13, SEQUENCE PHOTOGRAPHS OF MBGF BARRIER TEST.
(View Parallel To Rail Member)

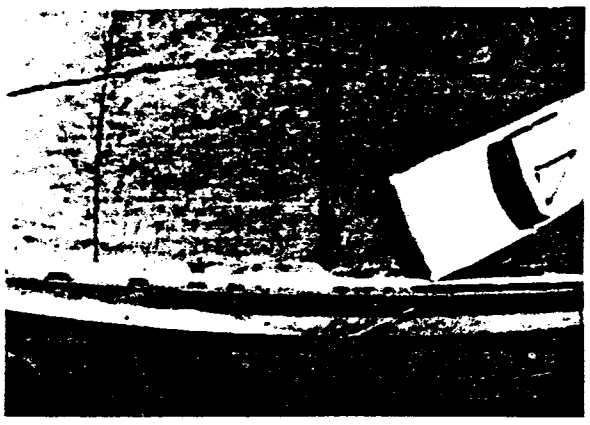

t = 0.000 sec

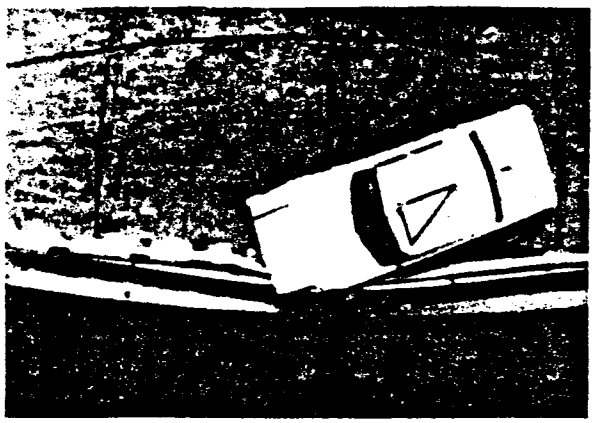

t = 0.101 sec

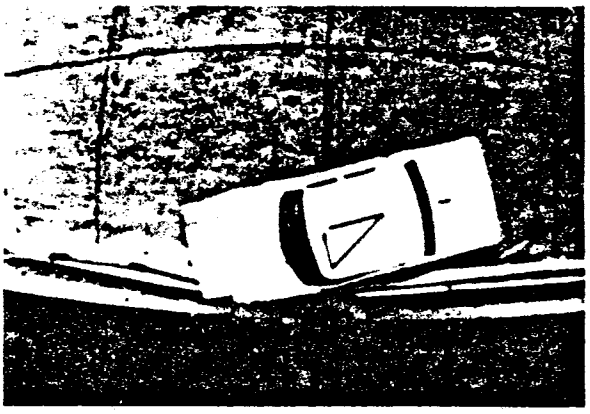

t = 0.155 sec

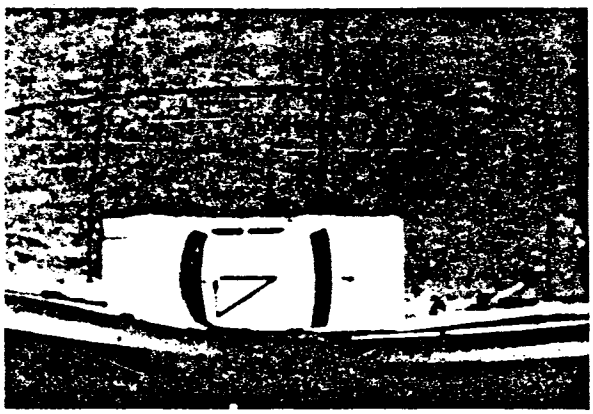

t = 0.239 sec

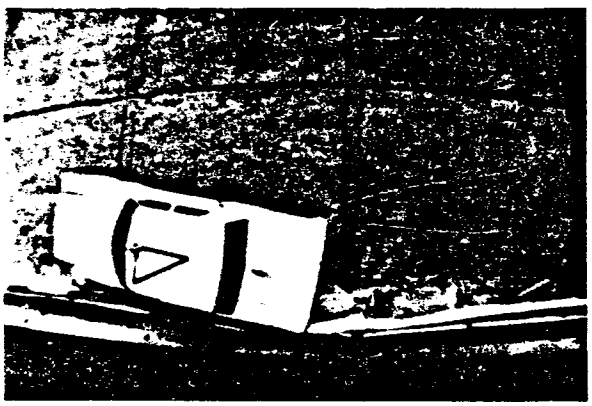

t = 0.352 sec

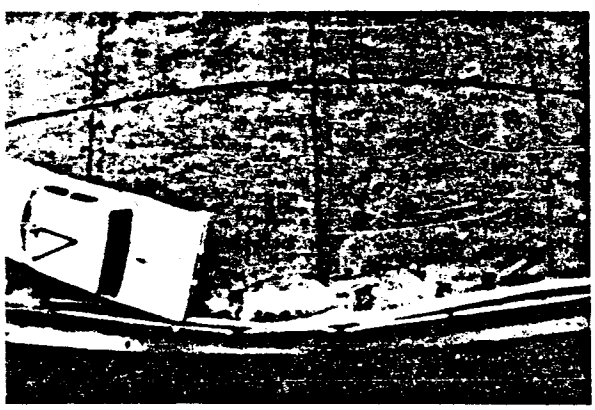

t = 0.457 sec

FIGURE 14, SEQUENCE PHOTOGRAPHS OF MBGF BARRIER TEST.
(Overhead View)

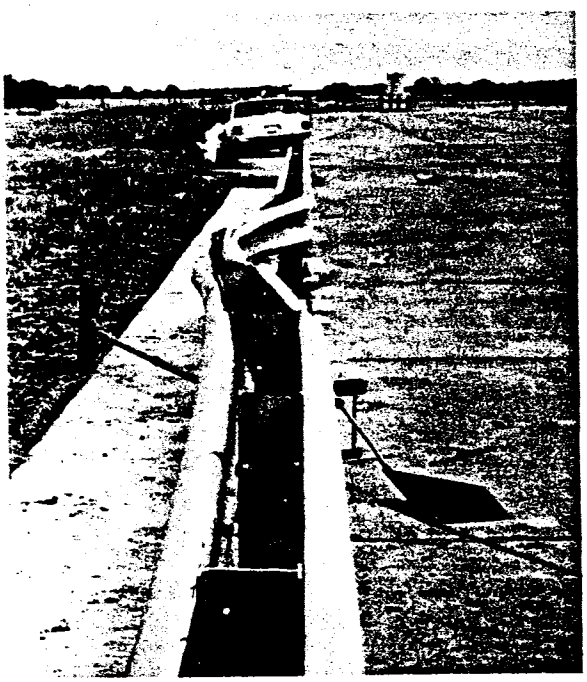

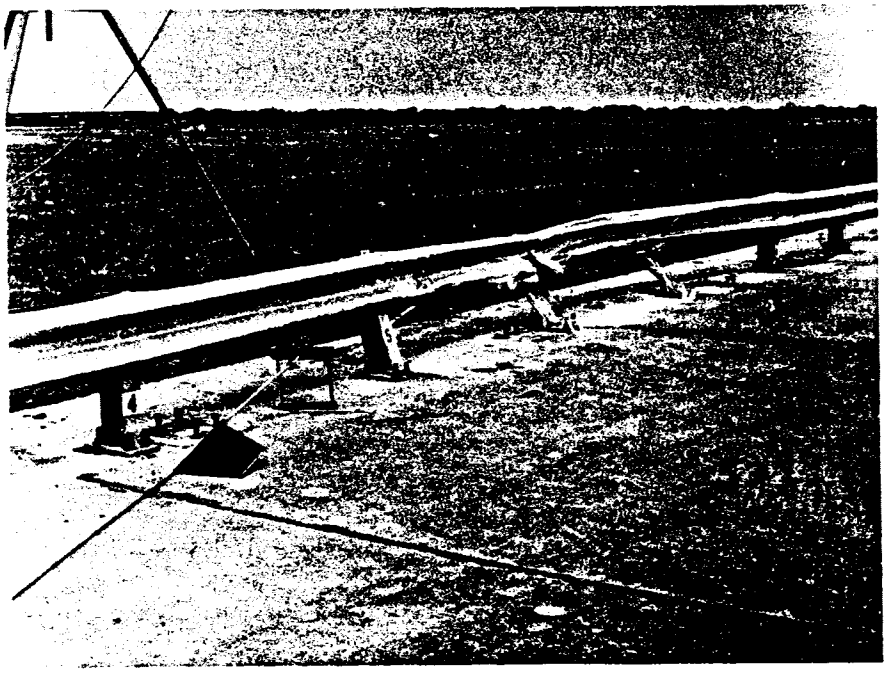

FIGURE 15, DAMAGE TO MBGF BARRIER.

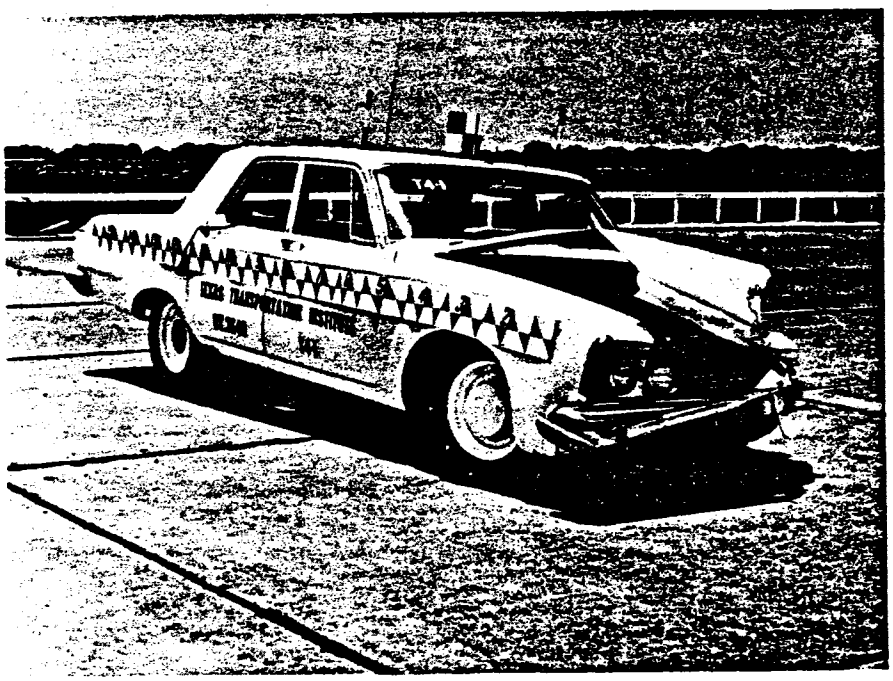

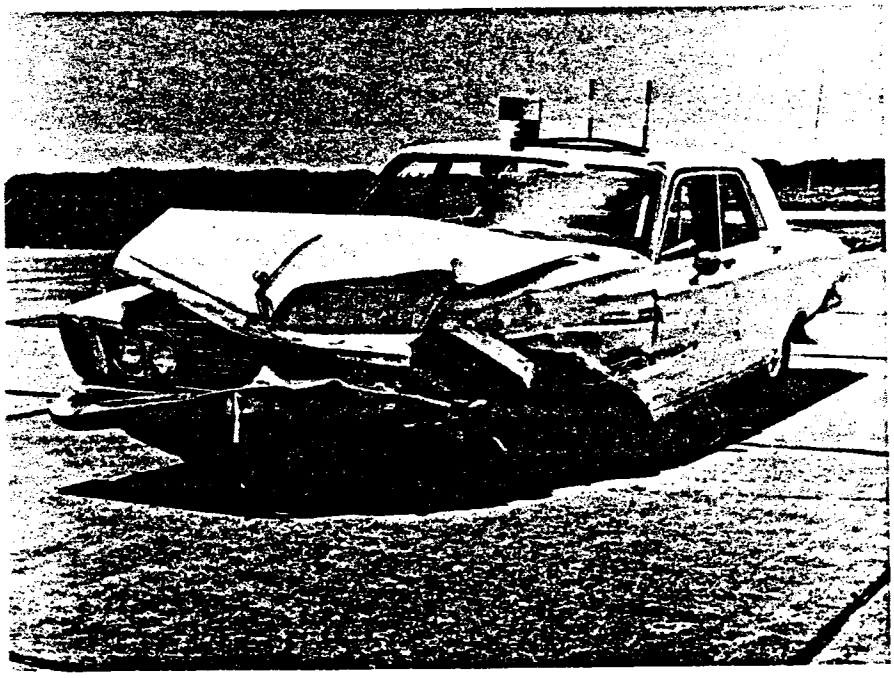

FIGURE 16, VEHICLE AFTER MBGF BARRIER TEST.

Concrete Median Barrier Test CMB-1

The first rigid concrete median barrier test, designated CMB-1, was conducted to determine if a standard size 4,000 lb. vehicle would snag and knock down the luminaire pole mounted on top of the barrier under the impact conditions of about 60 mph and 25 degrees. The centerline of the vehicle was directed at the center of the luminaire support, thus placing the initial contact point of the left front fender with the median barrier approximately 9 ft. upstream from the luminaire pole position. Photographs of the barrier and vehicle before the crash are shown in Figures 17 and 18.

Initially, the left front fender was crushed; then, as the vehicle was redirected, it rode partially up the side of the barrier lightly scraping the attached fence and luminaire pole. When the vehicle lost contact with the barrier, it was airborne until landing on the edge of the right front tire as shown in the sequential photographs in Figures 19 and 20. The vehicle took two more severe bounces, alternately lifting the front and back ends of the vehicle off the ground. The severely damaged left front quarter and wheel of the vehicle caused it to swerve back toward the barrier. The final position of the vehicle was approximately 155 ft. downstream of the initial point of impact and it was facing back toward the point of impact.

A summary of the test data based on an analysis of the high speed film and accelerometer traces is shown in Table 2. The change in heading speed during redirection was 15 mph; the average lateral vehicle deceleration was 8.0 G's; and, the departure angle from the barrier was 7

degrees.

The damaged vehicle is shown in Figure 18. As can be seen the front quarter and wheel were severely damaged, the door on the driver's side was sprung open, and the windshield was cracked.

TABLE 2

SUMMARY OF TEST DATA FOR CMB TESTS

DATA	BARRIER TEST			
	CMB-1	CMB-2	CMB-3	CMB-4
VEHICLE				
Year	1963	1964	1963	1963
Make	Plymouth	Chevrolet	Chevrolet	Chevrolet
W, Weight (lbs)	4000	4230	4210	4210
θ, Impact Angle (deg)	25	25	7	15
FILM DATA				
V_I, Initial Impact Speed (mph)	62.4	55.7	60.9	60.7
V_P, Speed at Parallel (mph)	47.2	--	58.8	50.5
S_{long}, Longitudinal Distance to Parallel (ft)	15.3	--	17.6	23.0
D, Dynamic Barrier Deceleration (ft)	0.0	0.0	0.0	0.0
S_{lat}, Lateral Distance to Parallel (ft)	2.9	2.9	0.85	1.74
Δt, Time to Parallel (sec)	0.223	0.320	0.206	0.298
a. G_{long}, Average Longitudinal Deceleration (G's) (Parallel to Barrier)	2.0	--	0.4	1.3
b. G_{lat}, Average Lateral Deceleration (G's) (Normal to Barrier)	8.0	6.4	2.2	4.7
Departure Angle (deg)	7.3	6.0	6.5	11.5
ACCELEROMETER DATA				
Longitudinal Deceleration (G's) (parallel to long. axis of vehicle)				
Maximum	8.7	10.3	8.4	7.8
Average	3.2	1.8	0.5	1.4
Time (sec)	0.184	0.271	0.325	0.244
Transverse Deceleration (G's) (normal to long. axis of vehicle)				
Maximum	16.1	13.3	29.2	14.0
Average	4.4	2.8	1.8	3.0
Time (sec)	0.254	0.280	0.282	0.264

a and b -- see Table 1.

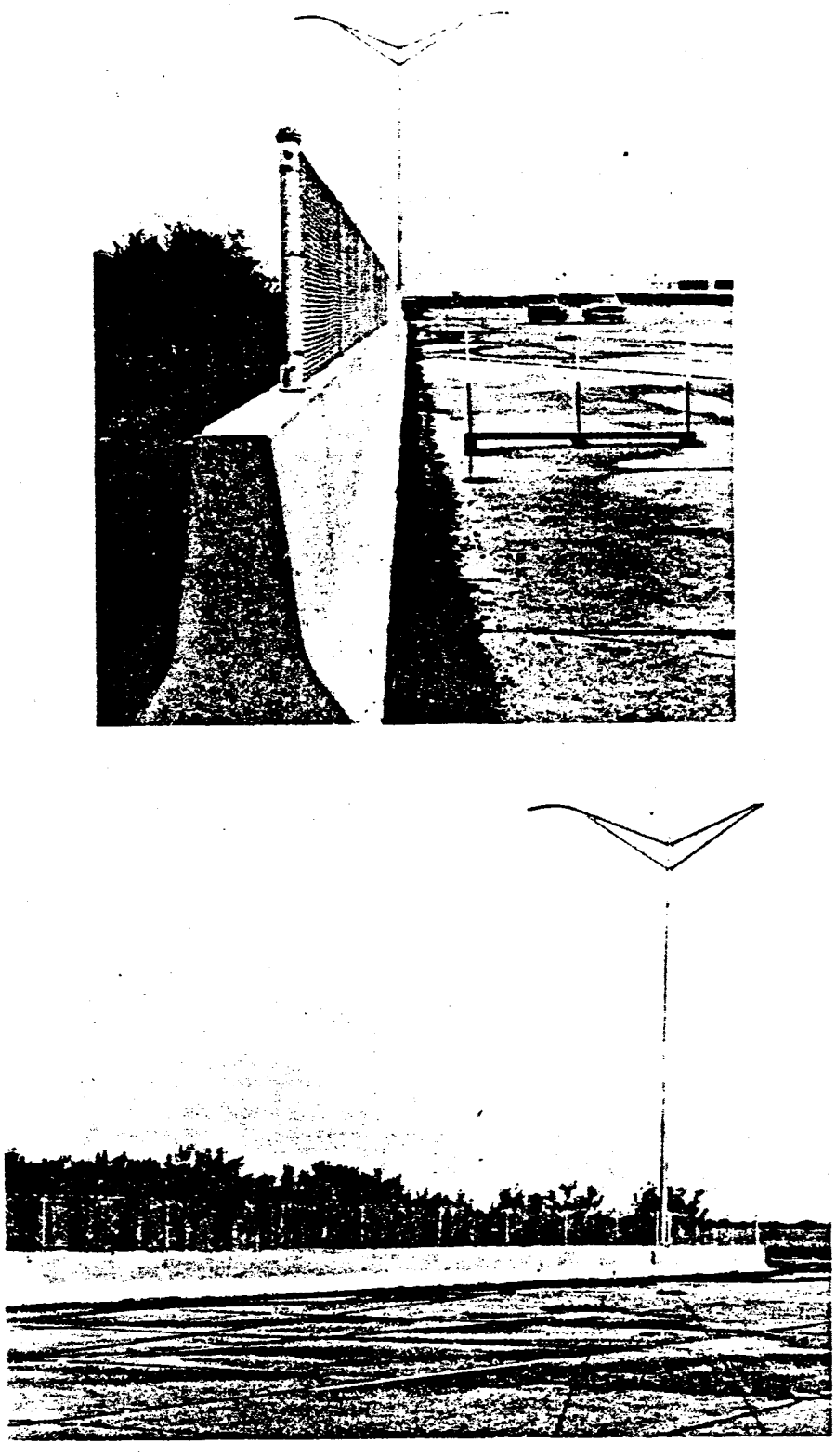

FIGURE 17. CONCRETE MEDIAN BARRIER BEFORE TEST CMB-1.

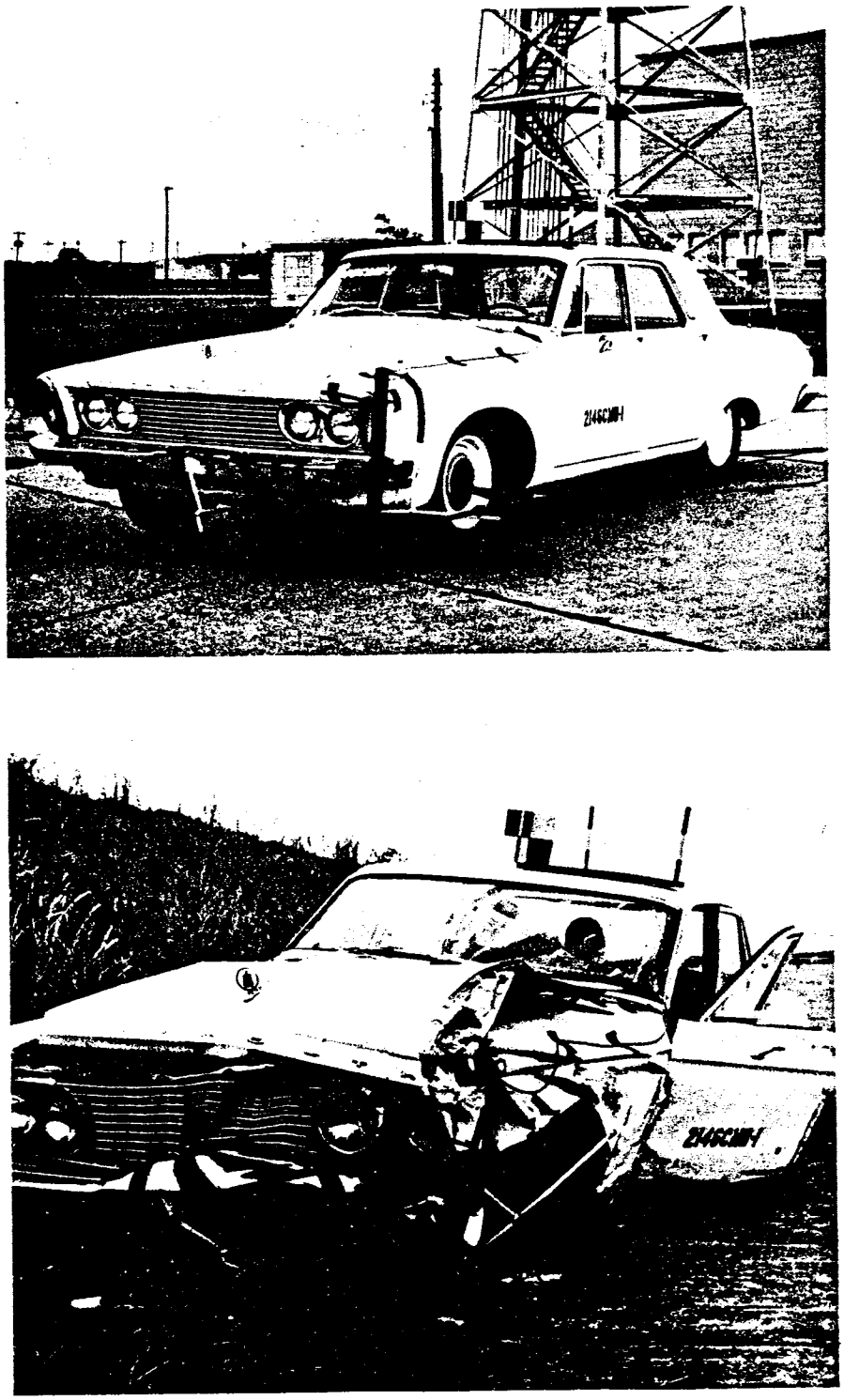

FIGURE 18. VEHICLE BEFORE AND AFTER TEST CMB-1.

t = 0.000 sec

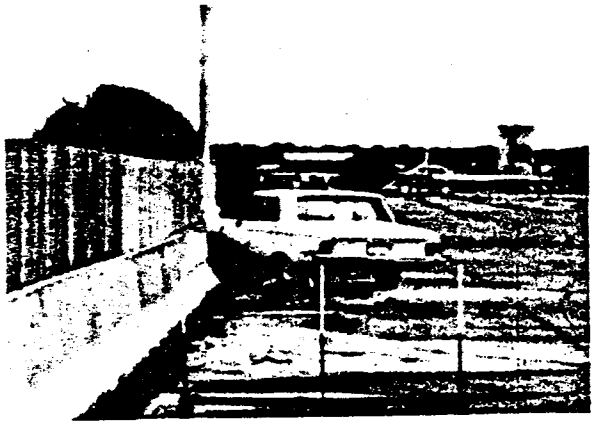

t = 0.040 sec

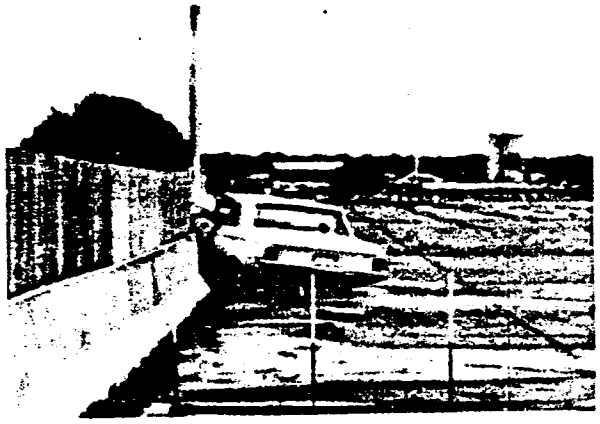

t = 0.094 sec

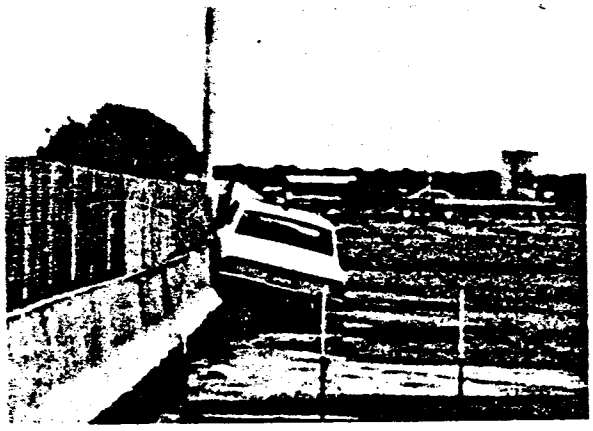

t = 0.169 sec

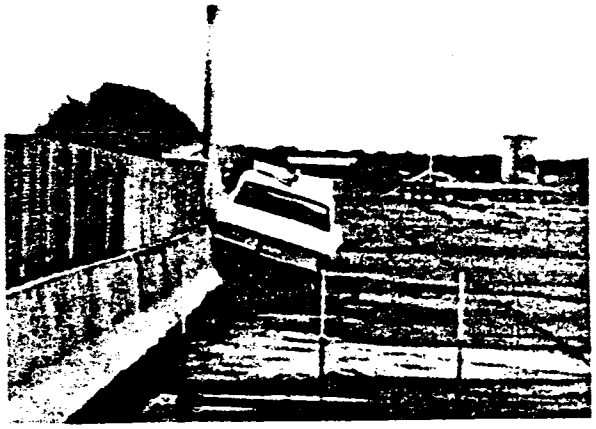

t = 0.223 sec

FIGURE 19. SEQUENCE PHOTOGRAPHS OF TEST CMB-1.
(View Parallel To Concrete Median Barrier)
(Continued)

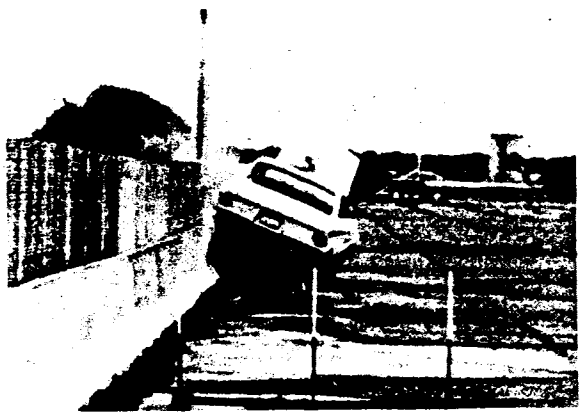

t = 0.341 sec

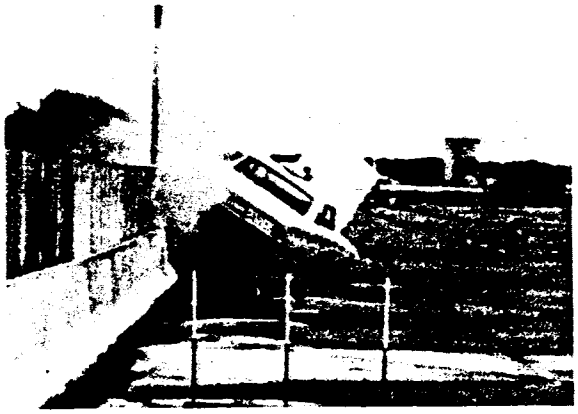

t = 0.587 sec

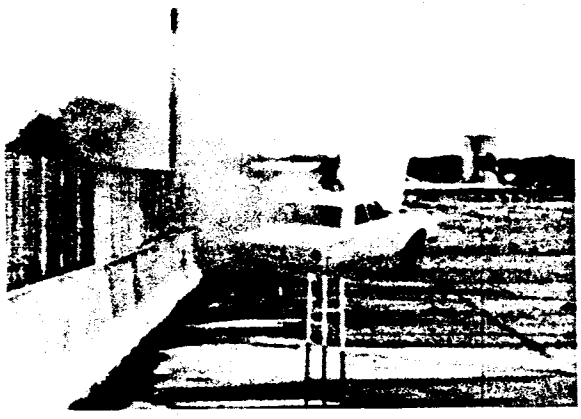

t = 0.954 sec

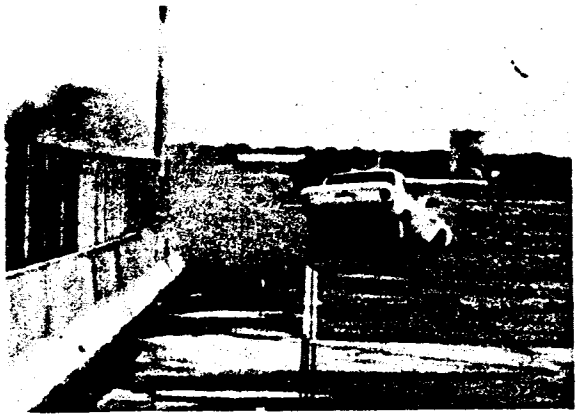

t = 1.396 sec

t = 1.990 sec

FIGURE 19. (Concluded)

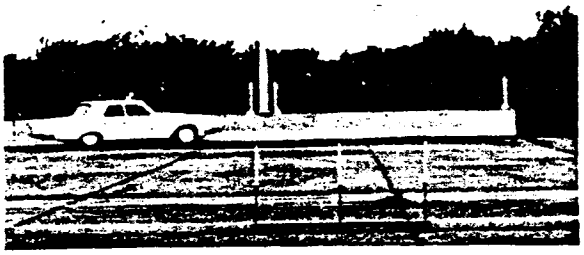

t = 0.000 sec

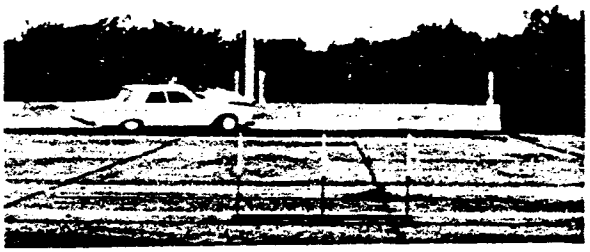

t = 0.067 sec

t = 0.138 sec

t = 0.223 sec

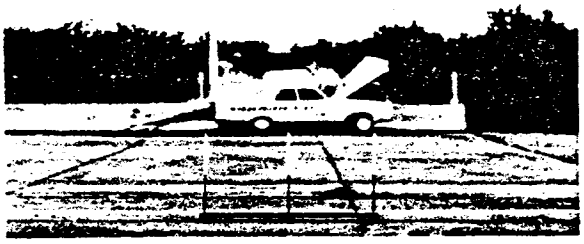

t = 0.302 sec

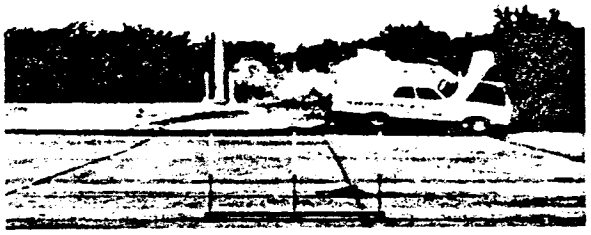

t = 0.456 sec

t = 0.631 sec

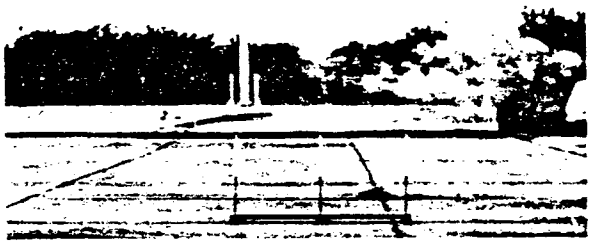

t = 0.742 sec

FIGURE 20. SEQUENCE PHOTOGRAPHS OF TEST CMB-1. (View Perpendicular To Concrete Median Barrier)

Concrete Median Barrier Test CMB-2

This test, designated CMB-2, was conducted to determine if the 150 ft. unanchored section of the CMB barrier, with continuous steel reinforcement, would slide and/or rotate in restraining and redirecting a standard size 4,000 lb. passenger vehicle under the impact conditions of about 60 mph and 25 degrees. Photographs of the barrier and vehicle prior to impact are shown in Figure 21.

The vehicle-barrier interaction in the CMB-2 test was similar to that of the first test, CMB-1. While the vehicle was being redirected, the left front fender was crushed and the vehicle rode up the side of the barrier. The tire marks go all the way up the side of the concrete barrier as can be seen in Figure 24. At loss of contact with the barrier, the right front wheel had already recontacted the pavement. Two more severe bounces followed this, alternately lifting the front and rear of the car off the ground. The drag forces from the severely damaged left front quarter caused the vehicle to swerve back toward the barrier. Sequential photographs of the vehicle collision and redirection are shown in Figure 22.

Strain gages were placed on the backside of the barrier to measure the barrier displacement during the collision. The gage which was placed 2.25 in. above the ground showed a maximum displacement of 0.03 in., while the other gage, placed near the top of the barrier showed a maximum displacement of 0.09 inches.

A summary of the test data based on an analysis of the high speed film and accelerometer traces is shown in Table 2. As can be seen in

Table 2, the average lateral vehicle deceleration in this test of 6.4 G's was smaller than that in previous tests because the impact speed was about 6 mph less. For all practical purposes, the departure angle of 6 degrees in this test was the same as in the previous test.

The damaged vehicle is shown in Figure 23. It can be seen that the 6 mph lower impact speed in this test also resulted in slightly less vehicle damage than that encountered in the previous CMB-1 test. For instance, the door is not sprung open in this test, whereas, in the CMB-1 test the door was sprung open.

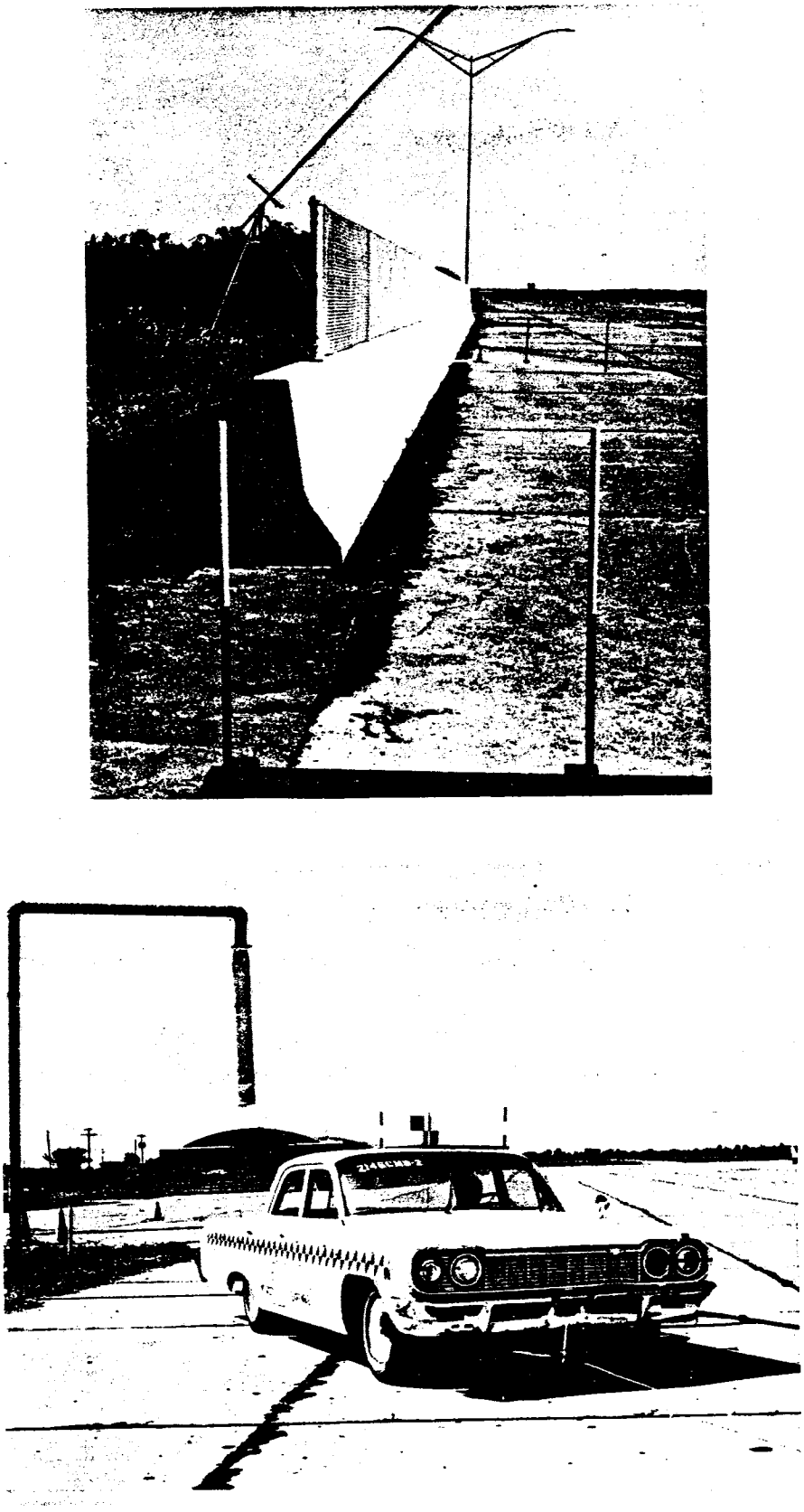

FIGURE 21. CONCRETE MEDIAN BARRIER AND VEHICLE BEFORE TEST CMB-2.

t = 0.000 sec

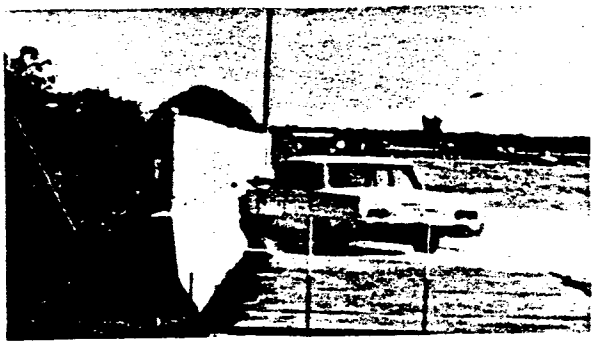

t = 0.033 sec

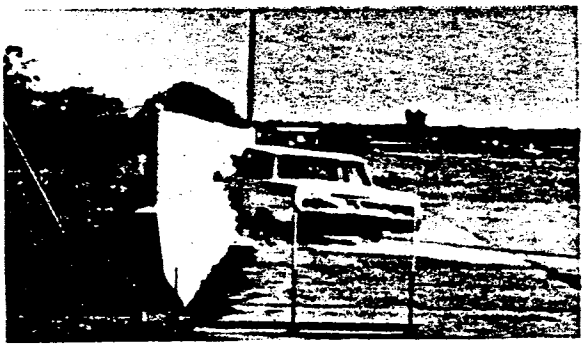

t = 0.099 sec

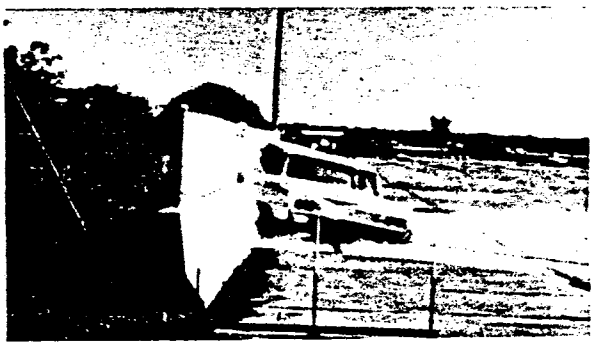

t = 0.144 sec

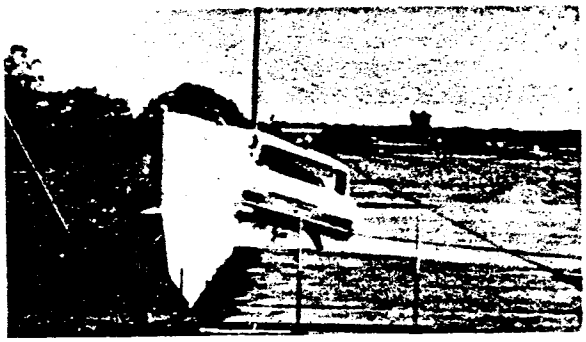

t = 0.207 sec

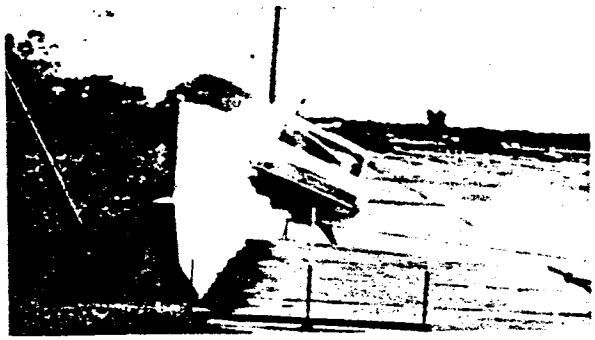

t = 0.320 sec

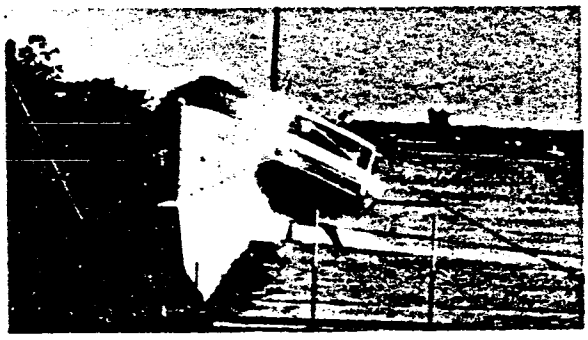

t = 0.390 sec

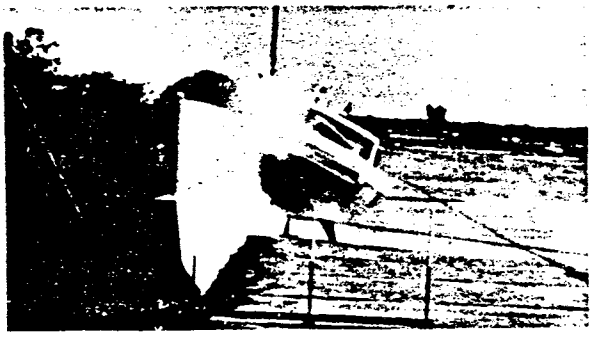

t = 0.450 sec

FIGURE 22. SEQUENCE PHOTOGRAPHS OF TEST CMB-2.
(View Parallel to Concrete Median Barrier)

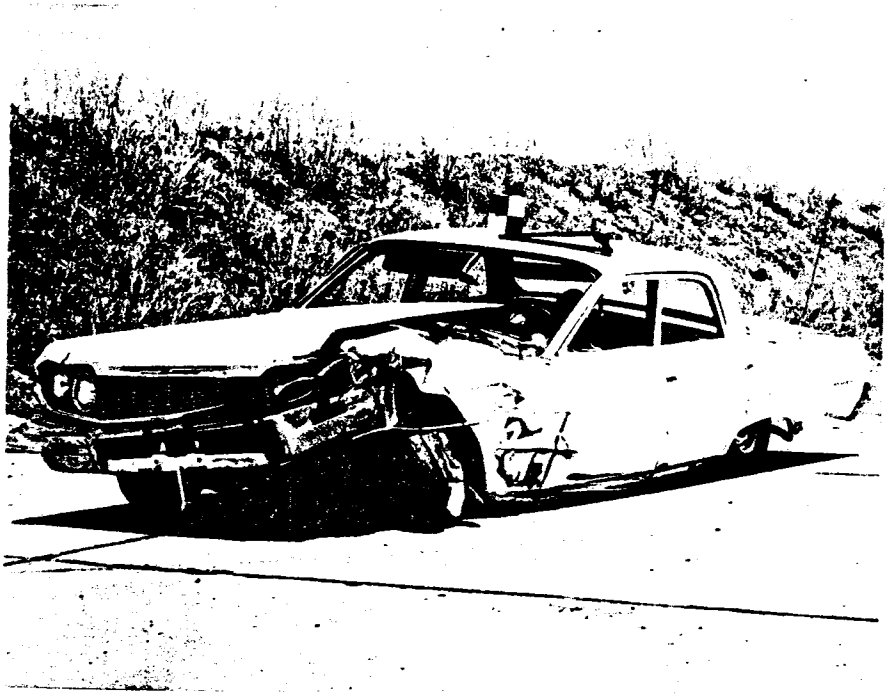

FIGURE 23. VEHICLE AFTER TEST CMB-2.

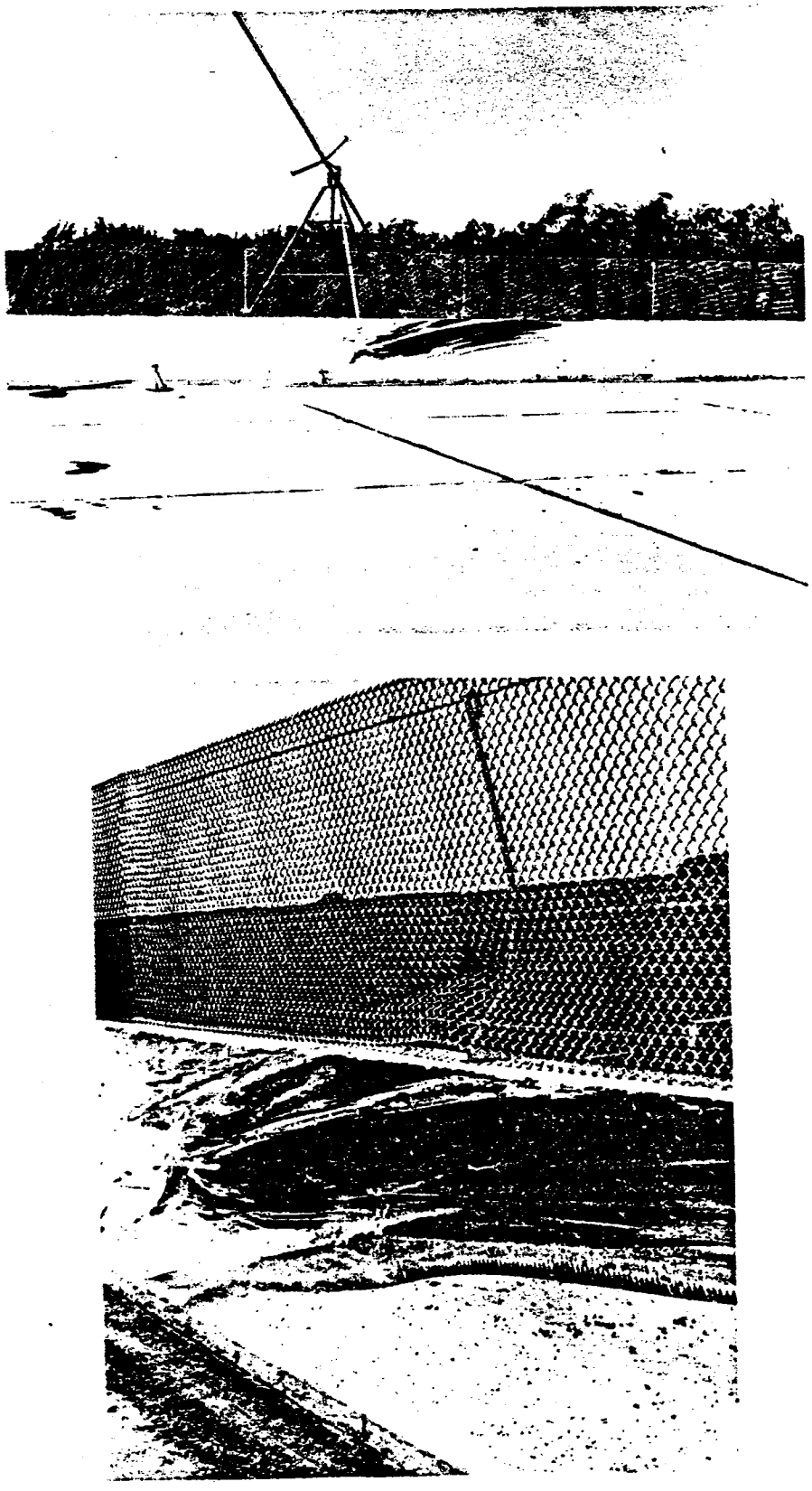

FIGURE 24. DAMAGE TO CONCRETE MEDIAN BARRIER AFTER TEST CMB-2.

Concrete Median Barrier CMB-3

Concrete median barriers with sloping faces are currently being used mostly on urban roadways having narrow medians and carrying a high traffic volume. The majority of the accidents under these conditions usually occur at shallow angles of 15 degrees and less. This test, designated CMB-3, was therefore conducted to evaluate the performance of the barrier in redirecting a 4,000 lb. passenger vehicle under representative inservice impact conditions of about 60 mph and 7 degrees.

This test was again run on the 150 ft. length section of the CMB barrier that was not anchored to the roadway. A photograph of the barrier prior to the test, which shows the tire scrub markings of the previous CMB-2 test run, is shown in Figure 25. And, a photograph of the vehicle prior to the test is shown in Figure 26.

Sequential photographs of the vehicle collision and redirection are shown in Figures 27 and 28. As can be seen by the tire scrub markings in Figure 25, the vehicle quickly climbed up the lower face of the barrier and was redirected when the tire contacted the steeper upper face of the barrier. The maximum height of climb was approximately 18 in. The vehicle lost contact with the barrier after 46 ft. of travel. At a point 72 ft. downstream from the point of impact, the vehicle again recontacted the barrier.

A summary of the test data based on an analysis of the high speed film and accelerometer traces is shown in Table 2. The departure angle was, for all practical purposes, the same as the two previous 25 degree

angle collisions. The change in the vehicle heading speed of 2 mph was much lower than in the 25 degree angle collision because the redirection of the vehicle occurred primarily as the result of an interaction between the vehicle tire and barrier. Also, it can be seen in Table 2 that the average lateral vehicle decelerations of 2.2 G's are very low in comparison to the previous tests.

The damaged test vehicle is shown in Figure 26. The relatively minor damage consisted of bumper and sheet metal crushing.

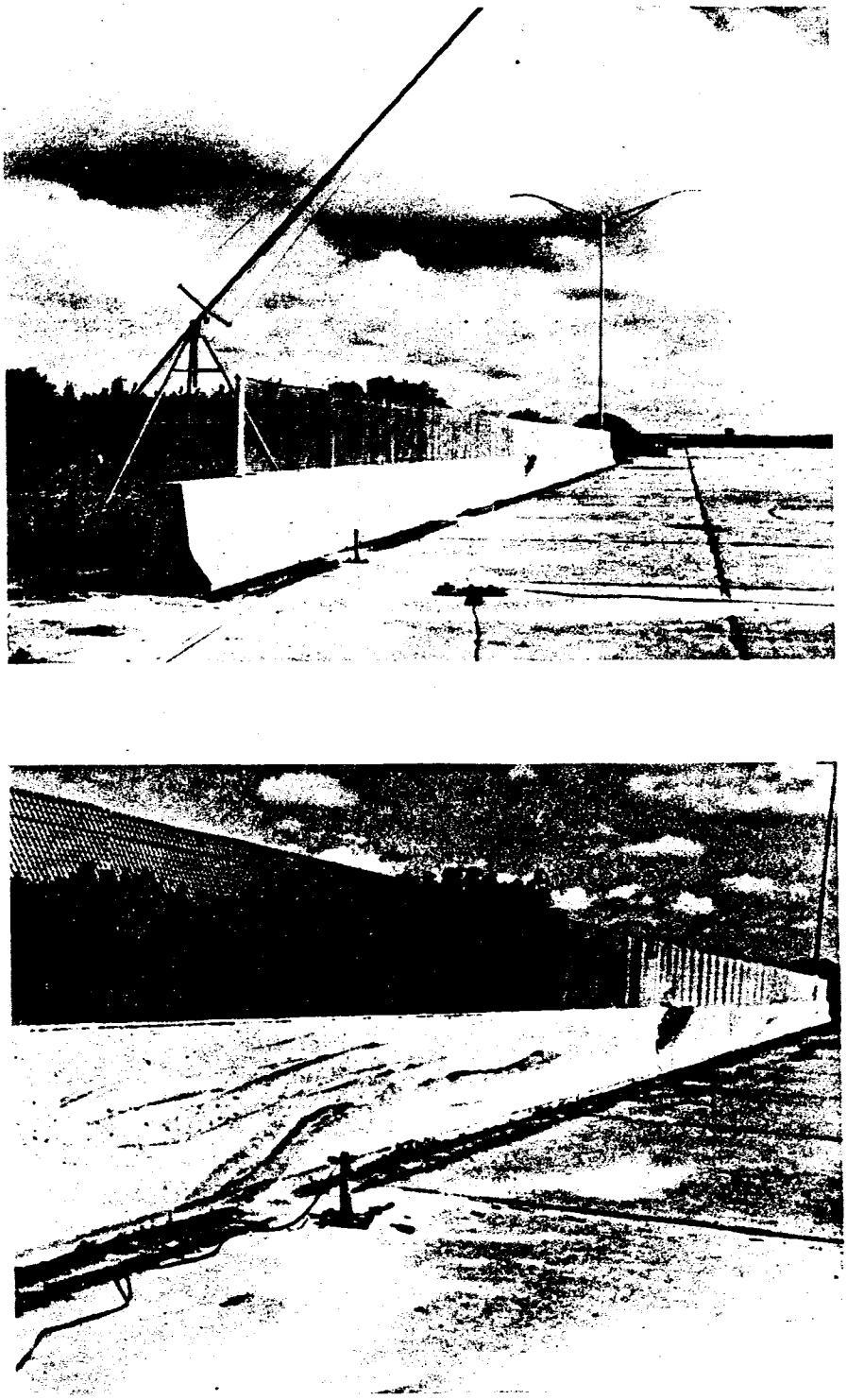

FIGURE 25. CONCRETE MEDIAN BARRIER BEFORE AND AFTER TEST CMB-3. (Darkest Tire Mark is from Test CMB-2.)

FIGURE 26. VEHICLE BEFORE AND AFTER TEST CMB-3.

t = -0.033 sec

t = 0.019 sec

t = 0.057 sec

t = 0.100 sec

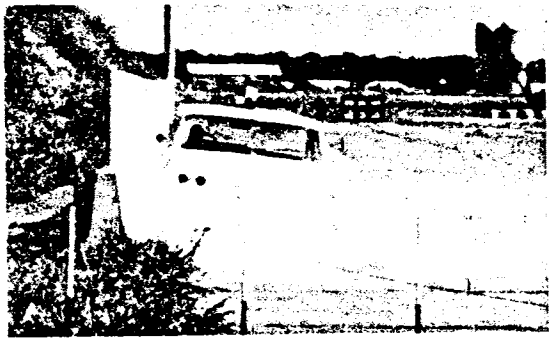

t = 0.112 sec

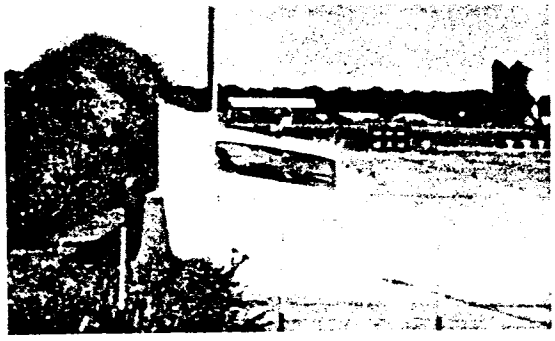

t = 0.150 sec

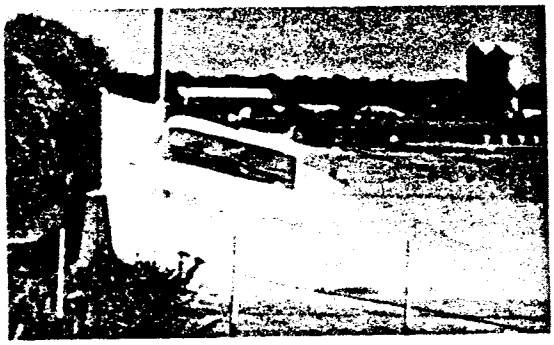

t = 0.211 sec

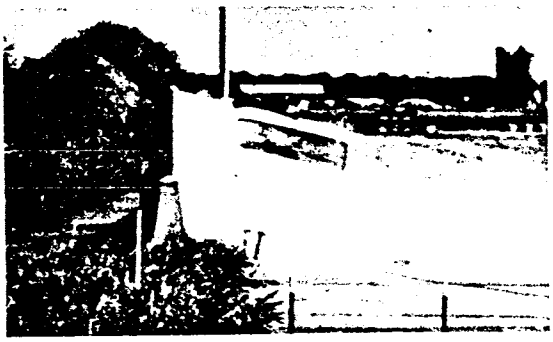

t = 0.242 sec

FIGURE 27. SEQUENCE PHOTOGRAPHS OF TEST CMB-3.
(View Parallel to Concrete Median Barrier)

t = 0.000 sec

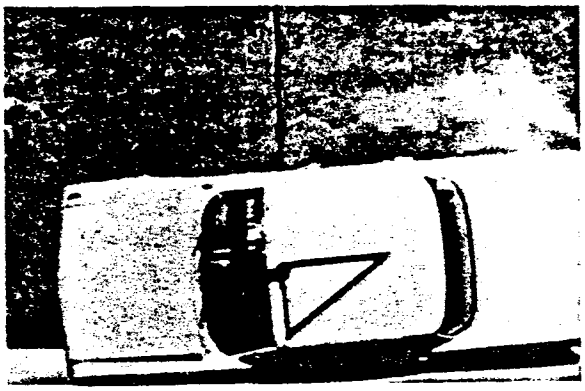

t = 0.101 sec

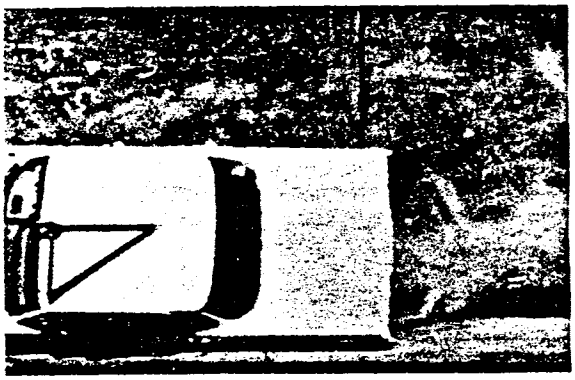

t = 0.207 sec

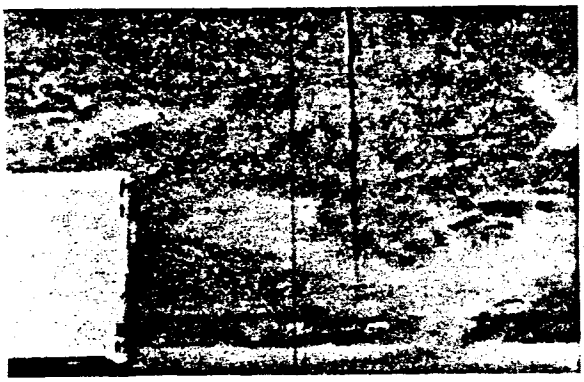

t = 0.304 sec

FIGURE 28. SEQUENCE PHOTOGRAPHS OF TEST CMB-3.
(Overhead View)

Concrete Median Barrier Test CMB-4

This test, designated CMB-4, was conducted to determine the performance of the barrier in redirecting a 4,000 lb. passenger vehicle under somewhat of an upper bound on inservice type collisions of 60 mph and 15 degrees.

The 150 ft. unanchored section of the CMB barrier was used. A photograph of the barrier prior to the test, which shows the tire scrub markings of the two previous CMB-2 and CMB-3 test runs, is shown in Figure 29.

Sequential photographs of the vehicle collision and redirection are shown in Figures 31 and 32. The sequential photographs and the photograph of the tire scrub markings in Figure 29 show that the vehicle climbed all the way to the top of the barrier. Sheet metal contact caused relatively minor damage to the fence as can be seen in Figure 29. After losing contact with the barrier, the vehicle took two more severe bounces, alternately lifting the right side and the back end off the ground.

A summary of the test data based on an analysis of the high speed film and accelerometer traces is shown in Table 2. For some unknown reason, the change in the vehicle heading speed of 11 mph was roughly double the speed of the previous CMB-1 test which was run at a much larger impact angle, and hence, probably developed greater sheet metal friction forces. However, the greater change in heading speed could be the reason for the departure angle of 12 degrees also being roughly double the angles in previous test runs. In any event, it appears that this larger departure angle would most likely not create any hazardous situation to other nearby

vehicles because the drag forces of the damaged front wheel pulled the vehicle back toward the barrier as can be seen in Figure 29.

The damaged vehicle is shown in Figure 30. The damage to the vehicle in this test was somewhat less than the damaged vehicles in the previous CMB-1 and CMB-2 tests which were run at larger impact angles.

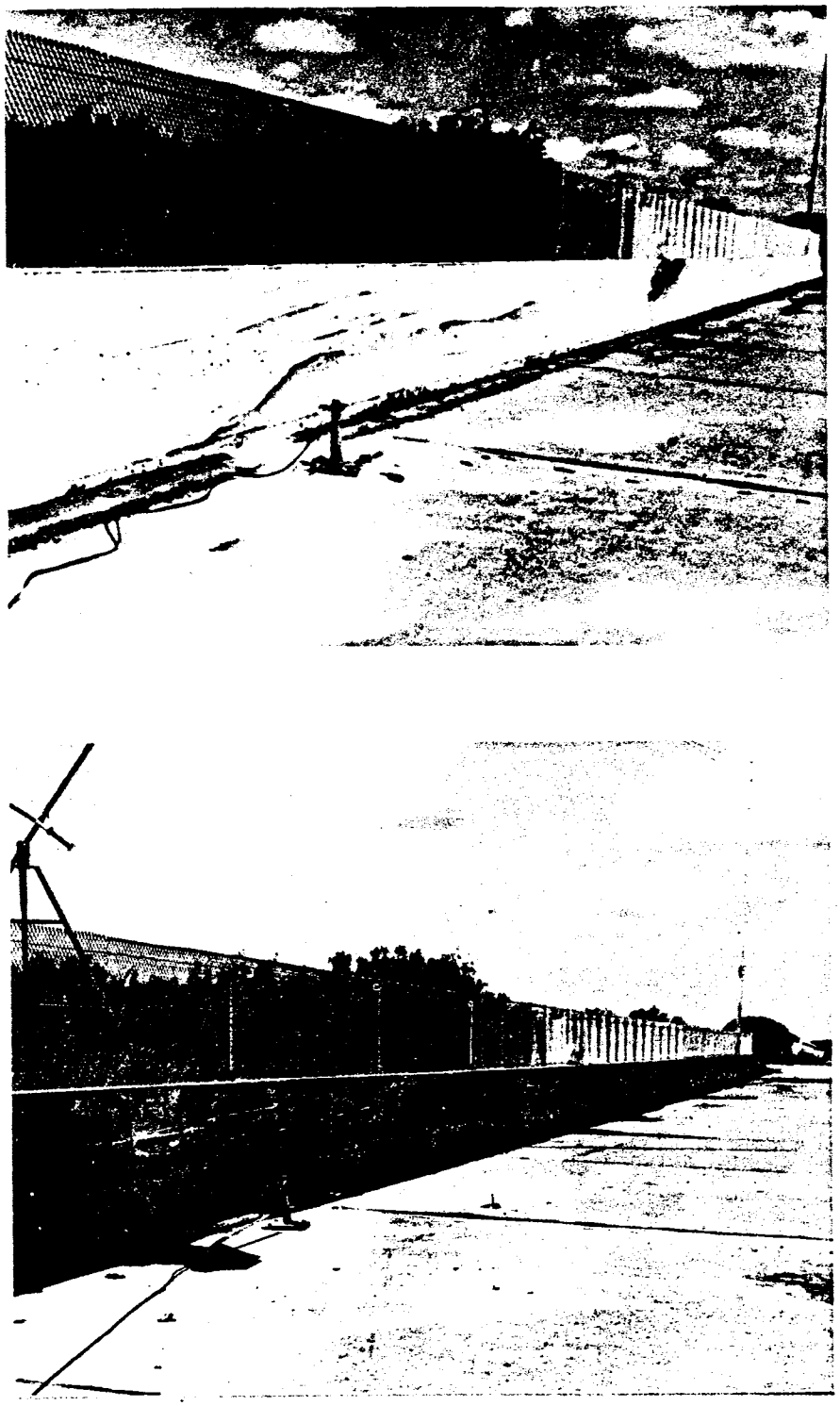

FIGURE 29. CONCRETE MEDIAN BARRIER BEFORE AND AFTER TEST CMB-4.

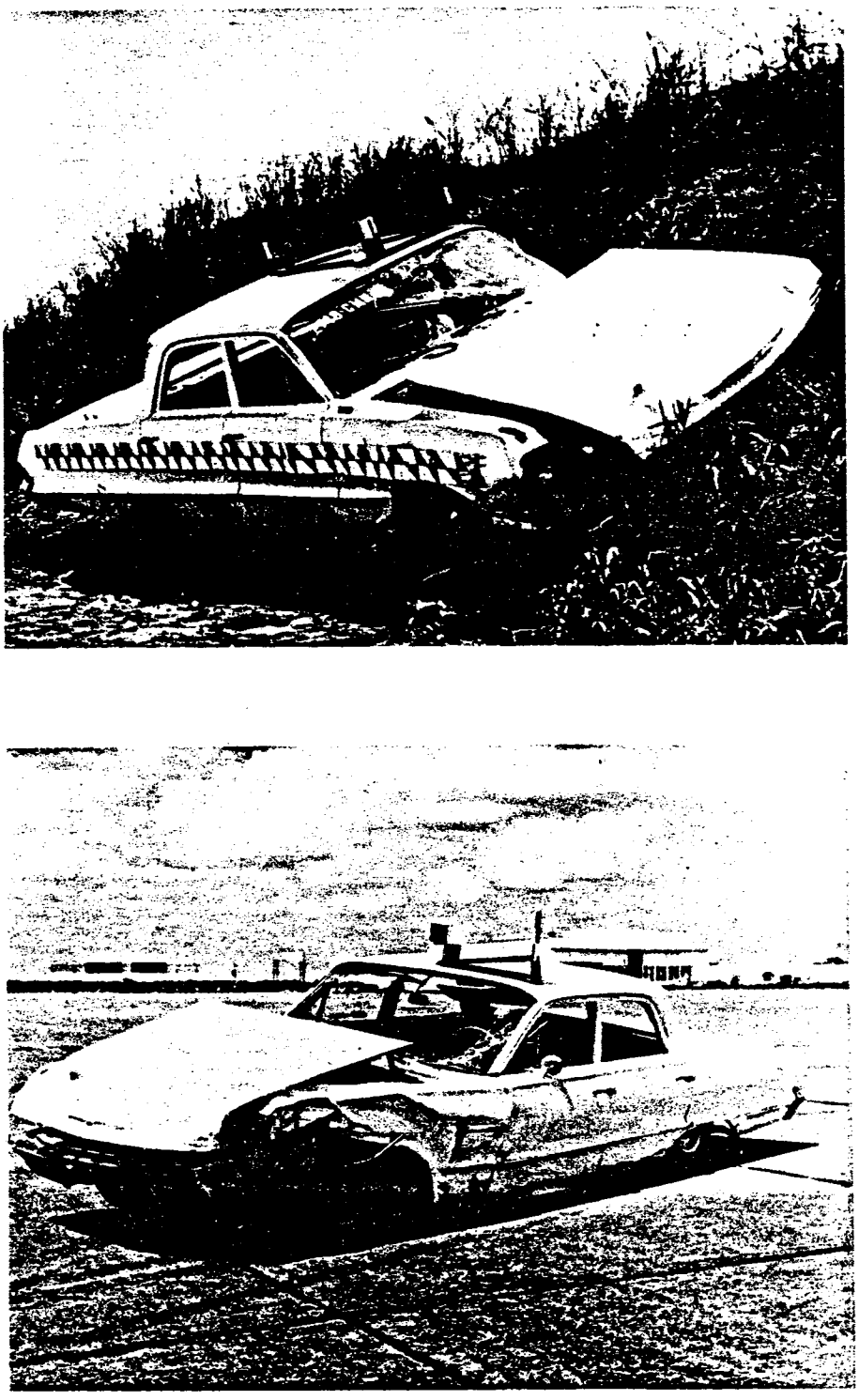

FIGURE 30. VEHICLE DAMAGE AFTER TEST CMB-4.

t = -0.010 sec

t = 0.023 sec

t = 0.077 sec

t = 0.128 sec

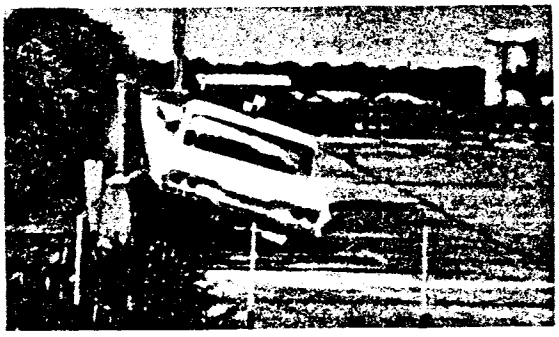

t = 0.176 sec

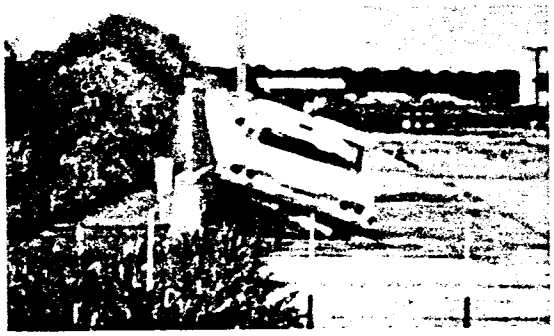

t = 0.199 sec

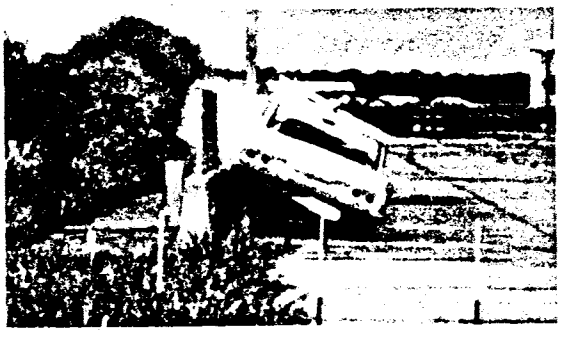

t = 0.273 sec

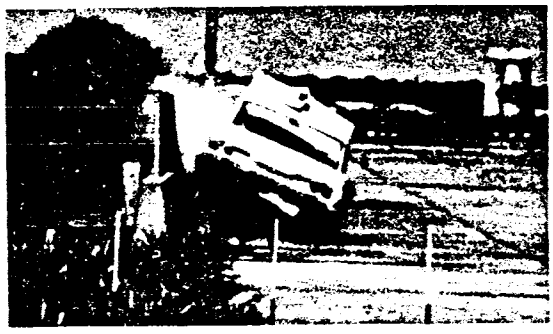

t = 0.327 sec

FIGURE 31. SEQUENCE PHOTOGRAPHS OF TEST CMB-4.
(View Parallel to Concrete Median Barrier)

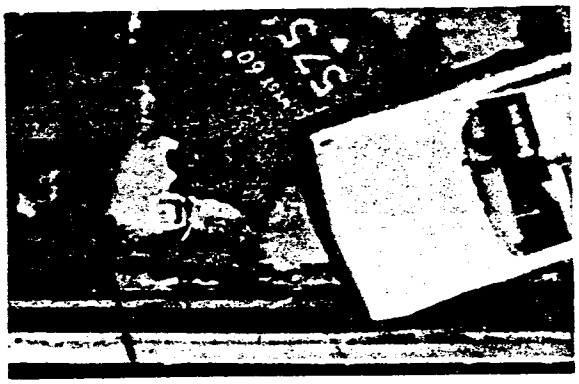

t = 0.000 sec

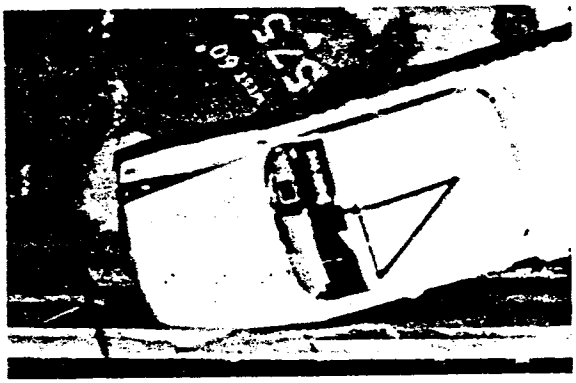

t = 0.079 sec

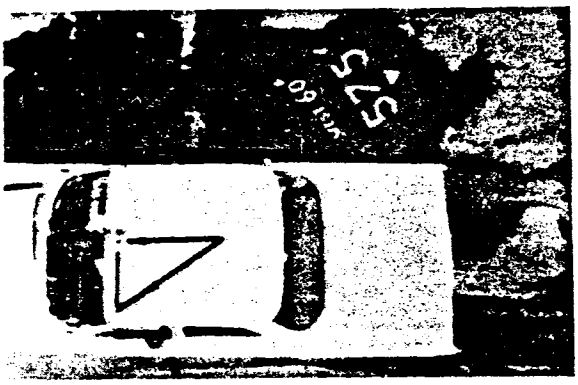

t = 0.225 sec

t = 0.298 sec

FIGURE 32. SEQUENCE PHOTOGRAPHS OF TEST CMB-4.
(Overhead View)

IV. INJURY SEVERITY

Vehicle damage and vehicle accelerations appear to be, at the present time, good indicators of the severity of occupant injury. Michalski (3) of the National Safety Council recently established from a statistical analysis of accident information a relationship between type of collision, vehicle damage, and the percentage of vehicles in which injuries occurred to unrestrained occupants. Shortly thereafter, Olson (4) in NCHRP 86 extended the work of Michalski (3) to include the average decelerations of vehicles involved in head-on collisions with roadside fixtures and angle collisions with traffic barriers. The combined efforts of Michalski (3) and Olson (4) are shown in Figure 33 for angle impacts. The equations relating the variables in Figure 33 are:

$$G_{lat} = \frac{V_I^2 \sin^2 \theta}{2g\{AL \sin\theta - B(1-\cos\theta) + D\}} \qquad (1)$$

...(NCHRP 86 Eq. 5)

$$G_{lat} = 0.204\ R^2 = 10.0\ P \qquad (2)$$

...(NCHRP 86 Eq. 11)

in which

G_{lat} = average lateral deceleration of vehicle normal to barrier from instant of impact to the time the vehicle is parallel to barrier

V_I = vehicle impact speed

θ = vehicle impact angle

AL = distance from front bumper to center-of-mass of vehicle

2B = overall width of vehicle

D = dynamic barrier displacement

R = vehicle damage rating using NSC 7-point photographic guide (Ref. 5)

P = percentage of vehicles in which injuries will occur (occupants unrestrained)

In addition, Michalski (3) determined upon examining only those accidents in which injuries occurred that injury accidents corresponded to a *mean* damage rating of R = 4.73. Referring to Figure 33, this mean damage rating corresponds to a mean average lateral deceleration of about 4.6 G's and a mean probability of injury considering *all* accidents of 46 percent. Probability is used as a shorthand notation for the "percentage of vehicles in which injuries occurred". Since the injury type accidents ranged from minor (not defined by Michalski) to fatalities, it is reasonable to regard the above *mean* values as representing a division between minor and major injuries.

Independently of the above work, a *severity-index* concept was developed by Weaver (6), Ross (7, 8) and Young (9) for predicting the severity of injuries to unrestrained occupants of vehicles involved in median and roadside traversals and rigid traffic barrier collisions. As shown in the equation below, the severity-index takes into consideration the longitudinal, lateral, and vertical acceleration components at the center-of-mass (CM) of the vehicle.

$$SI = \sqrt{\left(\frac{G_{long}}{G_{XL}}\right)^2 + \left(\frac{G_{lat}}{G_{YL}}\right)^2 + \left(\frac{G_{vert}}{G_{ZL}}\right)^2} \qquad (3)$$

in which

G_{long} = longitudinal acceleration of vehicle at CM (parallel to long. axis of vehicle)

G_{lat} = lateral acceleration of vehicle at CM (normal to long. axis of vehicle)

G_{vert} = vertical acceleration of vehicle at CM

G_{XL} = tolerable longitudinal acceleration limit

G_{YL} = tolerable lateral acceleration limit

G_{ZL} = tolerable vertical acceleration limit

The tolerable accelerations used by Ross (7, 8) and Young (9) for *unrestrained* occupants and a time duration of 50 milliseconds were:

$$G_{XL} = 7$$

$$G_{YL} = 5$$

$$G_{ZL} = 6$$

The vehicles' accelerations in Eq. 3 can be measured or computed from the mathematical model (HVOSM) developed by McHenry (10) and modified for specific applications by Young (9, 11).

A severity-index of *unity* and less indicates that an unrestrained occupant will not be seriously injured. The relationship between the *severity-index* concept and the *probability of injury* concept was found by Post and Young (21) to be approximately:

$$P(\%) = 30\ SI \qquad (4)$$

It can be seen from Eq. 4 that the findings of Michalski (3) and Olson (4) differs slightly from the findings of Post and Young (21).

That is, the work of Post and Young (21) indicates that major injuries would occur at a probability of 30 percent, whereas, the work of Michalski (3) and Olson (4) indicates that major injuries would occur at a probability of 46 percent.

The results of Michalski (3) and Olson (4) were based on a statistical analysis of accident information and a rational analytical approach; whereas, the selection of the tolerable acceleration limits in the severity-index equation for unrestrained occupants were extrapolated in a somewhat subjective manner from acceleration limits established by Hyde (13) for a fully restrained vehicle occupant. Rather than attempt to redefine the tolerable acceleration limits to obtain results that would agree with that of Michalski (3) and Olson (4), Post and Young (21) had elected to define a severity-index value of SI = 1.5 as an indicator of major injuries with a probability injury level of 46 percent. An interpretation of the entire range of severity-index values from a low probability of 10 percent (SI = 0.4) to a probability of 100 percent (SI = 3.3) are defined in the CMB barrier report by Post and Young (21).

The available information presented above on probability of injuries and injury severity will now be used to evaluate the full-scale tests on the three median barriers selected by THD.

Predictions on the probability and severity of injuries on the three barriers of different configuration and lateral stiffness are shown in Figure 34. The probability of injury values were computed from Eq. 2 using the average lateral vehicle decelerations in Tables 1 and 2 obtained by an analysis of high speed film. The corresponding severity-index

values were obtained from Eq. 3. It can be seen in Figure 34 that the probability of injury (46%) and severity-index (1.5) were lowest for the semi-rigid MBGF barrier undergoing the largest displacement of 1.5 ft.; whereas, the probability of injury (72%) and severity-index (2.3) were highest for the rigid CMB barrier undergoing negligible displacements. The E-3 barrier, undergoing a lateral displacement of 0.7 ft., had a probability of injury (62%) and severity-index (2.0) in between that of the CMB and MBGF barriers. The comparison of the three barriers in Figure 34 clearly illustrates the desirable effect of barrier displacements in enhancing safety. However, under the severe impact conditions suggested by HRB Circular 482 (1) and used in this study, it can be predicted that major injuries will occur during collisions with the CMB and E-3 barriers, whereas, major injuries may or may not occur during collisions with the MBGF barrier. A small decrease in the lateral stiffness of the MBGF barrier appears desirable from a viewpoint of safety.

Predictions on the probability and severity of injuries associated with *rigid* traffic barriers in general under various conditions of impact speed, impact angle, and vehicle weight are presented for simplicity in one overall view in Figure 35. The probability curves were obtained from Eq.'s 1 and 2. The relationships between the vehicle dimensions in Eq. 1 and vehicle weight were obtained from a recent NCHRP 86 continuation study by Olson (12).

The four full scale test runs on the rigid CMB barrier at different impact speeds and angles are plotted in Figure 35. Knowing the weight

of the test vehicles, one can readily predict the probability of injuries. A comparison of injury probability by three different techniques are shown in Table 3. The probabilities based on test vehicle *damage* were obtained from Eq. 2 using the average damage rating values of nine research engineers in Table 4. The assessment of vehicle damage was based on the 7-point photographic scales developed by the National Safety Council (5). It can be seen in Table 3 that a good comparison exists between the three different prediction techniques. The excellent correlation between the measured and computed techniques indicates that the probability predictions shown in Figure 35 can be extended to any combination of impact speed, impact angle, and vehicle weight.

Before leaving this section on injury severity, a summary on several points of interest in Figure 35 will be presented:

1. A large 5,000 lb. passenger vehicle can strike a rigid barrier at a larger angle than a compact 3,000 lb. vehicle with no difference in injury probability. Interpolation can be used for intermediate weight vehicles.
2. Major injuries will occur under impact conditions exceeding an injury probability of 46 percent and a severity-index of 1.5. For example, major injuries may occur during a rigid barrier redirection of a 4,000 lb. vehicle under the impact conditions of about 60 mph and 17 degrees; to reduce the probability and severity of injury for possible angles of impact greater than 17 degrees, one would need to consider a semi-rigid barrier.

3. A probability injury level of about 20 percent (G_{lat} = 2 from Eq. 2) corresponds to impact conditions in which minor sheet metal damage occurs during collisions with the CMB barrier. Further verification of this fact can be easily obtained by examining the results of tests conducted by California (14, 15). The effectiveness of the CMB barrier beyond this level is similar to that of a vertical concrete barrier.

4. *Live driver* tests lend considerable support to the probability and injury severity predictions of Michalski (3) and Olson (4) in Figure 35. Tests run by Lunstrom (16) on the General Motors (GM) rigid concrete barrier at 50 mph/8 deg. resulted in minor vehicle damage and no driver concern. The GM test conditions in Figure 35 would correspond to a low injury probability of about 15 percent and an injury severity of minor. The tests conducted by the Ontario Department of Highways (19) on the New Jersey concrete median barrier at 10, 20, 30, 40 mph/10 deg. and 20 mph/25 deg. resulted in minor vehicle damage, little driver discomfort, and good driver control of the vehicle both when in contact with the barrier and on exit. The test conditions of Ontario (19) in Figure 35 would correspond to a low probability of about 11 percent and less and an injury severity of minor.

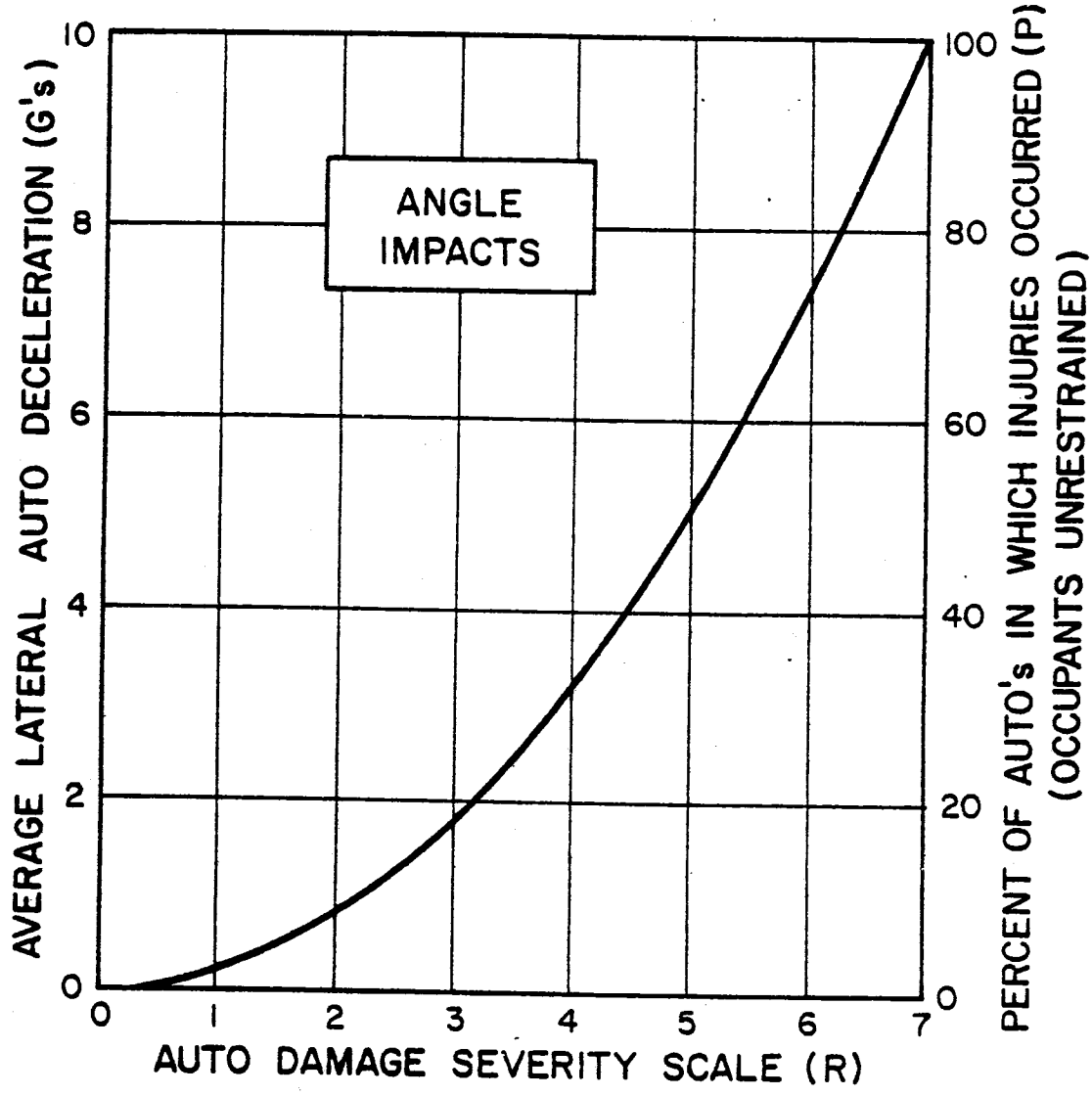

FIGURE 33 CURVE RELATING AUTO LATERAL DECELERATION, INJURIES, AND DAMAGE SEVERITY (Refs. 3,4)

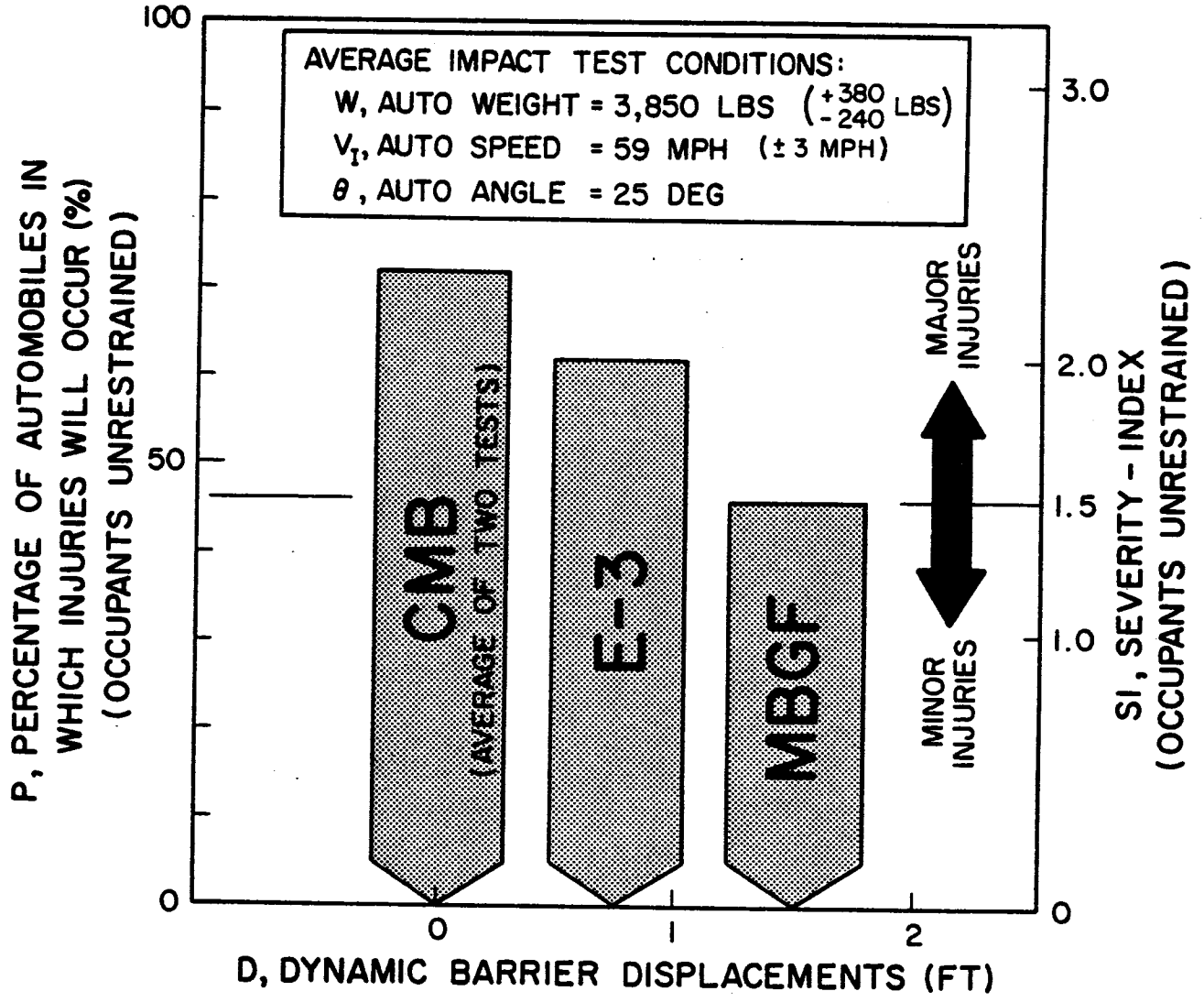

FIGURE 34 COMPARISON OF SELECTED BARRIERS FROM A VIEWPOINT OF INJURY SEVERITY

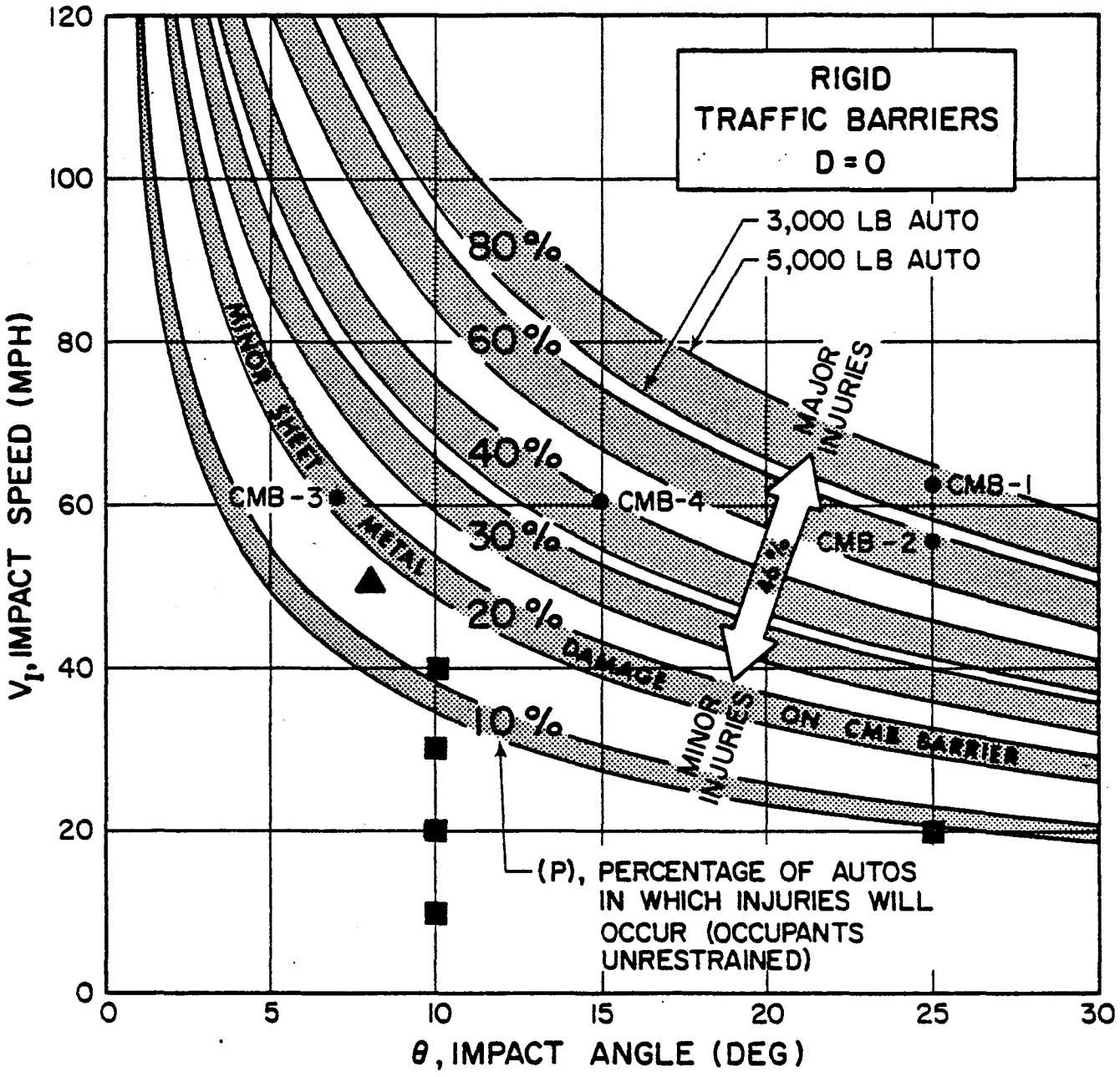

FIGURE 35 PREDICTED PROBABILITY AND INJURY SEVERITY UNDER VARIOUS IMPACT CONDITIONS INVOLVING RIGID BARRIERS

TABLE 3

COMPARISON OF INJURY PROBABILITIES
OBTAINED BY THREE TECHNIQUE METHODS

TECHNIQUE METHOD	MEDIAN BARRIER TESTS					
	E3	MBGF	CMB1	CMB2	CMB3	CMB4
PROBABILITIES BASED ON DECELERATIONS OBTAINED BY ANALYSIS OF HIGH SPEED FILM	62%	46%	80%	64%	22%	47%
COMPUTED PROBABILITY CURVES IN FIGURE 35	---	---	82%	63%	19%	43%
PROBABILITIES BASED ON DAMAGE RATINGS IN TABLE 4	76%	55%	66%	69%	9%	62%

TABLE 4

DAMAGE RATINGS OF TEST VEHICLES USING NSC
7-POINT PHOTOGRAPHIC SCALES

TTI RESEARCH RATING ENGINEER	MEDIAN BARRIER TESTS					
	E3	MBGF	CMB1	CMB2	CMB3	CMB4
EDWARD R. POST	LFQ6	LFQ5	LFQ6	LFQ6	FL2	LFQ5
EUGENE MARQUIS	FL5	FL4	LFQ5	LFQ5	FL1	FL5
ROBERT M. OLSON	LFQ7	LFQ5	LFQ5	LFQ7	LFQ3	LFQ7
HAYES E. ROSS	FL5	FL5	FL5	FL5	FL1	FL5
RONALD YOUNG	LFQ7	LFQ5	LFQ6	LFQ5	LFQ3	LFQ5
TEDDY J. HIRSCH	FL5	FL4.5	FL5.5	FL5.5	FL1	FL3.5
NEILON J. ROWAN	FL6	FL6	FL7	FL6	FL2	FL6
NED E. WALTON	LFQ7	LFQ6	LFQ6	LFQ7	LFQ3	LFQ6
GRAEME D. WEAVER	LFQ7	LFQ6	LFQ5.5	LFQ5.5	LFQ3	LFQ6.5
R, AVERAGE RATING	6.1	5.2	5.7	5.8	2.1	5.5

V. ESTIMATED CONSTRUCTION COSTS AND REPAIR COST

In order to properly evaluate the three selected barriers, it is important that one take into consideration the initial costs of construction and the maintenance costs.

Initial construction costs for the three selected barriers are presented in Table 5. The unit cost breakdowns were adjusted to agree with the total cost per linear foot figures obtained from a Texas Highway Department D-8 Interoffice Memorandum (20) dated April 10, 1972. As evident, the construction cost of $19.20/ft for the E-3 barrier is relatively high in comparison to the more efficient CMB barrier with a cost of $13.40/ft and the MBGF barrier with a cost of $11.75/ft.

The estimated maintenance costs for the three barriers after the comparable 4,000 lb. automobile tests of 60 mph/25 deg. are presented in Table 6. The initial construction costs for the E-3 and MBGF barriers were increased by a *factor* of 1.5 for purposes of repair to a small section.

TABLE 5

COMPARATIVE STUDY
ON
INITIAL CONSTRUCTION COSTS*

TYPE MEDIAN BARRIER	STRUCTURAL COMPONENT	UNIT COST INCLUDING LABOR	COST PER LINEAR FOOT ($/FT)
CMB(70) 9,181 LF	Steel Forms (Rental and Labor)	--------	4.00
	8 pcs #5 Reinforcing Steel	$0.30/Ft	2.40
	Concrete (Ready-Mix)	$ 45/cyd	5.50
	Site Preparation; Stabilize Soil; 1-in. Asphalt at base; Contingencies	--------	1.50
			13.40
E - 3 72,778 LF	Top Rail Member (7.25 lbs/ft)	$0.60/lb	4.35
	Bottom Rail Member (12.89 lbs/ft)	$0.60/lb	7.75
	Fabricated Posts (10 ft. on centers)	--------	4.25
	Drilled Concrete Shafts (18-in. dia.)	--------	1.00
	Base Plates and Anchor Bolts	--------	1.00
	Contingencies	--------	0.85
			19.20
MBGF(B)-69 36,079 LF	2-12 Ga. Steel W-Beams	$0.45/lb	6.00
	6 B 8.5 Posts (6 ft. 3 in. on Centers)	$0.45/lb	1.50
	Drilled Concrete Shafts (18-in. dia.)	--------	1.80
	Base Plates and Anchor Bolts	--------	1.60
	Contingencies	--------	0.85
			11.75

* These costs do not include the costs of the fence and luminaire poles because in roadway medians the fence and luminaire poles would be common to all three barriers. It is estimated that the fencing would cost about $1.00/ft. Steel 40 ft. luminaire poles (Galv.) with 12 ft. mast and 15 ft. mast would cost about $3.30/ft. and $3.60/ft., respectively. Steel 50 ft. luminaire poles (Galv.) with 12 ft. mast and 15 ft. mast would cost about $2.90/ft. and $3.10/ft., respectively. Luminaire pole costs include conduit, dual cable, service pole, and installation. Aluminum luminaire poles are considerably higher in cost. Luminaire costs obtained from Highway Research Record No. 377 (Ref. 17).

TABLE 6

ESTIMATED
MAINTENANCE COSTS

Barrier	Required Maintenance	*Cost/ft ($/ft)	**Total Cost ($)
CMB(70)	• Occasional Sandblasting Job to remove tire scrub marks	- - - -	Nil
E-3	• Replace one 10-ft. length section upper rail • Straighten one support post • Paint touchup	19.20 (1.5)	290
MBGF	• Replace one 25-ft. length section of 2 back-to-back W-beam guardrails • Replace 3 breakaway support posts	11.75 (1.5)	440

* The initial construction costs for the E-3 and MBGF barriers were increased by a *factor* of 1.5 for purposes of repair to a small section.

** Values rounded off to the nearest $10.

VI. CONCLUSIONS

A summary of the comparative results made on the three Texas median barriers is presented in Table 7. The barriers are compared on the basis of:

1. Initial construction cost
2. Estimated maintenance following a 4,000 lb. automobile impact at 60 mph/25 deg.
3. Predicted probability and severity of injuries to *unrestrained* occupants during a 4,000 lb. 60 mph/25 deg. impact.
4. National Safety Council vehicle damage rating after 4,000 lb. automobile 60 mph/25 deg. impact.
5. Applicability for *narrow* medians with luminaire poles for probably 4,000 lb. automobile 60 mph/25 deg. impact.
6. Appearance

One could conclude from the results in Table 7 that the MBGF barrier is the most economical concerning initial construction costs, and that the barrier is the safest concerning probability and injury severity to unrestrained occupants during a 4,000 lb. automobile 60 mph/25 deg. impact. However, the MBGF barrier would cost the most to maintain and its use in *narrow* medians is *not* desirable due to the possibility of the vehicle displacing the barrier a sufficient distance and knocking the luminaire pole onto the roadway. It appears that the MBGF barrier would probably be satisfactory for use on rural type roadways with wide shoulders, wide medians and relatively high speed but low traffic volume.

One could further conclude from the results in Table 6 that the CMB barrier is the most economical when both initial construction costs and estimated maintenance costs are considered. The CMB barrier with luminaire poles would be very desirable for use on urban type roadways with narrow medians and carrying high speed and high traffic volume. In addition, low maintenence reduces the amount of exposure time, and hence, increases safety to maintenance personnel.

It is important that one keep in mind that all three median barriers investigated in this study have performed adequately while in service on our highways. Also, other factors in addition to those presented here should be considered when selecting a barrier. For example, Hutchinson and Kennedy (18) present data which indicates approximately 75% of the vehicle collisions will be at angles of 15 deg. or less. At lower impact angles, the safety and maintenance aspects of all three median barriers would improve. A graph (Figure 35) is presented from which a highway engineer can examine the probability and severity of injury associated with *rigid* type traffic barriers under various combinations of impact speed, impact angle, and passenger vehicle weight.

TABLE 7

COMPARATIVE SUMMARY ON THREE TEXAS MEDIAN BARRIERS

Basis for Comparison	CMB(70) (Long. Reinf. Concrete)	E - 3 (Tubular Rails)	MBGF (Back-to-Back W-Beams)
1. Initial Construction Cost*	$13.40/ft	$19.20/ft	$11.75/ft
2. Estimated Maintenance after 4,000 lb. Auto 60 mph/25 deg. impact	Nil	$290	$440
3. Predicted probability and severity of injury during 4,000 lb. Auto 60 mph/25 deg. impact	72% Major Injuries	62% Major Injuries	46% Threshold of Major Injuries
4. National Safety Council Vehicle Damage Rating after 4,000 lb. Auto 60 mph/25 deg. impact	5.8	6.1 (snagging)	5.2
5. Should barrier be used in *Narrow* Medians with Luminaire Poles for Probable 4,000 lb. Auto 60 mph/25 deg. impact	YES Negligible Barrier Displacements	PROBABLY Small Barrier Displacements of 0.7 ft. Should raise lower rail to prevent snagging.	PROBABLY NOT Barrier Displacements of 1.5 ft. may allow auto to knock down luminaire pole
6. Appearance	Simple and smooth lines	Smooth and Thin Tubular rails	Adequate

* Cost does not include chain link fence (glare screen) or luminaire poles.

ACKNOWLEDGMENTS

This study was conducted under an interagency contract between the Texas Transportation Institute and the Texas Highway Department. It was sponsored jointly by the Texas Highway Department and the Federal Highway Administration. Liaison was maintained through Mr. John Nixon and Mr. Paul Tutt, contact representatives for the Texas Highway Department.

REFERENCES

1. Committee on Guardrail and Guide Posts, HRB *Circular 482* (Sept. 1962).

2. New Jersey State Highway Department, "Center Barrier Save Lives", 1966, 15 pp.

3. Michalski, C. S., "Model Vehicle Damage Scale: A Performance Test". *Traffic Safety*, Vol. 12, No. 2 (June 1968), pp. 34-39.

4. Olson, R. M., Post, E. R., and McFarland, W. F., "Tentative Service Requirements for Bridge Rail Systems". *NCHRP Report 86*, 1970, 62 pp.

5. "Vehicle Damage Scale for Traffic Accident Investigation". Traffic Accident Data Project, National Safety Council, *TAD Project Technical Bull. No. 1* (1968), 18 pp.

6. Weaver, G. D., "The Relation of Side Slope Design to Highway Safety". Final Report on Task Order No. 2, Report No. 626-2, NCHRP Project 20-7, Texas Transportation Institute, Texas A&M University, May 1970.

7. Ross, H. E., and Post, E. R., "Criteria for the Design of Safe Sloping Culvert Grates," Vol. 1: Development of Criteria, Research Report 140-3, Texas Transportation Institute, Texas A&M University, August 1971, 23 pp.

8. Ross, H. E., and Post, E. R., "Criteria for Guardrail Need and Location on Embankments," Vol. 1: Development of Criteria, Research Report 140-4, Texas Transportation Institute, Texas A&M University, April 1972, 63 pp.

9. Young, R. D., Ross, H. E., and Post, E. R., "Rigid Traffic Barrier Study," First Rough Draft, Texas Transportation Institute, Texas A&M University, Nov. 1971.

10. McHenry, R. R., and Deleys, N. J., "Vehicle Dynamics in Single Vehicle Accidents: Validation and Extension of a Computer Simulation," Cornell Aeronautical Laboratory Report No. VJ-2251-V-3, Buffalo, N. Y., Dec. 1968, 276 pp.

11. Young, R. D., Edwards, T. C., Bridwell, R. J., and Ross, H. E., "Documentation of Input for Single Vehicle Accident Computer Program," Research Report 140-1, Texas Transportation Institute, Texas A&M University, July 1969, 110 pp.

12. Olson, R. M., Ivey, D. L., Post, E. R., Gunderson, R. H., and Cetiner, A., "Bridge Rail Service Requirements as a Basis for Design Criteria," Final Report to NCHRP 12-8/1, Texas Transportation Institute, Texas A&M University, Feb. 1972.

13. Hyde, A. S., "Biodynamics and the Crashworthiness of Vehicle Structures," Wyle Laboratories - Research Staff, Huntsville Facility, Report WR 68-3, Vol. III of V, March 1968.

14. Nordlin, E. F., and Field, R. N., "Dynamic Tests of Steel Box-Beam and Concrete Median Barriers," *Highway Research Record 222*, 1968, pp. 61-88.

15. Nordlin, E. F., Hackett, R. P., Woodstrom, J. H., and Folsom, J. J., "Dynamic Tests of the California Type 20 Bridge Barrier Rail," Presented at the 50th Annual Meeting of the Highway Research Board, Jan. 1971.

16. Lunstrom, L. C., Skeels, P. C., Englund, B. R., and Rogers, R. A., "A Bridge Parapet Designed for Safety," *Highway Research Record No. 83*, 1965, pp. 169-187.

17. McFarland, W. F., and N. E. Walton, "Economic and Accident Potential Analysis of Roadway Lighting Alternatives," *Highway Research Record 377*, 1971, pp. 92-102.

18. Hutchinson, J. W., and Kennedy, T. W., "Medians of Divided Highways - Frequency and Nature of Vehicle Encroachments," *Bulletin 487*, University of Illinois Engineering Experiment Station, 1966.

19. Smith, P., "Development of a Three Cable Guide Rail System and Other Guide Rail Tests, 1967-1968".

20. Texas Highway Department D-8 Interoffice Memorandum to Mr. John Nixon from R. S. Williamson, April 10, 1972.

21. Post, E. R., and Young, R. D., "Tentative Relationship Between Injury Probability, Injury Severity and Severity-Index," Work-In-Progress as part of THD 2140-5 Project, Texas Transportation Institute, August 1972.

A P P E N D I X

HIGH-SPEED FILM DATA FOR E-3 BARRIER TEST

Time (msec)	Displacement (ft)	Time (msec)	Displacement (ft)
-51	-4.4	(Continued)	
-41	-3.5	203	12.8
-30	-2.7	213	13.4
-20	-1.8	223	13.7
-10	-0.9	233	14.1
0 Impact	0	254	14.8
10	0.9	274	15.6
20	1.7	294	16.3
30	2.6	315	17.1
41	3.4	335	17.8
51	4.3	355	18.6
61	5.1	376	19.5
71	5.9	396	20.4
81	6.6	416	21.2
91	7.3	436	22.1
102	8.0	457	22.9
112	8.6	477	23.8
122	9.2	497	24.6
132	9.7	518	25.4
142	10.2	538	26.2
152	10.6	558	27.0
162	11.1	579	27.7
173	11.5	599	28.6
183	11.9	619	29.3
193	12.4		

HIGH-SPEED FILM DATA FOR MBGF BARRIER TEST

Time (msec)		Displacement (ft)
-61		-5.2
-51		-4.3
-41		-3.4
-31		-2.6
-20		-1.7
-10		-0.8
0	Impact	0

HIGH-SPEED FILM DATA FOR TEST CMB-1

Time (msec)	Displacement (ft)	Time (msec)	Displacement (ft)
-61	-5.6	(Continued)	
-51	-4.6	183	13.4
-41	-3.7	203	14.8
-30	-2.8	223	16.3
-20	-1.9	243	17.7
-10	-0.9	264	19.1
0 Impact	0	284	20.5
20	1.8	304	21.9
41	3.5	324	23.3
61	5.1	345	24.8
81	6.6	365	26.1
101	8.1	385	27.5
122	9.4	406	28.9
142	10.8	426	30.3
162	12.1		

HIGH-SPEED FILM DATA FOR TEST CMB-2

Time (msec)		Displacement (ft)
-71		-5.8
-57		-4.6
-43		-3.4
-29		-2.3
-14		-1.2
0	Impact	0

HIGH-SPEED FILM DATA FOR TEST CMB-3

Time (msec)		Displacement (ft)
-68		-6.1
-61		-5.5
-46		-4.1
-30		-2.7
-15		-1.4
0	Impact	0
15		1.4
30		2.7
46		4.0
61		5.3
76		6.5
91		7.7
106		9.0
122		10.3
137		11.5
152		12.8
167		14.1
175		14.8
190		16.0
205		17.4
220		18.7
236		20.0
251		21.4
266		22.6
281		24.0
296		25.2
312		26.6

Time (msec)	Displacement (ft)
(Continued)	
327	27.9
342	29.2
357	30.4
372	31.8
388	33.1
403	34.3
418	35.6
433	37.0
448	38.2
464	39.5
479	40.9
494	42.1
509	43.5
524	44.8
532	45.4
547	46.7
562	48.0
578	49.3
593	50.6
608	51.9

HIGH-SPEED FILM DATA FOR TEST CMB-4

Time (msec)	Displacement (ft)
-23	-2.0
-15	-1.3
-8	-0.7
0 Impact	0
129	10.8
144	12.1
159	13.3
174	14.7
189	15.9
204	17.0
234	19.2
264	21.4
280	22.5
294	23.6
310	24.7
317	25.3

Time (msec)	Displacement (ft)
(Continued)	
393	31.0
476	37.3
514	40.2
529	41.3
536	41.8
552	43.0
567	44.2
587	45.3
594	45.9

POSITION OF DATA POINTS FOR

TRIANGULATION DATA

ROOF TARGETS: Shown in relation to vehicle

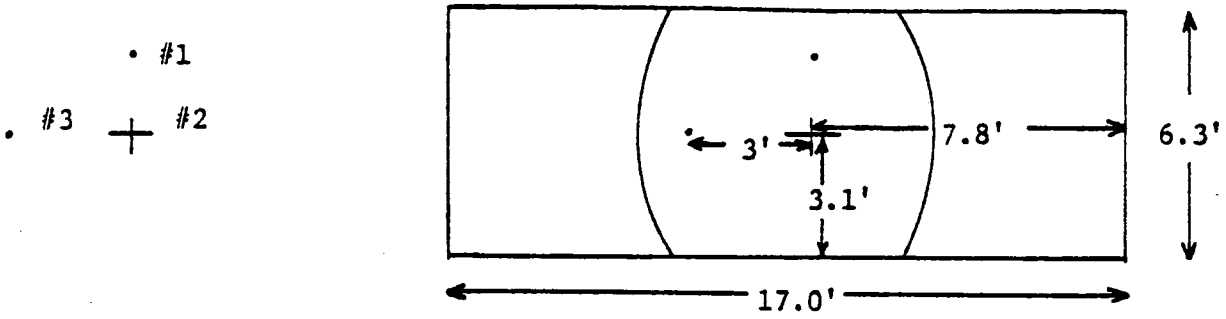

x,y COORDINATES: Shown in relation to median barrier

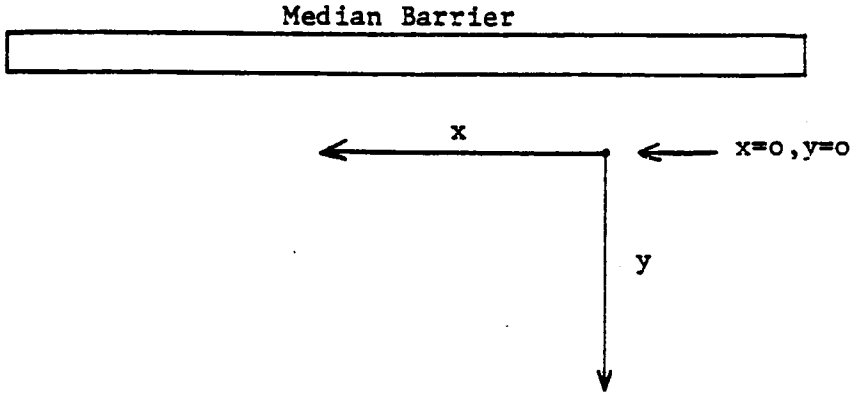

TRIANGULATION DATA FOR E-3 BARRIER TEST

x,y coordinates of roof target 3. Point where x = 0 and y = 0 is 33 ft north and 5.5 ft east of the south end of the barrier.

Time (msec)	x (ft)	y (ft)
-10	13.6	2.9
0	12.8	2.5
40	9.8	1.1
80	6.9	0.03
120	4.6	-0.7
160	2.6	-0.9
200	0.6	-1.2
240	-1.3	-1.3
280	-3.1	-1.2
320	-4.7	-1.1
360	-6.4	-1.1
400	-8.1	-1.1
440	-9.7	-1.1
480	-11.2	-1.1
520	-12.9	-0.9
560	-14.2	-0.7
600	-15.7	-0.4

TRIANGULATION DATA FOR MBGF BARRIER TEST

x,y coordinates of roof target 2 (above c.g.). Point where x = 0 and y = 0 is 32.1 ft north and 3.9 ft east of the south end of the barrier.

Time (msec)	x (ft)	y (ft)	Time (msec)	x (ft)	y (ft)
-40	14.2	4.3		(continued)	
-30	13.9	3.9	275	-6.5	-1.6
-20	13.5	3.6	300	-7.7	-1.4
-10	12.0	3.3	325	-8.9	-1.1
0	11.2	2.9	350	-10.2	-0.7
25	9.3	2.0	375	-11.4	-0.4
50	7.4	1.2	400	-12.7	0
75	5.5	0.4	425	-13.8	0.3
100	3.7	-0.2	450	-15.0	0.6
125	1.9	-0.7	475	-16.2	1.1
150	0.3	-1.1	500	-17.4	1.6
175	-1.1	-1.3	525	-18.6	2.0
200	-2.6	-1.6	550	-19.7	2.5
225	-4.0	-1.8	575	-20.9	3.0
250	-5.4	-1.6	585	-21.4	3.1

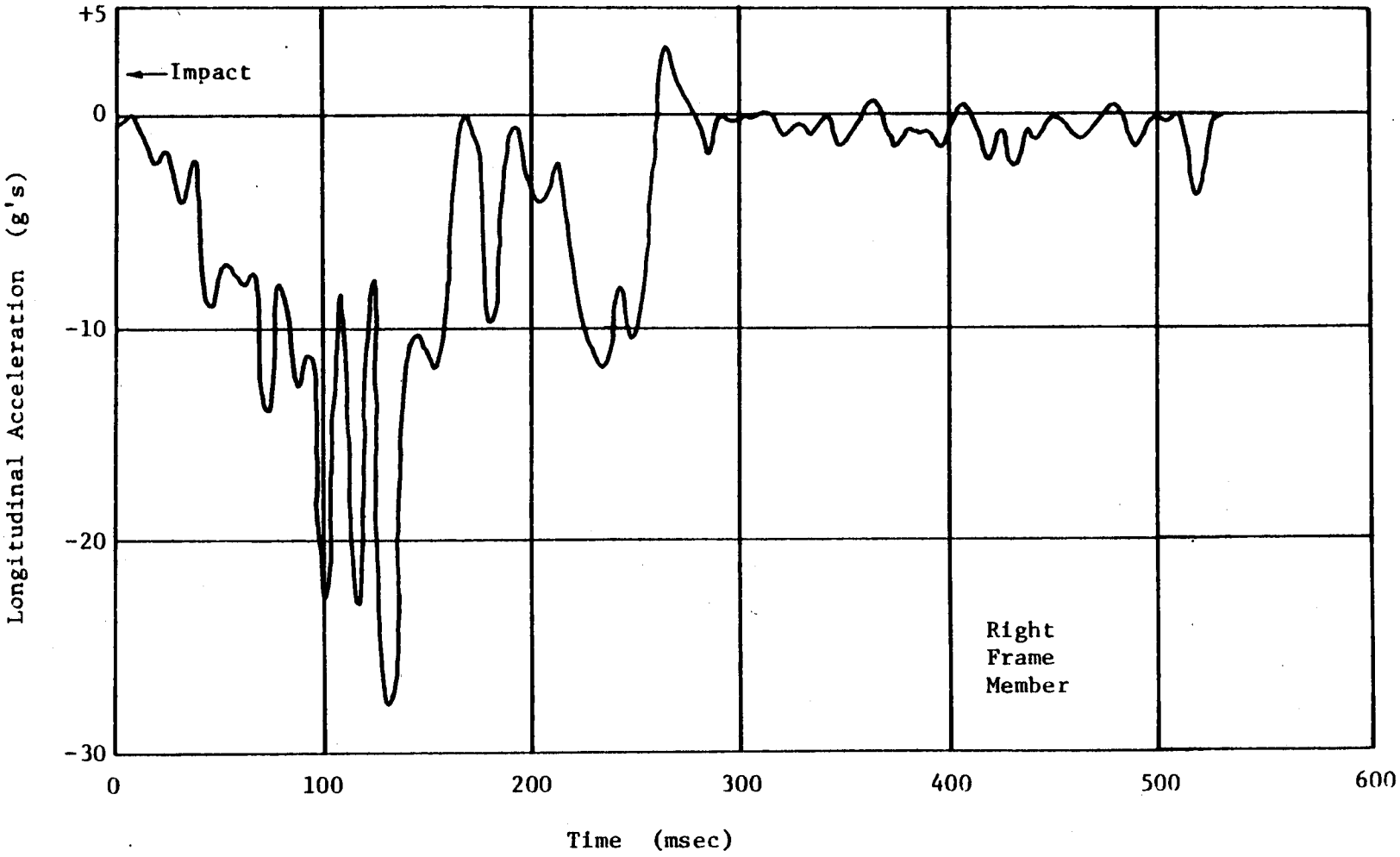

FIGURE 36. LONGITUDINAL ACCELEROMETER DATA FOR E-3 BARRIER TEST.

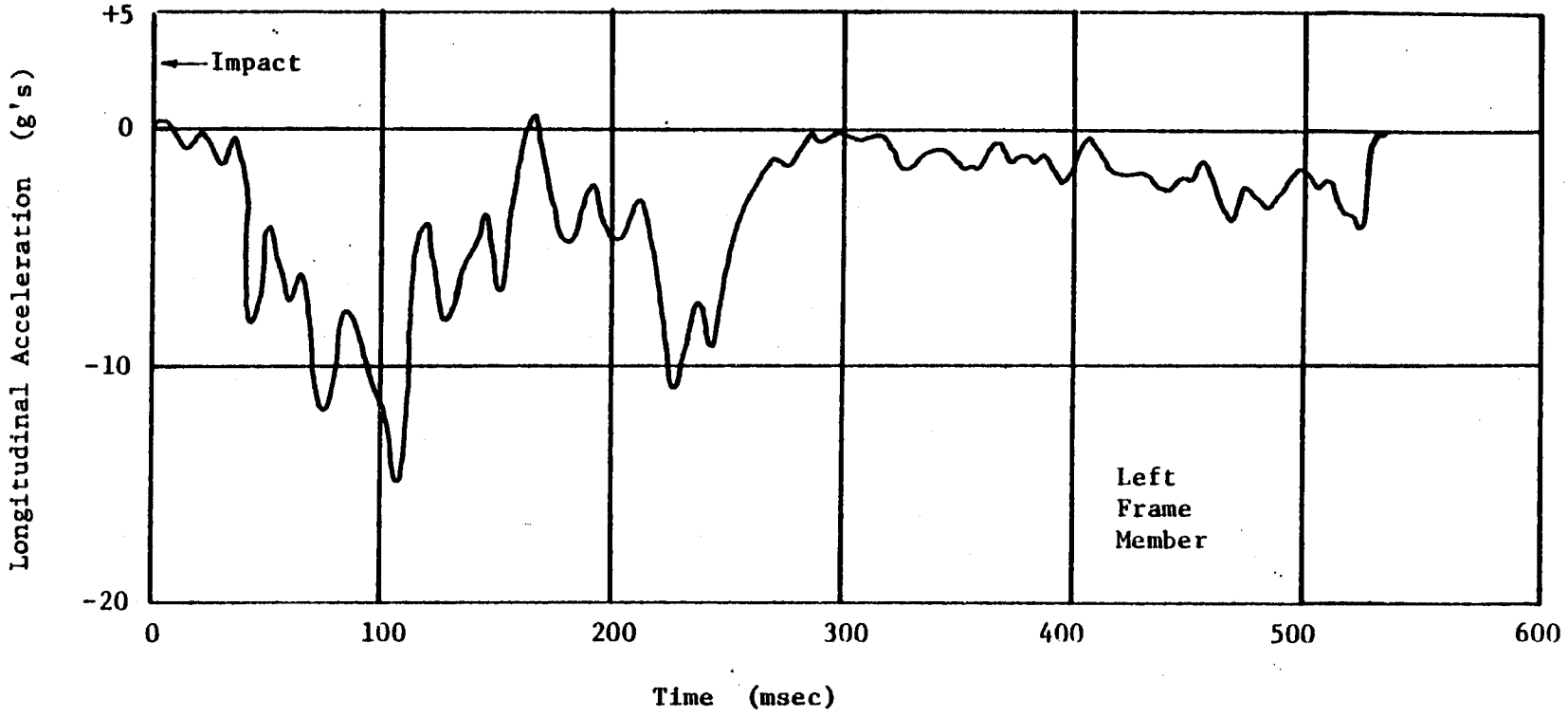

FIGURE 37. LONGITUDINAL ACCELEROMETER DATA FOR E-3 BARRIER TEST.

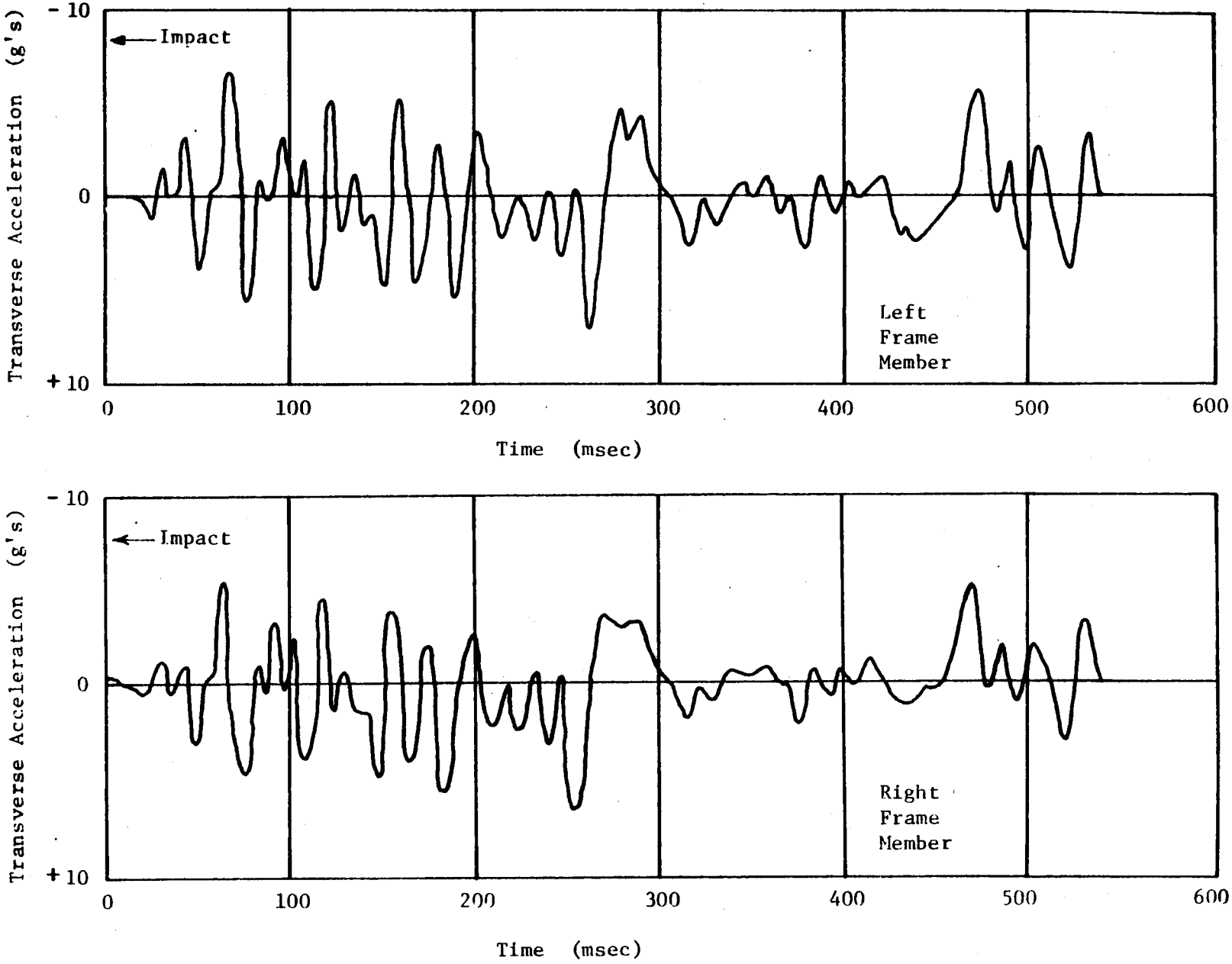

FIGURE 38. TRANSVERSE ACCELEROMETER DATA FOR E-3 BARRIER TEST.

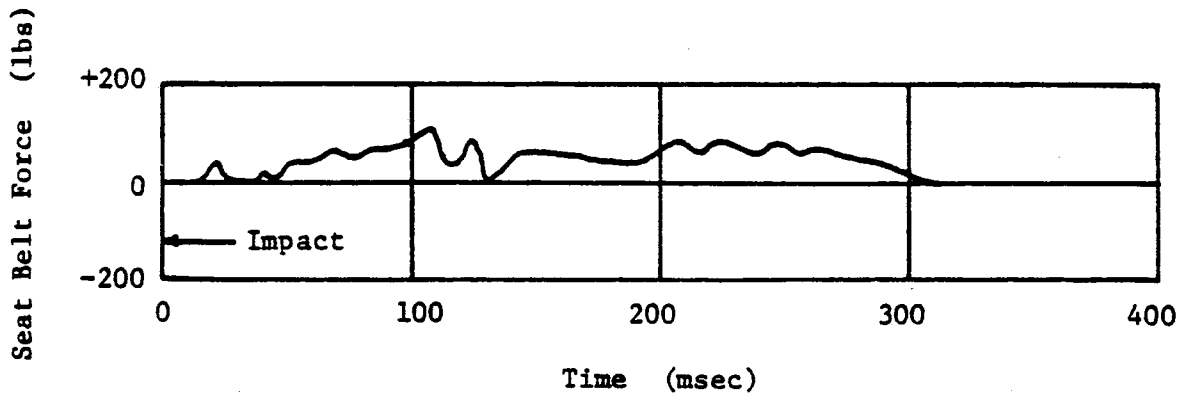

FIGURE 39. SEAT BELT DATA FOR E-3 BARRIER TEST.

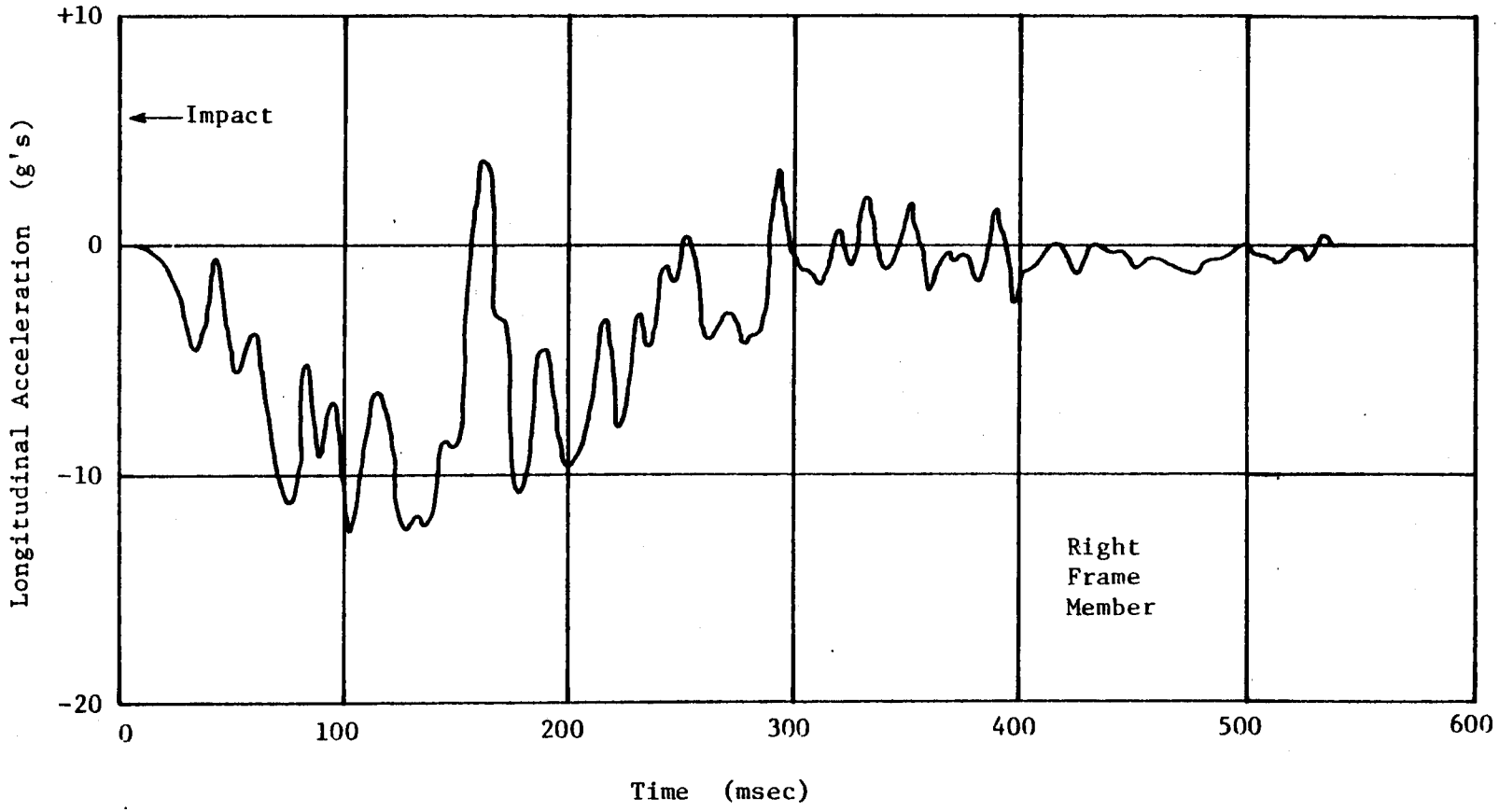

FIGURE 40. LONGITUDINAL ACCELEROMETER DATA FOR MBGF BARRIER TEST.

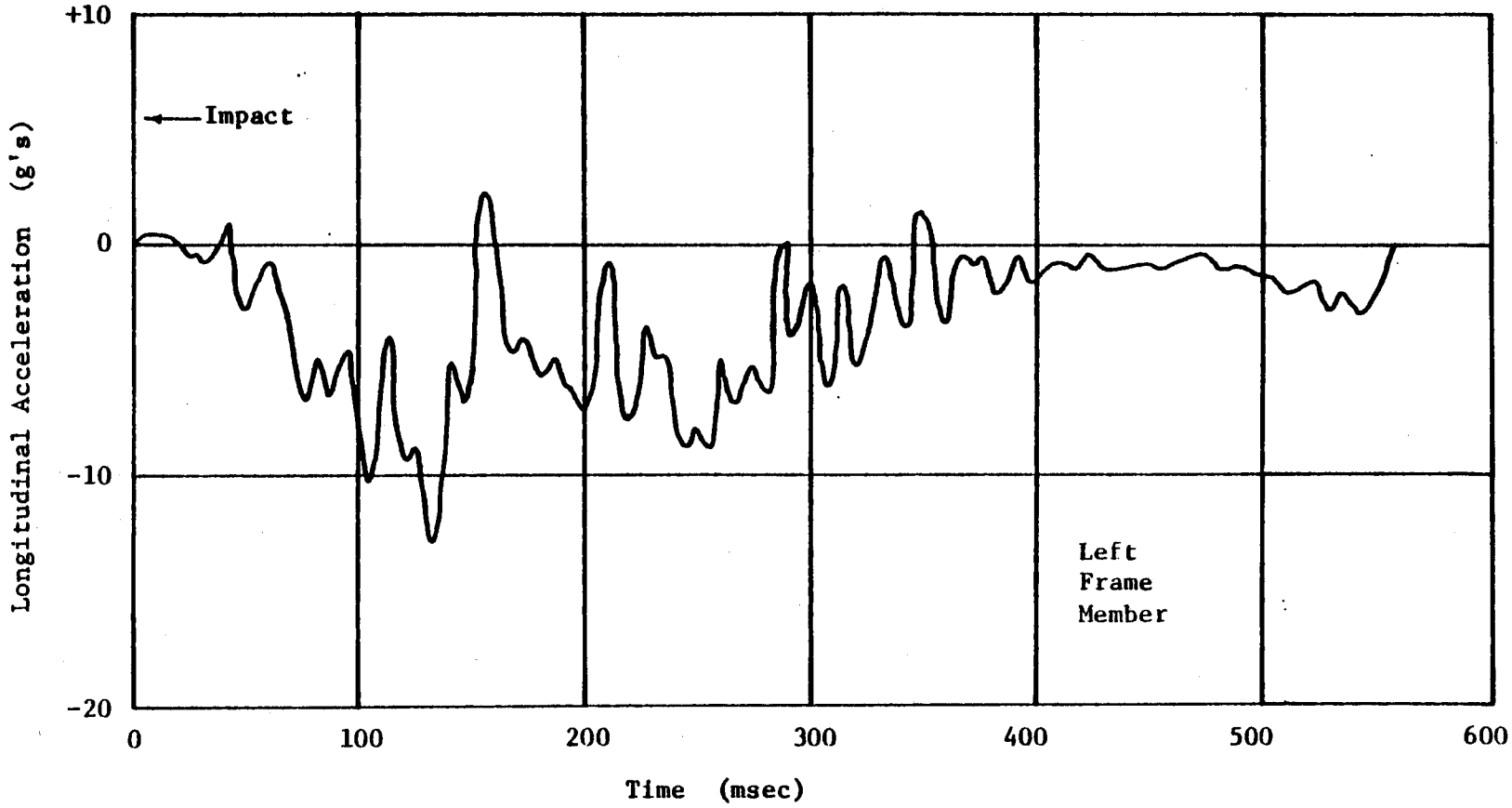

FIGURE 41. LONGITUDINAL ACCELEROMETER DATA FOR MBGF BARRIER TEST.

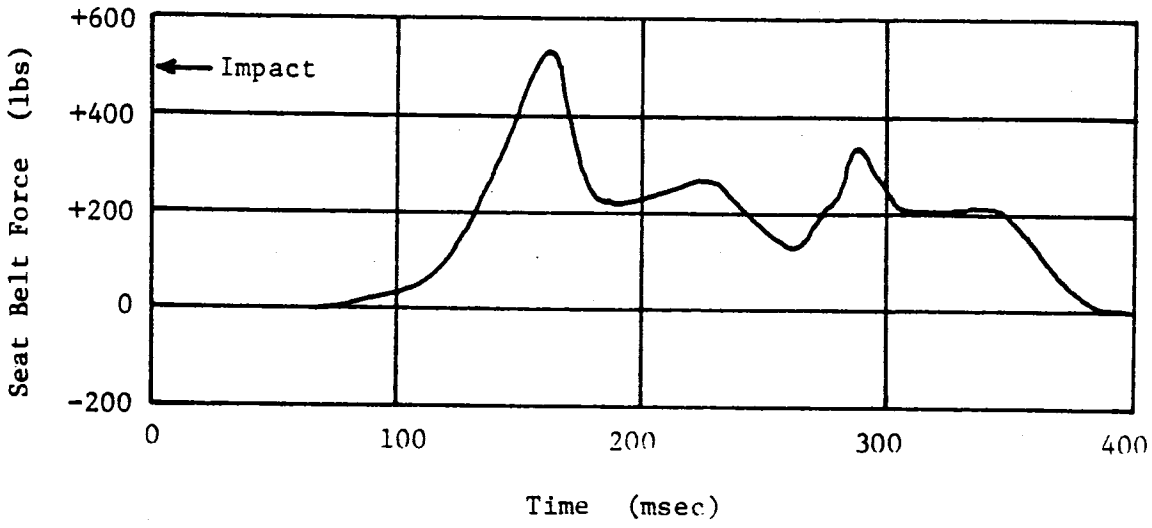

FIGURE 42. SEAT BELT DATA FOR MBGF BARRIER TEST.

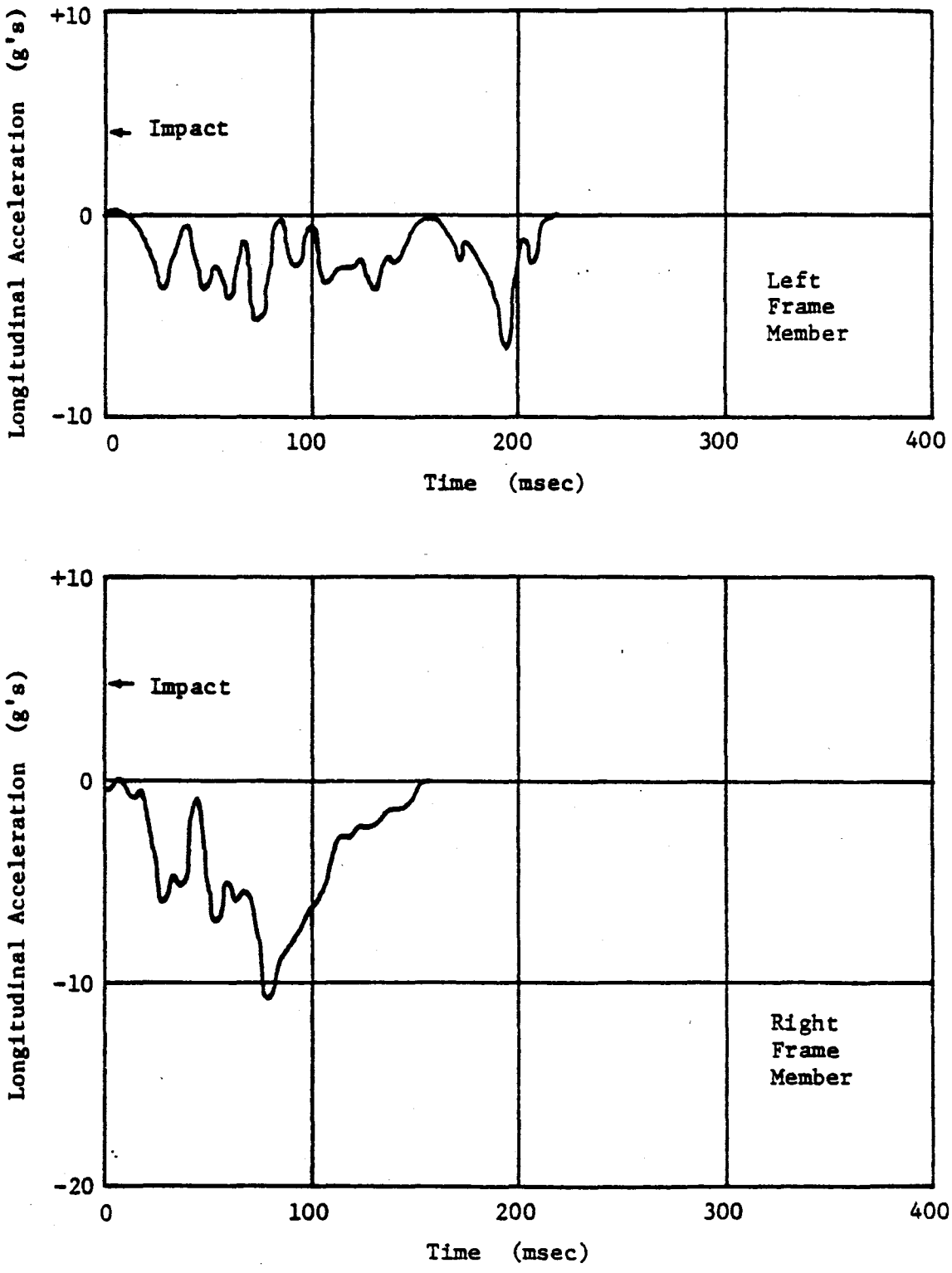

FIGURE 43. LONGITUDINAL ACCELEROMETER DATA FOR TEST CMB-1.

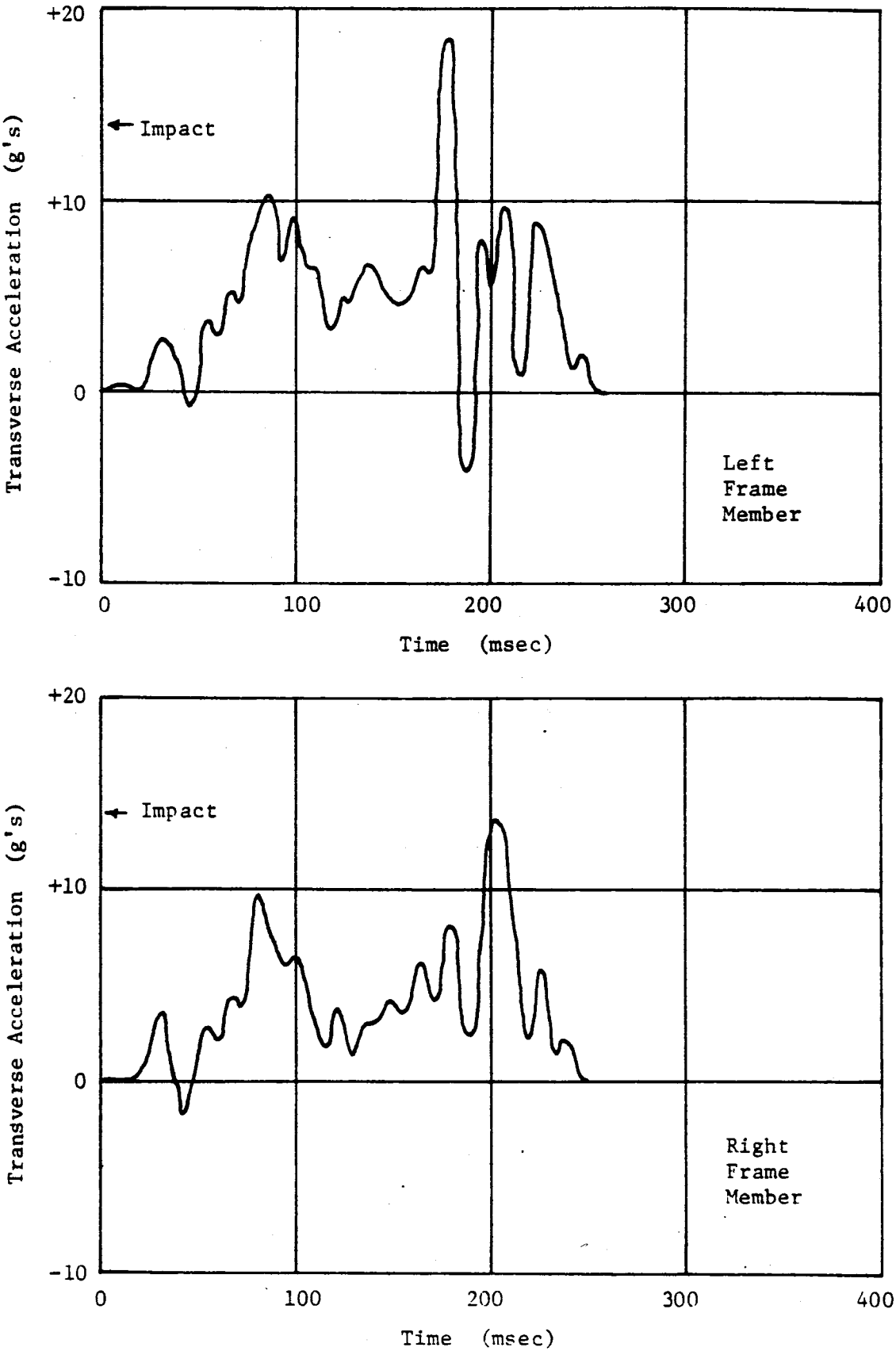

FIGURE 44. TRANSVERSE ACCELEROMETER DATA FOR TEST CMB-1.

(Positive acceleration is acceleration to the right of the vehicle.)

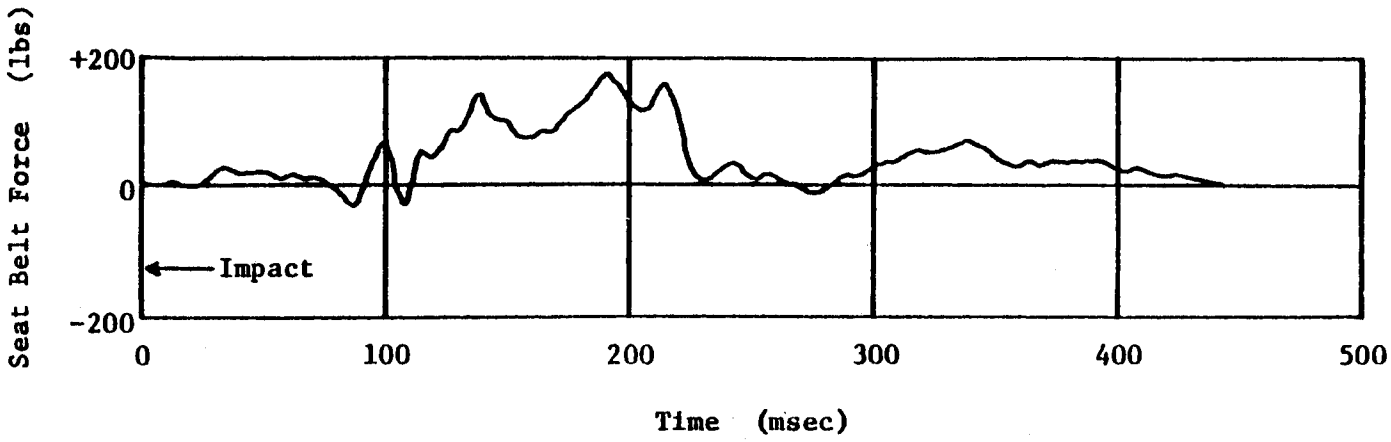

FIGURE 45. SEAT BELT DATA FOR TEST CMB-1.

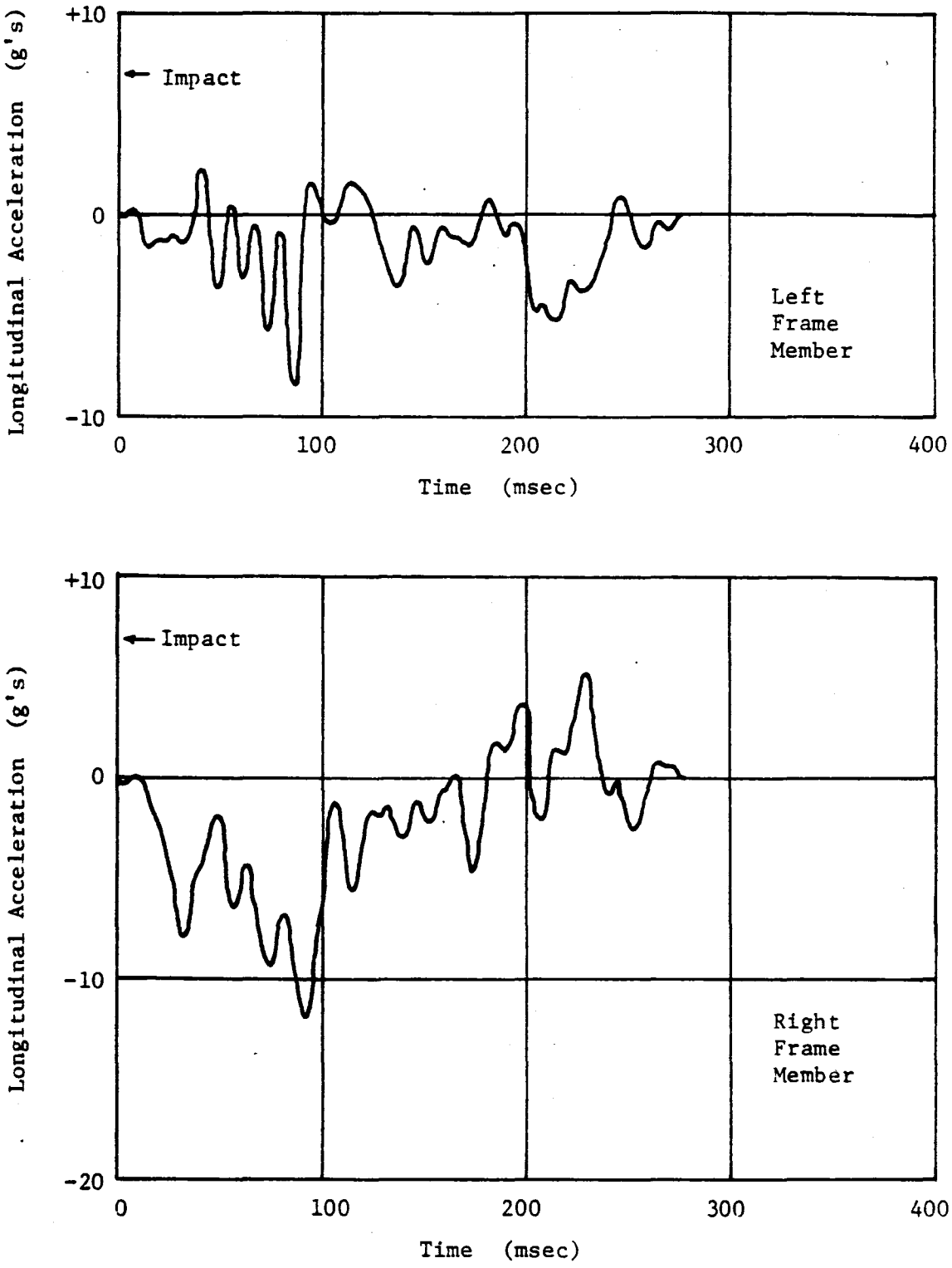

FIGURE 46. LONGITUDINAL ACCELEROMETER DATA FOR TEST CMB-2.

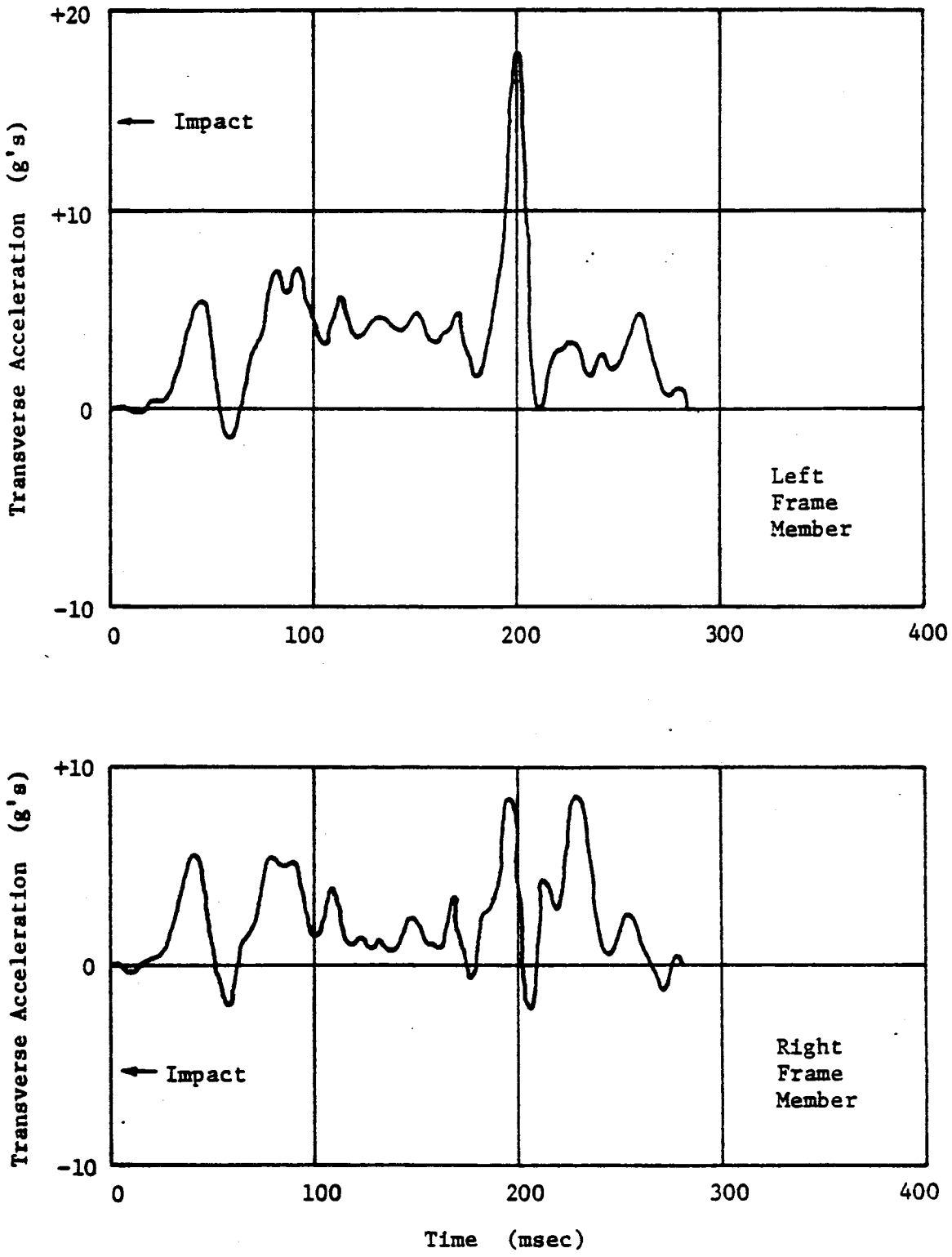

FIGURE 47. TRANSVERSE ACCELEROMETER DATA FOR TEST CMB-2.
(Positive acceleration is acceleration to the right of the vehicle.)

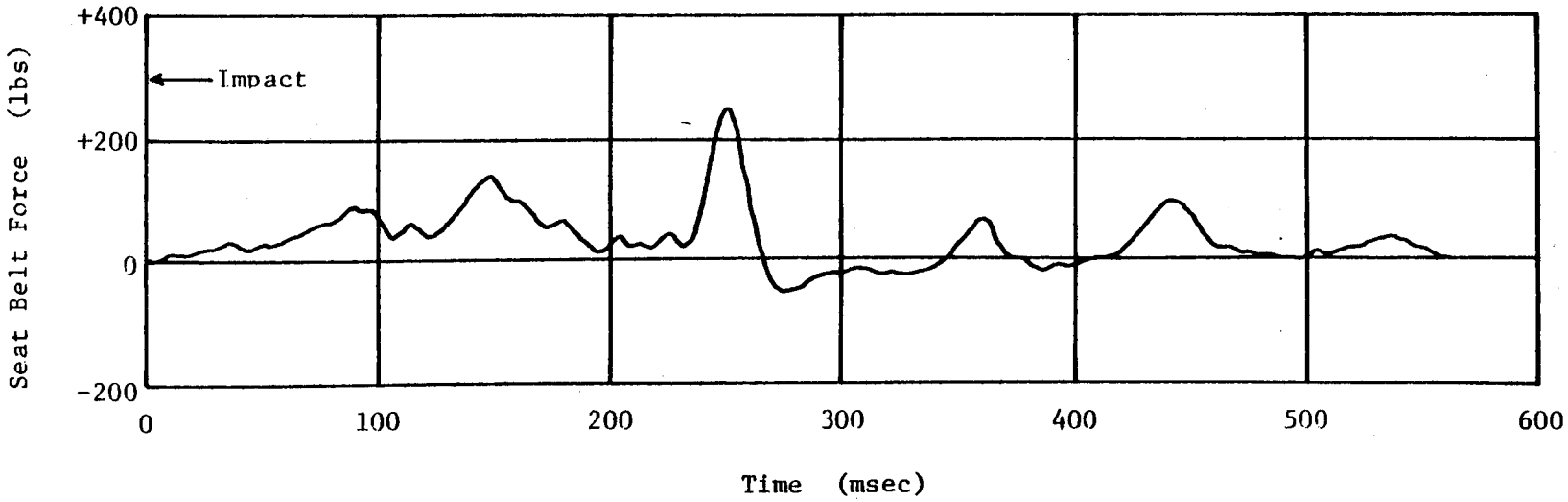

FIGURE 48. SEAT BELT DATA FOR TEST CMB-2.

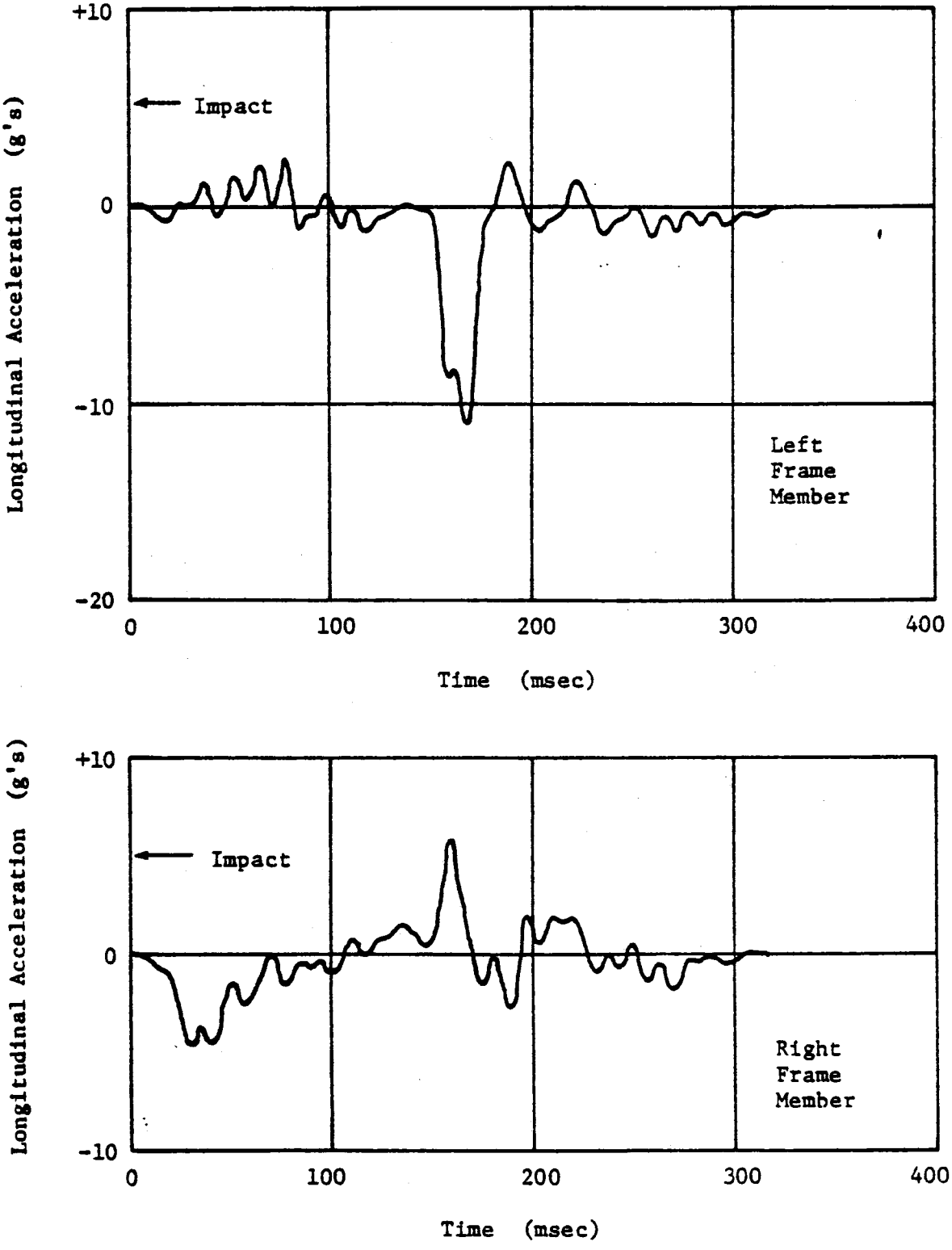

FIGURE 49. LONGITUDINAL ACCELEROMETER DATA FOR TEST CMB-3.

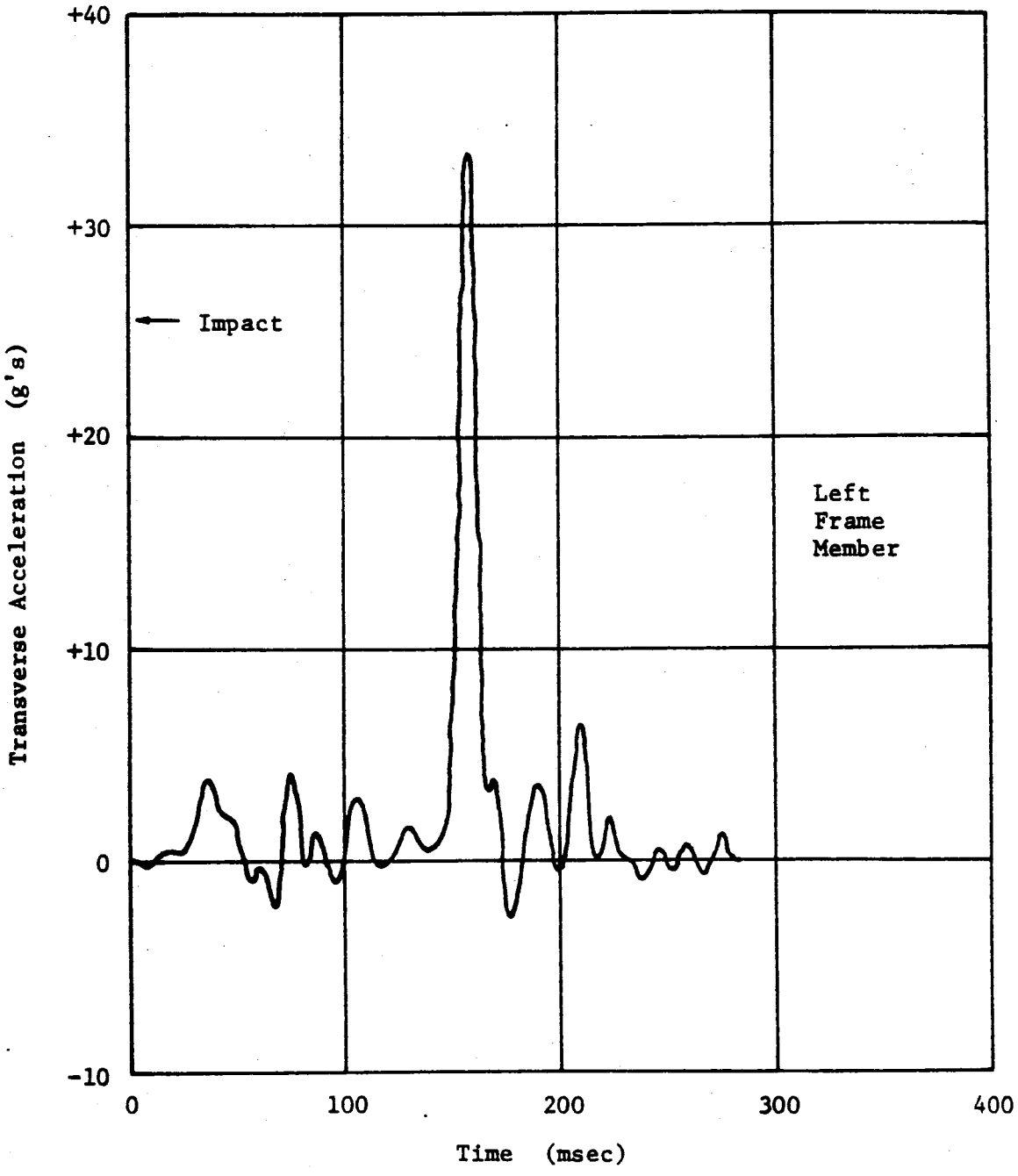

FIGURE 50. TRANSVERSE ACCELEROMETER DATA FOR TEST CMB-3.

(Positive acceleration is acceleration to the right of the vehicle.)

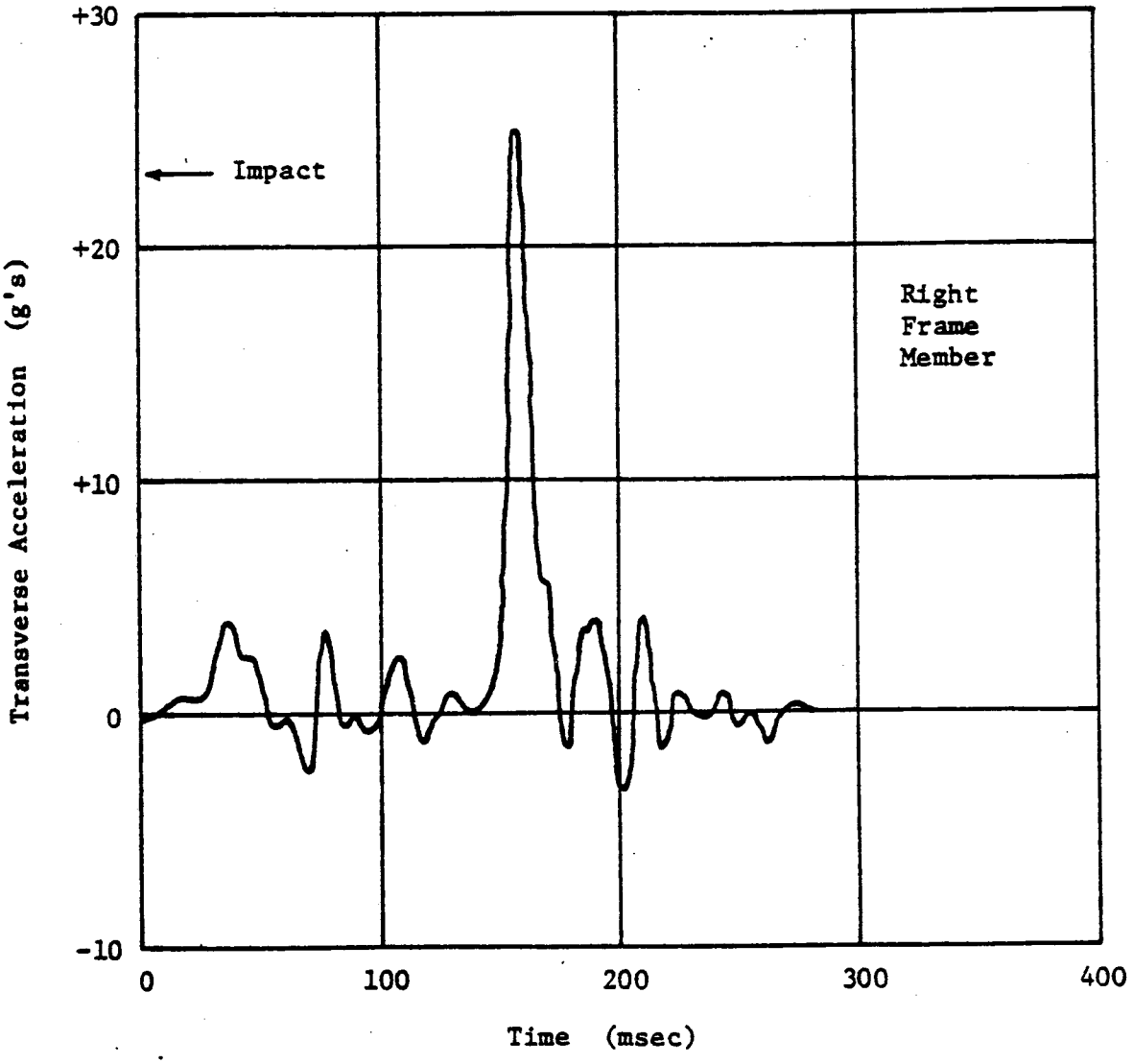

FIGURE 51. TRANSVERSE ACCELEROMETER DATA FOR TEST CMB-3.

(Positive acceleration is acceleration to the right of the vehicle.)

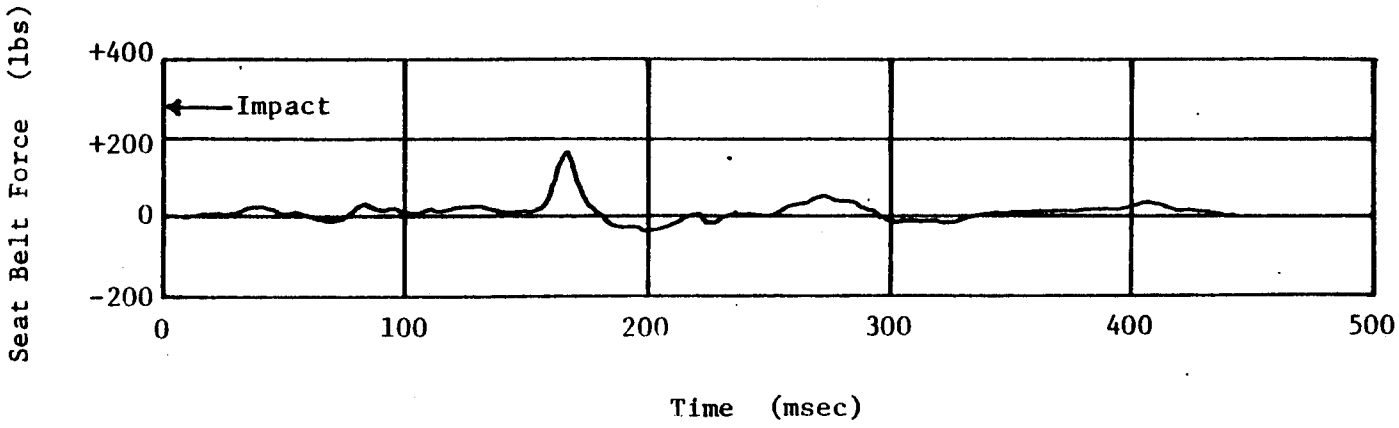

FIGURE 52. SEAT BELT DATA FOR TEST CMB-3.

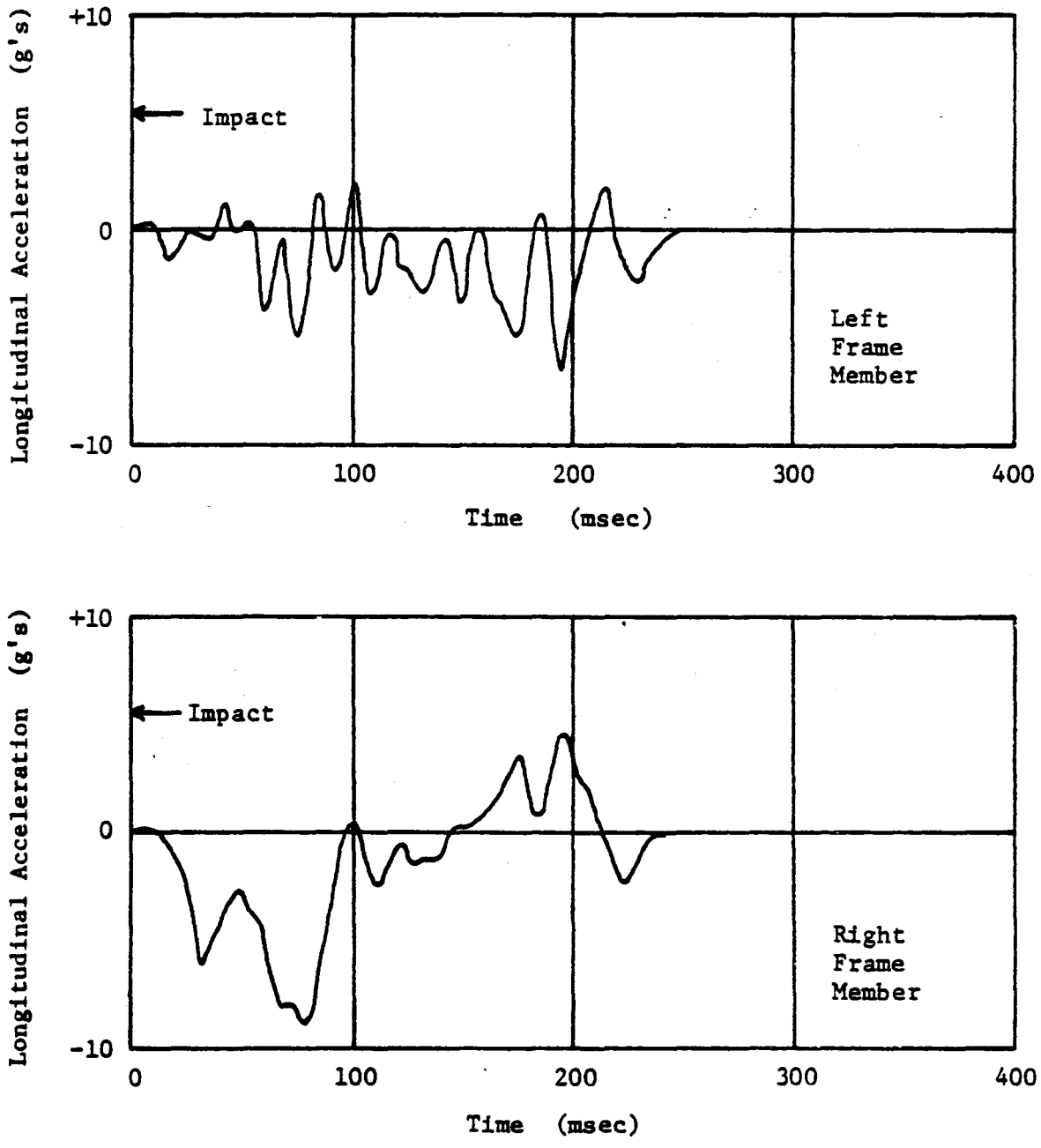

FIGURE 53. LONGITUDINAL ACCELEROMETER DATA FOR TEST CMB-4.

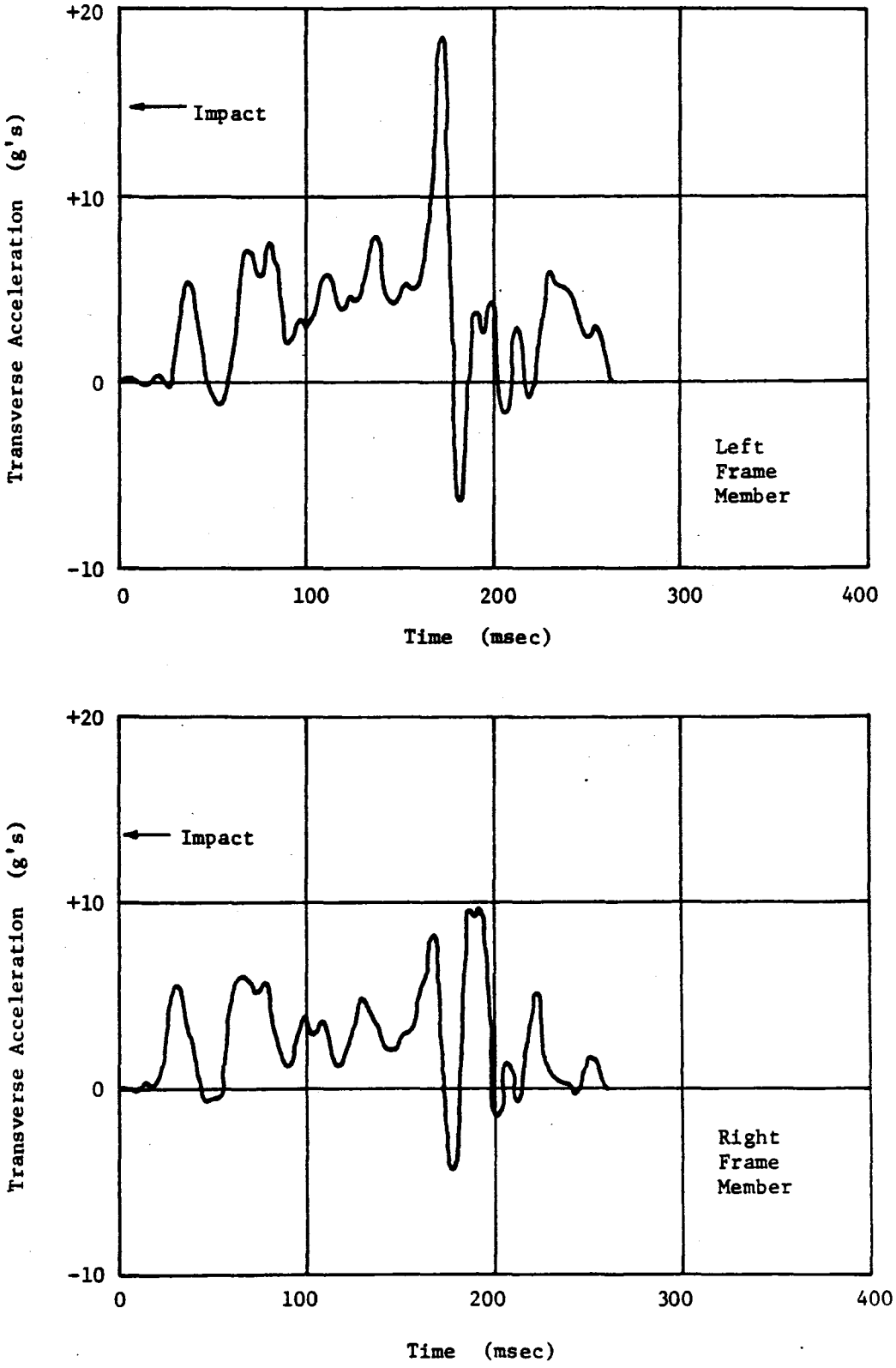

FIGURE 54. TRANSVERSE ACCELEROMETER DATA FOR TEST CMB-4.

(Positive acceleration is acceleration to the right of the vehicle.)

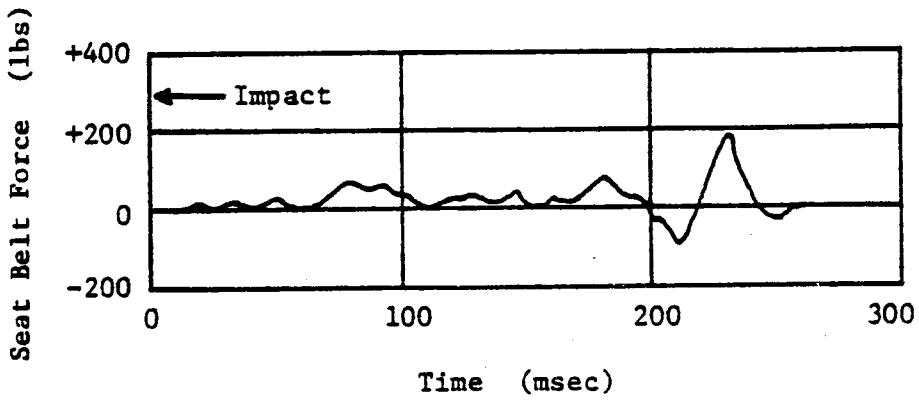

FIGURE 55. SEAT BELT DATA FOR TEST CMB-4.